Coastal inundation by storm-tides and waves in the Auckland region

Prepared for Auckland Council

September 2013

Authors/Contributors:

Scott Stephens
Sanjay Wadhwa
Richard Gorman
Nigel Goodhue
Mark Pritchard
Ron Ovenden
Glen Reeve

For any information regarding this report please contact:

Scott Stephens
Coastal Scientist
Coastal and Estuarine Processes Group
+64-7-856 7026
scott.stephens@niwa.co.nz

National Institute of Water & Atmospheric Research Ltd
Gate 10, Silverdale Road
Hillcrest, Hamilton 3216
PO Box 11115, Hillcrest
Hamilton 3251
New Zealand

Phone +64-7-856 7026
Fax +64-7-856 0151

Contents

Tables

Figures

Reviewed by   Approved for release by

Dr Emily Lane   Dr Rob Bell

Formatting checked by

Executive summary

Auckland Council commissioned NIWA in March 2013 to calculate extreme sea level elevations and their likelihood around the entire coastline of the Auckland region, and to map selected inundation areas.

Coastal extreme sea-level elevations resulting from storm-tides and wave setup were calculated for annual exceedance probabilities of 39%, 18%, 10%, 5%, 2%, 1% and 0.5% (corresponding to 2, 5, 10, 20, 50, 100 and 200-year average recurrence intervals, respectively). These extreme storm-generated sea levels are likely to persist for only short periods of 1–2 hours around the coincident high tide.

The study used hydrodynamic models calibrated against tide-gauge and wave buoy measurements to calculate storm-tide and wave setup along the coastline, and applied robust joint-probability modelling techniques to calculate the occurrence likelihood of the extreme sea-level elevations. The modelling was divided into the major harbours (Waitemata, Manukau and Kaipara), the beaches of the east and west coasts, and inside the small east-coast estuaries, according to geographical influences on models and the processes controlling extreme sea level.

The extreme sea-level elevations were spatially interpolated along the coastline, and intersected with a digital elevation model of the land surface produced from LiDAR, to produce maps of inundation associated with a subset of annual exceedance probabilities of 18%, 5%, 2% and 1% (5, 20, 50 and 100-year average recurrence intervals).

The inundation levels and inundation maps were calculated relative to Auckland Vertical Datum 1946 (AVD-46), and they include the present-day mean-sea-level offset added to AVD-46 (e.g., +0.15 m at Auckland). Further inundation maps were produced for additional sea-level rise scenarios of +1 m and +2 m above present-day mean-sea-level, added to the 1% annual exceedance probability elevation.

This report presents tables that include the coastal extreme sea-level elevations used to generate the coastal storm inundation maps, and presents the data, models and methods that were employed in the study.

1   Introduction and project scope

Coastal hazards are a significant issue within the Auckland region and Auckland Council are tasked with managing such hazards under the RMA and associated NZ Coastal Policy Statement (e.g., Policies 24–27). Coastal hazards include, tsunami, storm erosion and storm-tide inundation.

Added to these are the increasing effects of climate change and especially the prospect of a projected rise in sea level of 0.5–0.8 m (or greater) by the 2090s (Ministry for the Environment 2008) or 0.7–1.0 m (or greater) in the next 100 years, by 2115 (Britton et al. 2011)[1].

Auckland Council requires estimates of extreme sea level elevations and their likelihood around the whole coastline of the Auckland region that are well-founded on robust and defendable science. Auckland Council requested that the coastal inundation elevations be translated into inundation maps within a geographic information system (GIS) for some scenarios.

High storm-tides and large waves contribute to storm erosion and flooding on the open-coast of the Auckland region. There are a number of meteorological and astronomical phenomena involved in the development of a combined extreme storm-tide and wave event, and these processes can combine in a number of ways to inundate low-lying coastal margins, or cause coastal erosion. Storm-tide is defined as the sea-level peak reached during a storm event, from a combination of monthly mean sea-level anomaly + tide + storm surge. Waves also further raise the effective storm-tide level at the coastline. Wave setup is the increase in the sea level within the surf zone from the release of wave energy. Flooding, from rivers, streams and stormwater, is another contributor to coastal inundation when the flood discharge is constrained inside narrower sections of estuaries. Flooding from rivers was not considered in this phase of the project. Coastal inundation by tsunami and coastal erosion were also not considered in this study.

Mean sea level (MSL) is rising, which will raise the base level for wave attack on the coastline and storm-tide inundation of low-lying land. Estimates of long-term sea-level rise are required, along with methods to include sea-level rise into coastal hazard assessments. Climate change will also cause acceleration in long-term trends of sea-level rise, but recent research in New Zealand shows only minor increases will occur in the drivers (winds, barometric pressure) that produce storm surges (Mullan et al. 2011).

Coastal extreme sea-level elevations were calculated previously for parts of the Auckland region now under Auckland Council's jurisdiction. Former Manukau City Council (MCC) and Auckland City Council (ACC) respectively commissioned NIWA to assess extreme sea levels for the coastlines under their jurisdiction (Ramsay et al. 2008a; Ramsay et al. 2008b). Likewise, former North Shore City Council and Rodney District Council commissioned Tonkin and Taylor to calculate sea inundation levels for their coastlines (Andrews 2004; Reinen-Hamill & Shand 2005). Projections of future sea-level rise were under constant debate and review over the period spanning these studies, and the studies applied different sea-level rise estimates for different planning timeframes. Also, the NIWA and Tonkin and Taylor studies used different techniques to calculate extreme storm-tide levels. NIWA rationalised

---

[1] http://www.niwa.co.nz/sites/default/files/pathways_to_change_nov2011.pdf

these four studies to the common datum of 1980–99 mean sea level in Auckland Vertical datum 1946 (AVD–46) (Stephens et al. 2011c). The rationalisation study dealt only with storm-tides, and not waves, since NIWA's studies inside the Waitemata and Manukau Harbours did not consider wave setup. Since those studies, new techniques have become available to calculate the joint-probabilities (frequency–magnitude relationships) of large storm-tides and large waves occurring together, and these techniques are applied here. Previous coastal inundation studies were undertaken individually for Territorial Local Authorities, so they only covered the coastline under the individual TLA jurisdictions. The present study provides complete coverage of the entire Auckland region using recent developments in dynamic and probabilistic modelling.

NIWA's Waves And Storm Surge Prediction (WASP)[2,3] project has provided a regionally consistent set of wave and storm surge predictions, both a 40-year hindcast and projections of future climate-induced changes. The WASP project allows both the magnitude and joint-probability of storm surges and waves to be calculated, offshore of the open coast, and has been used here for open-coast locations, after cross-checking and calibrating against available tide-gauge and wave-buoy data.

Study output

Coastal extreme sea-level elevations resulting from storm-tides and wave setup were calculated for annual exceedance probabilities of 39%, 18%, 10%, 5%, 2%, 1% and 0.5% (which correspond to 2, 5, 10, 20, 50, 100 and 200-year average recurrence intervals). These elevations were calculated at intervals along the entire coastline of the Auckland region, including the major harbours (Waitemata, Manukau and Kaipara), the beaches of the east and west coasts, and inside the small east-coast estuaries.

The extreme sea-level elevations were spatially interpolated along the coastline, and intersected with a digital elevation model of the land surface produced from LiDAR, to produce inundation area maps. Inundation areas were mapped for annual exceedance probabilities of 18%, 5%, 2% and 1% (5, 20, 50 and 100-year average recurrence intervals).

The inundation levels and inundation area maps were calculated relative to AVD-46, and they include the present-day mean-sea-level offset added to AVD-46. Auckland Council requested that further inundation area maps be produced for additional sea-level rise scenarios of +1 m and +2 m above present-day mean-sea-level, added to the 1% and 2% annual exceedance probability elevations. Table 1-1 summarises the study output.

Table 1-1:   Coastal extreme sea-level elevation and inundation map outputs.

Annual exceedance probability	0.39	0.18	0.1	0.05	0.02	0.01	0.005
Average recurrence interval (years)	2	5	10	20	50	100	200
Present-day extreme sea-level elevations	✕	✕	✕	✕	✕	✕	✕
Present-day inundation maps		✕		✕	✕	✕	
+1 m SLR inundation maps					✕	✕	
+2 m SLR inundation maps					✕	✕	

The GIS inundation maps supplied to Auckland Council are the primary output of this study (e.g., Figure 8-7). This report presents tables that include the coastal extreme sea-level elevations used to generate the inundation area maps. The report also presents the data, models and methods used to calculate the extreme sea-level elevations and generate the inundation area maps.

The report is structured as follows: Section 2 presents the methods used to generate the extreme sea-level elevations and the inundation area maps; Sections 3 and 4 present location-specific information on the data and models used, and calculated extreme sea-level elevations.

2   How inundation areas were calculated and mapped

This section outlines the methods used to calculate extreme storm-tide plus wave setup elevations around the coastline of the Auckland region. It also describes the process used to convert the elevations into inundation area maps, within GIS. The method description in this section is designed to be generic. Location-specific details, such as data and models relevant to the application of these methods, are given in later sections.

2.1   Processes contributing to sea-level variability (and extreme sea levels)

Extreme sea levels in the Waitemata, Manukau and Kaipara Harbours were estimated from calculations of storm-tide elevations within the harbours, whereas extreme sea levels on the open coast were estimated from calculations of combined storm-tide plus wave setup elevations. The "open coast" is coastline located outside of sheltered harbours and estuaries, in locations subject to ocean swell. In this study we have modelled wave effects at all locations outside from harbours and estuaries, including the inner Hauraki Gulf, which is treated as open coast.

2.1.1 Sea level (excluding waves)

There are a number of meteorological and astronomical phenomena involved in the development of extreme sea level events. These processes can combine to inundate low-lying coastal margins. The processes involved are:

- Astronomical tides.

- Storm surge.

- Monthly mean sea level (MMSL), which can vary up or down over time periods of months up to decades.

- Climate-change effects including sea-level rise. Sea-level rise was considered in this study as +1 m, and +2 m above present-day mean sea level.

- Tsunami – not considered in this study.

The astronomical tides are caused by the gravitational attraction of solar-system bodies, primarily the Sun and the Earth's moon, which then propagate as forced long waves in the ocean interacting in a complex way with continental shelves. In New Zealand the astronomical tides have by far the largest influence on sea level, followed by storm surge (in most locations).

Low-pressure weather systems and/or adverse winds cause a rise in water level known as storm surge. Storm surge results from two processes: 1) low-atmospheric pressure relaxes the pressure on the ocean surface causing a temporary rise in sea-level, and 2) wind stress on the ocean surface pushes water down-wind, or alternatively, to the left of an alongshore wind (in the southern hemisphere) from a persistent wind field, piling up against any adjacent coast e.g., for the Auckland east coast, this would occur for onshore winds (from NE quadrant) and alongshore winds from SE respectively, and for the Auckland west coast, onshore winds from south-west and alongshore winds from north-west. Wind setup within

harbours varies according to the fetch present at various tide states, but at high tide can be several cm.

Storm-tide is defined as the sea-level peak reached during a storm event, from a combination of **MMSL + tide + storm surge** (see below for description of MMSL). It is the storm-tide that is primarily measured by sea-level gauges such as the Ports of Auckland Ltd gauges analysed here. Throughout this report, we refer to storm-tide as the sea-level quantity relevant to coastal inundation.

The mean sea level describes the variation of the non-tidal sea level on longer time scales ranging from a monthly basis, through an annual sea-level cycle, up to decades due to climate variability, including the effects of El Niño–Southern Oscillation (ENSO) and the Interdecadal Pacific Oscillation (IPO) patterns on sea level, winds and sea temperatures, and seasonal effects. The following bullet points describe mean sea level definitions and how mean sea level measurements were obtained from sea-level gauge records:

- Tidal harmonic analysis was used to resolve the astronomical tide from the sea-level measurement record. The tide was then subtracted to produce a non-tidal residual sea-level record.

- The non-tidal residual sea-level record was then low-pass filtered (using a wavelet filter) to remove variability with periods of less than 1 month. The remaining sea-level time-series contained only sea-level variations with periods of motion of one month or greater, and this low-frequency time-series is termed the "Monthly Mean Sea Level" (MMSL). A simple way to obtain MMSL is to remove the tidal component of sea-level variability from the sea-level record, and then average the non-tidal residual on a monthly basis.

- When MMSL is averaged over a defined time period (usually several years), the Mean Sea Level (MSL) is obtained. New Zealand's local vertical datums were obtained in this way. Auckland Vertical Datum 1946 (AVD-46) was established as the mean sea level (MSL) at Port of Auckland (Waitemata) from 7 years of sea level measurements collected in 1909, 1917–1919 and 1921–1923. MSL (AVD-46) is +1.743 m relative to tide gauge zero at Port of Auckland, which equals Chart Datum (CD) for Waitemata Harbour. Thus, for the purposes of this report, MSL is the average sea level over a defined time period. The mean sea level changes in time, due to climate variability and long-term sea-level rise. Therefore the mean sea-level offset to AVD-46 changes depending on the sea-level averaging epoch used. Sea level has risen since the years of measurements used to establish AVD-46 datum, at a long-term rate of 1.5 mm/yr at Auckland relative to the land (Auckland Regional Council 2010). Thus, the mean sea level from 1999–2008 was 1.89 m CD, which is +0.15 relative to AVD-46.

- The Mean Monthly Sea Level Anomaly (MMSLA) was obtained by detrending MMSL time-series and removing the time-series mean (mean of zero). MMSLA defines the monthly (and greater) sea-level anomaly due to climate variability such as seasonal effects, ENSO and IPO.

- All storm-tide plus wave setup and runup elevations were calculated relative to a zero MSL. Thus a MSL offset is subsequently required to relate the results to AVD-46.

Climate change will also cause acceleration in long-term trends of sea-level rise (Ministry for the Environment 2008) and could cause minor increases in the drivers (winds, barometric pressure) that produce storm surges (Mullan et al. 2011)[4].

Tidal hysteresis is an additional setup in mean sea level in harbours relative to the open coast, caused by the differential speed of the tidal wave between low and high tides in shallow harbours.

2.1.2 Wave setup and runup

Waves also raise the effective sea level at the coastline (Figure 2-1). Wave setup describes an average raised elevation of sea level when breaking waves are present. Wave runup is the maximum vertical extent of wave "up-rush" on a beach or structure above the instantaneous still water level (that would occur without waves), and thus constitutes only a short-term fluctuation in water level relative to wave setup, tidal and storm-surge time scales. Wave runup includes the wave setup component. When offshore waves are large, wave setup and runup can raise the water level at the beach substantially.

Which of wave *setup* or wave *runup* is most important to widespread inundation? Wave runup elevations are considerably higher than wave setup elevations, being about 2.5 $\times$ larger for a steep beach and about 10 $\times$ larger for a dissipative beach. The two processes are important for different reasons. Wave setup is an integral component of the total water level that potentially could cause direct inundation of coastal margins. The combined storm-tide plus wave setup level is important for large-scale inundation. The combined storm-tide plus wave runup level is important to any overtopping of dunes and seawalls, beach erosion and wave impact on seawalls. Generally, overtopping by wave runup will not cause substantial flooding, compared to more direct inundation from wave setup, but this also depends on the capacity of the drainage system behind the overtopped barrier, and the safety of vehicles and pedestrians if close to a road. For seawalls, formulae exist to calculate the number of waves overtopping in one hour, the probability of overtopping per wave, and the mean overtopping discharge that enables estimates of damage to buildings and seawalls (EurOtop 2007). Note: this approach was used for the design of the north-western motorway causeway at Waterview.

In this study, calculated extreme sea-level elevations and inundation maps include wave setup (in open-coast locations) but <u>do not include wave runup</u> elevations.

There are a number of different approaches to calculating wave setup. The Stockdon et al. (2006) formula were developed from empirical measurements made on 10 sandy beaches on USA and Netherlands coastline with different morphologies; so it is expected to be appropriate for sandy beaches along the coastline of the Auckland region. Depending on the nature of the coastline at each location, it may be more appropriate to use empirical formulae designed for gravel beaches, rock revetments or sea walls (e.g., EurOtop 2007; HR Wallingford ; Van Rijn 2010)[5]. The Stockdon et al. (2006) formula (Equation 2-1) estimates

[4] http://www.niwa.co.nz/sites/default/files/slmacc_extremewinds_slew093_may2011.pdf
[5] http://www.overtopping-manual.com/calculation_tool.html

wave setup using the offshore significant wave height[6] and wavelength and the slope of the upper beach face.

Wave setup is highly sensitive to the beach profile shape (Stephens et al. 2011b) and likewise, calculations made using the empirical wave setup equation (Equation 2-1) are also sensitive to the beach slope parameter. Thus there is considerable uncertainty around the use of empirical wave setup calculations, because beach profiles are in a constant state of evolution, and it is often difficult to pick a representative beach slope from a profile.

What beach slope should be used in the wave setup equation?

For future planning purposes, a sound approach is to use historical beach profiles where available, locate the upper beach face near the high tide mark, examine the beach slope variability and choose a relatively steep beach slope to be conservative (steep beach = larger setup). For sandy beaches the calculated wave setup is more sensitive to choice of beach slope than to calibration factors or the particular equation chosen. Choice of beach slope for this study is described in Section 7.4.

Equation 2-1: Empirical wave setup formula (Stockdon et al. 2006). H_0 = Deep-water significant wave height (m). L_0 = Deep-water wave length (m). β_s = Beach slope (m/m = dimensionless).

$$\text{Wave setup (m)} = 0.35\beta_s(H_0 L_0)^{\frac{1}{2}}$$
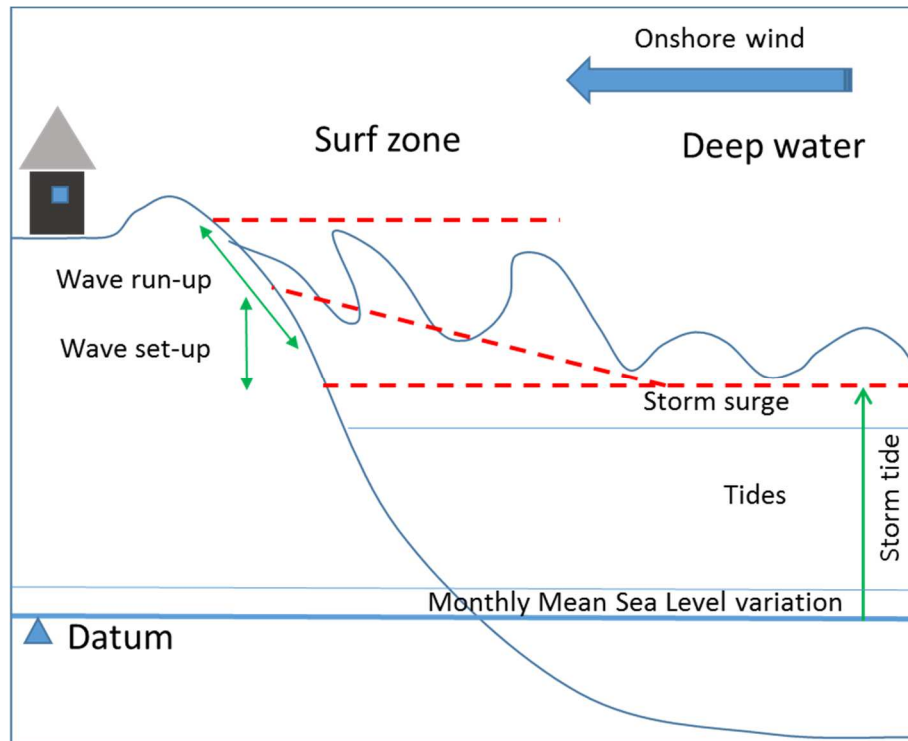
Figure 2-1: Schematic illustrating the various processes that contribute to coastal inundation.

---

[6] The average wave height of the highest 33% of waves.

2.2 Sea-level datum and mean sea level (MSL)

All data in this report are referenced relative to Auckland Vertical Datum–1946 (AVD-46), unless otherwise stated.

Before the introduction of New Zealand Vertical Datum 2009 (NZVD2009) in September 2009, land heights in New Zealand were referred to one of 13 local vertical datums, two of which are applicable to the Auckland region, being Auckland Vertical Datum–1946 and One Tree Point Datum–1964[7].

These local datums were established historically by determining mean sea level (MSL) at a tide-gauge and then transferring this level by precise levelling to benchmarks in the surrounding hinterland.

Sea level is known to vary around the coast of New Zealand and the local datums were set a different times during last century. This means that the level of MSL determined at each datum's tide-gauge will be different and that offsets will occur between adjacent datums. Also, in most cases the level of MSL for the vertical datums was determined many decades ago (apart from One Tree Point in the 1960s) and has not been officially updated since then to include the effect of sea level rise. Recent MSL values relative to these local vertical datums have been reported by Hannah and Bell (2012).

At a particular port the level of the water is expressed as a height above a local datum which is also the datum used for the depths of the sea on nautical charts, known as Chart Datum (CD). This datum is defined with reference to permanent benchmarks ashore and the zero of the tide gauge. The Chart Datum adopted usually approximates Lowest Astronomical Tide (LAT) which is the lowest tide predicted to occur under normal meteorological conditions.

Auckland Vertical Datum 1946

Auckland Vertical Datum 1946 (AVD-46) was established as the mean sea level (MSL) at Port of Auckland from 7 years of sea level measurements collected in 1909, 1917–1919 and 1921–1923 (Hannah & Bell 2012). Based on these historical measurements, the MSL for Auckland Vertical Datum-1946 (AVD-46) was set in 1946 to +1.743 m relative to the present tide gauge zero at Port of Auckland, which equals Chart Datum.[8] For the Manukau Harbour, Chart Datum at the Port of Onehunga is 2.201 m below AVD-46, being lower than the Waitemata Harbour because of the larger tide range (i.e., lower low tides).

One Tree Point Datum 1964

One Tree Point Datum-1964 (OTP-64) was established as the mean sea level (MSL) at Marsden Point from 4 years of sea level measurements collected between 1960–1963. The historic MSL set in 1964 was +1.676 m relative to local Chart Datum at Marsden Point.

Offset between datums

From the official offsets of the two local vertical datums from NZVD2009, LINZ implies that OTP-64 is 0.28 m higher than AVD-46 on average, based on several benchmarks in both local datums. There is uncertainty however, because the New Zealand geoid varies spatially, therefore it is difficult to define the offset as it depends on where it is measured, and the

---

[7] http://www.linz.govt.nz/geodetic/datums-projections-heights/vertical-datums/mean-sea-level-datums
[8] Note: prior to the present Chart Datum set in 1 Jan 1973, the old Auckland Harbour Board Chart Datum was 0.15 m lower

accuracy of past precise surveying levels. Also, the offset between local vertical datums depends on the relative accuracy between the two surveys. For example, the offset between datums at benchmark ABHL at Wellsford is 0.206 m, and in earlier research on developing a geoid model for New Zealand, Amos (2007) shows a 0.25 m offset between the two local vertical datums. Overall, OTP-64 is about 25 cm higher than AVD-46, but its exact value at any location is unknown and could differ by about ± 4 cm. Note: a progressive move towards using NZVD2009 for land elevations will eventually eliminate these cross-boundary issues with the offsets between adjoining local vertical datums. NZVD2009 is based on a New Zealand-wide geoid model – the geoid varies spatially. We have adopted a +0.25 m offset (OTP-64 = AVD-46 + 0.25 m) for this study. The estimated ±4 cm uncertainty is not significant in the comparison of extreme sea levels between coasts.

2.2.1 Defining present mean sea level

The aforementioned local vertical datums were established from the mean sea level, averaged over several years during different historical periods. Sea level has risen since the AVD-46 datum was established, at a long-term rate of 1.5 mm/yr at Auckland relative to the land (Auckland Regional Council 2010). Thus, mean sea level is now higher than when the local vertical datum were established. The OTP-64 datum is somewhat of an anomaly as present MSL is still below the OTP-64 datum zero at Marsden Point (partly due to the short record used from the 1960s and the way it was defined – not known).

To define MSL in the Auckland region, we need to calculate recent MSL by averaging modern sea-level gauge records, referenced to local vertical datum, as shown in Table 2-1. These tide-gauges are all surveyed to local vertical datum. For an exact comparison, the averaging periods used in Table 2-1 should be identical. We were reliant on quality-assured data that was available and so the averaging periods are a little different, but are mostly post-2001, whereas the two local vertical datums were set several decades earlier. Small (± 1 cm) uncertainties introduced from using slightly different averaging periods are insignificant for the purposes of establishing extreme sea-level inundation area maps.

Table 2-1:   Sea-level gauges with known offsets to local vertical datum used in this study.
Shown in italics is a MSL derived from Hannah and Bell (2012)* for a longer half nodal-tide period (10 years) which confirms the Auckland value. The local gauge-zero level for Pouto Point was obtained from Northland Regional Council (Dale Hansen, pers. com.); a corrected MSL offset (explained in the text) is also given.

Sea-level gauge location	Local vertical datum	Chart Datum (or gauge zero)	Mean sea level	Averaging period
Auckland	AVD-46	-1.743 (AVD-46)	+0.15 m (AVD-46)	2006–2011
			+0.15 m (AVD–46)	*1999–2008*
Marsden Point	OTP-64	-1.676 (OTP-64)	-0.09 m (OTP-64)	2001–2011
Onehunga	AVD-46	-2.201 (AVD-46)	+0.22 m (AVD-46)	2001–2009
Pouto Point	OTP-64	-1.687 (OTP-64)	+0.16 m (OTP-64)	2001–2011
			-0.02 m (OTP-64)	*Corrected*

The sea-level records and their associated assigned datum level indicate that mean sea level in the Kaipara Harbour at Pouto Point is about 26 cm higher than at Auckland (Waitemata) and 19 cm higher than at Port Onehunga (Manukau). The Pouto Point level is higher than we

would expect from tidal shoaling theory, and we suspect that the Pouto Point gauge level offset may need re-surveying. The Pouto Point gauge was buried by a sand wave in about September 2012, so at the time of writing it is not possible to re-survey the gauge offset. The gauge zero for the sea-level gauge that NIWA operated at Anawhata (now closed) is also likely to be inaccurate (appears to be lower than expected) due to the open-coast wave environment which makes it difficult to establish a datum without the use of a tide-board[9]. Thus we have lower confidence in the mean sea-level offsets for the Kaipara Harbour and the open west coast of the Auckland region.

The mean sea level for the open west coast was derived by subtracting 6 cm of tidal hysteresis from the mean sea level at the Onehunga sea-level gauge. Bell et al. (1998) calculated a rise in the mean tide level between the harbour entrance (Paratutae Island) and Onehunga Wharf of 4.5 cm using an M_2 tidal harmonic hydrodynamic model simulation, which is similar to an estimate of 6 cm derived from survey measurements (Tonkin & Taylor Ltd 1986).

Given our uncertainty in the levelling of the Pouto Point tide gauge, the mean sea level for the Kaipara Harbour was derived as follows. A hydrodynamic model of the Kaipara Harbour was used to calculate an approximate tidal hysteresis rate, giving an expected tidal hysteresis rise from Pouto Point to Ruawai of +0.083 m. An archived 1969–74 sea-level record from Ruawai (northern Kaipara Harbour) with known datum levelling (not shown), suggests Ruawai mean sea level is about +0.1 ±0.045 mm OTP-64 after accounting for sea-level rise of +0.15 mm/yr in the intervening period. This suggests Pouto Point MSL ≈ OTP-64, rather than +0.16 m as shown in Table 2-1 (which is very high relative to MSL at Auckland). MSL at Onehunga is +0.22 m AVD-46, with tidal hysteresis of 6 cm to entrance (Bell et al. 1998), that suggests +0.16 m AVD-46 for open west coast. The expected tidal hysteresis from open coast to Pouto Point (based on hydrodynamic model of upper harbour, but through larger entrance) is 7 cm. So Pouto Point MSL expected to be about +0.23 AVD-46, or similar to Onehunga, which makes sense dynamically. This is also similar to the 25 cm OTP-64 to AVD-46 offset. In conclusion, for the purposes of this study we estimate that the present-day mean sea-level offset from AVD-46 is +0.23 m at Pouto Point, and -0.02 m from OTP-64 (Table 2-1).

Table 2-2 gives the mean sea-level offsets to AVD-46 that were used in this study, based on the averaging epochs given in Table 2-1. For the purposes of this study, the values in Table 2-2 are taken as representative of "present-day" mean sea level.

Table 2-2:   Mean sea-level offsets to AVD-46 datum used in this study, at several locations in the Auckland region.

Location	Mean sea-level offset relative to AVD-46
Waitemata Harbour at Port of Auckland	+ 0.15 m
Open east coast	+ 0.15 m
Kaipara Harbour at Pouto Point	+ 0.23 m
Manukau Harbour at Onehunga	+ 0.22 m
Open west coast	+ 0.16 m

---

[9] A tide-board is a vertical ruler placed alongside a tide-gauge and surveyed to datum. The tide-gauge is calibrated against visual observations of sea level elevation relative to the tide-board.

2.3   How extreme sea-levels were calculated – overview

This section gives an overview of the calculation of extreme sea-levels around the Auckland coastline. This overview is designed to enable the reader to understand what was done and why, with a minimum of technical detail. Details are provided in Appendix A.

Extreme sea levels are, by definition, rare events. Only by observing a system for a long period of time can an understanding of the frequency and magnitude of extreme sea levels be attained. For the calculation of extreme sea levels, a sea-level record would ideally meet the following criteria:

- Sea-level gauge surveyed to datum.

- Accurate: no long-term drift or sensor subsidence, no siltation or blockage of the gauge. Known tectonic movement or subsidence at gauge site.

- ≥ 50-years length to incorporate approximately two IPO and multiple ENSO climate variability cycles.

- Sample at least hourly to capture storm tide peak.

- Include all extreme sea-levels that occurred (no data gaps at crucial times).

Because this is generally not the case, techniques have been developed to overcome the lack of long term records and calculate extreme events from shorter records. The method used for this project is the Monte Carlo joint-probability (MCJP) technique (Goring et al. 2010), which is explained further in Section 7.2.3. This method makes best use of short but regularly sampled (e.g., hourly or better) data records.

The MCJP method uses component parts of storm-tide: tide, storm surge and MMSLA, by assuming they are independent and reassembling them into a storm-tide sequence. Therefore, for each location where extreme storm-tides are required, we need to first obtain time-series for each of the three sea-level components, tide, storm surge and MMSLA.

Tide-gauge records at Ports of Auckland Ltd, Port of Onehunga, Pouto Point and Anawhata provide the required data within the Waitemata, Manukau and Kaipara Harbours, and the open west coast. These gauge records are crucial to the study because they allow extreme sea-level analyses to be made that are founded on actual sea-level measurements. These are then used to validate extreme sea-level estimates based on modelled data.

Extreme sea-level estimates are needed throughout the Auckland region, not just at the tide-gauge locations. Extreme sea-levels change with location as the tide, storm surges, MMSLA and wave setup all interact in different ways with the local environment such as the underwater bathymetry, topographic constriction, and wind and wave exposure.

Numerical hydrodynamic models, calibrated against sea-level measurements, were used to simulate tides, storm surges and wave setup at locations around the Auckland region. Extreme sea-levels were then modelled from the simulated time-series, at "model-output locations" around the coastline.

Sea-level components were calculated differently for locations in three different regions: the major harbours Waitemata, Manukau and Kaipara – which each have at least one sea level

---

gauge for validation; the open coast; and the minor harbours/estuaries. This is because of the different physical environment between the open coast and the harbours, and the need to deal with multiple small estuaries in an efficient way.

Open coast sites occasionally experience high wave energy as well as large storm-tides, so joint-probability methods were used to calculate the combined likelihood of large waves and storm-tides occurring simultaneously. The joint-probability method accounts for any dependence between waves and storm tide.

2.3.1 Major harbours

The following steps were used to calculate extreme sea-levels inside the Waitemata, Manukau and Kaipara Harbours:

- Tide-gauge data was decomposed into sea-level components: tide, storm-surge and MMSLA.

- Extreme sea levels were calculated from measured sea-level components at tide gauge sites.

- For model output locations away from tide gauge sites, time-series of sea-level components were simulated using hydrodynamic models, as follows:

  - *Tides* were simulated for a full lunar cycle (1-month). From this, scaling relationships were developed between the tide at the tide-gauge site and those at the model-output locations. Tides were predicted at the tide-gauge site (from tidal harmonic analysis) for > 45 years, to match available meteorological records, used for winds (see next bullet). The spatial scaling relationships from the 1-month tidal simulation were applied to the predicted tide-gauge time-series to simulate tidal time-series at the model-output locations.

  - The *wind-driven* component of *storm-surge* was simulated by matching the > 45-year meteorological records (1965–2011 for Waitemata and Manukau; 1960–2010 for Kaipara) to a wind setup response matrix, for each model-output location. The wind setup response matrices were created using hydrodynamic models to simulate wind setup along different fetches from a variety of wind speeds and directions. The wind response was simulated at high spring tide, when fetch is maximum.

  - The *inverse-barometer* component of *storm-surge* from low-pressure weather systems was calculated from the barometric pressure record, by applying Equation 7-1 (Section 7.3.1).

  - *MMSLA* was taken directly from the tide-gauge record, and assumed to be of uniform magnitude throughout the harbour. The MMSLA record does not need to match in time the simulated tide and storm-surge, because the cumulative distribution function of MMSLA is used in the MCJP extreme sea-level technique. MMSLA generally follows a normal (Gaussian) distribution above and below MSL.

– Tidal hysteresis relative to the tide-gauge location was calculated for all model-output locations, using the 1-month tidal simulation.

2.3.2 Open Coast

The following steps were used to calculate extreme sea-levels along the open coastlines of the Auckland region:

- Time-series of storm surge, tides and waves were extracted directly from WASP model simulations, for the 30-year hindcast period 1970–2000. For the east coast (Hauraki Gulf) where there are several islands, a SWAN wave model was used to transform the WASP offshore wave time-series (from the northern Gulf region) inshore to the coast.

- Storm-tide and wave height and period statistics were combined in a joint probability analysis, for each model-output location.

- Beach profile data were examined to establish a representative beach slope with which to calculate wave setup, using Equation 2-1.

- The maximum storm-tide plus wave setup elevation was calculated for various annual exceedance probabilities, at each model-output location.

The WASP programme was intended to provide long term time-series and statistics for both waves and storm surge around the New Zealand, based on (30 years or more) numerical simulations of historic conditions ('hindcasts'), as well as of conditions expected towards the end of this century ('projections') based on expected climate change. Results of the WASP modelling project are available at http://wrenz.niwa.co.nz/webmodel/coastal.

2.3.3 Small east-coast harbours and estuaries

Storm-tide elevations in the numerous relatively small east-coast harbours and estuaries were calculated as follows:

- The maximum storm-tide plus wave setup elevations calculated for the open east coast were applied to the harbour entrances.

- The storm-tide component is expected to amplify inside the harbours. An amplification factor that increased with distance from the harbour entrance was applied to the storm-tide component.

The applied amplification rate, in lieu of tidal height measurements inside these harbours, was equivalent to the tidal amplification between the Ports of Auckland Ltd and Salthouse Jetty (Lucas Creek) gauges in the Waitemata Harbour, being 4.2 mm of elevation per km of horizontal distance. There remains uncertainty in the amplification rates used for the smaller estuaries that have no sea-level records. The wave setup component at the entrance was assumed to translate inside the estuary without dissipation, so was added to the amplified storm tide elevations inside the estuary.

2.4 Inundation mapping

Inundation maps were created within GIS, for the scenarios outlined in Table 1-1. Extreme sea-level elevations from the sea-level modelling were input to GIS at model-output locations around the Auckland coastline. These were interpolated along the coastline and intersected with a digital elevation model of the land topography, to create GIS polygons that map the areas where extreme sea-level was higher than land level. For low-lying land areas that were not connected to the sea by rivers or drains, the "inundation" areas were removed from the maps. The GIS inundation mapping process is described, using examples, in Section 8.

The major assumption in the GIS mapping procedure was the use of a "bathtub" flooding approach, whereby every land area below the extreme sea-level is mapped as instantly flooded in its entirety. In reality, the peak of a storm-tide only lasts for about 1–2 hours centred around high tide, and this may not be enough time to flood a large area of the wider hinterland if the flow rate of the storm-tide is restricted by a narrow connection to the sea.

An example of this occurred at the Waitemata Golf Course near the suburb of Narrowneck, during the 23 January 2011 storm-tide, which is the highest storm-tide on record in the Waitemata Harbour. The modelled present-day 0.01 AEP extreme sea-level elevation closely matched the extreme sea-levels that were both simulated and measured during the 23 January 2011 storm-tide. The modelling agreed with observations of storm-tide breaching Lake Road into the golf course. However, whereas the bathtub mapping procedure predicted the entire golf course was inundated due to that breach, the storm-tide actually flowed over Lake Road for only an hour or so at the peak of the tide, and this did not cause substantial inundation in the golf course. In this instance, the present-day 0.01 AEP inundation map was hand-edited to remove excess flooding in the golf course.

The bathtub inundation mapping approach is conservative in that it tends to over-predict rather than under-predict inundation by storm-tides, although can be tempered by delays in inundation subsiding if drainage to the sea is inadequate. The bathtub mapping approach is best-suited to locations where the topography rises approximately continuously with distance from the coast, and without large low-lying areas behind coastal barriers. This is the case for most parts of Auckland city.

3 Extreme sea levels in the Waitemata, Manukau and Kaipara Harbours

In this section we provide location-specific information, such as data and models, required to explain how the methods from Section 2 and Appendix A (Section 7.3) were applied in the Waitemata, Manukau and Kaipara Harbours.

3.1 Waitemata Harbour

3.1.1 Tide-gauge analysis

Figure 3-1 plots the most up-to-date quality-analysed sea-level record for the Ports of Auckland Ltd gauge. This hourly sea-level record was digitised from archived records and has undergone considerable quality analysis as part of three studies of long-term sea-level rise in New Zealand (Hannah 1990; Hannah 2004; Hannah & Bell 2012), and has recently become available for analysis in this study. It provides an excellent record for extreme-sea-level analysis using direct extreme-value techniques (Table 7-4).

Two examples of the decomposition of the sea-level record are shown for 2006–2011 (Figure 3-2) and for the large (~0.6 m) storm surge that peaked on 26 July 2008 (Figure 3-3).

Previous extreme sea-level analyses conducted by Stephens et al. (2011c) used a digital sea-level record from 1974–May 2011, supplemented by a graph of annual maxima from 1925 onward from Auckland Harbour Board records (Auckland Harbour Board 1974). Subtle differences in the processing of the datasets has led to differences, generally of ±1 cm in the elevations of sea-level maxima between the two records, which are insignificant for the extreme sea-level analyses. Of more importance to the extreme sea-level analysis is the length and coverage of the dataset. We consider the following extreme sea-level analyses to be more robust than those of Stephens et al. (2011c) owing to longer and more complete record used here.
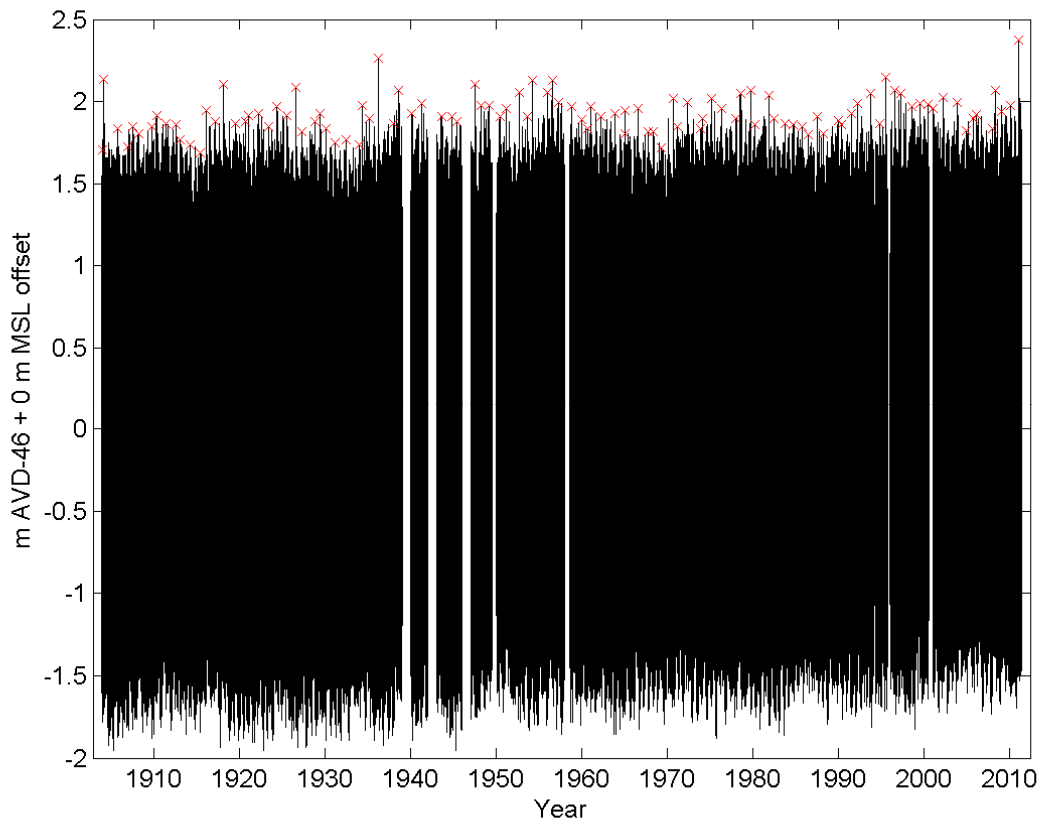
Figure 3-1: Ports of Auckland hourly sea-level record 26 Oct 1903 – 31 May 2012. Data is relative to AVD-46, with no (0 m) mean-sea-level offset applied. Crosses mark annual maxima.
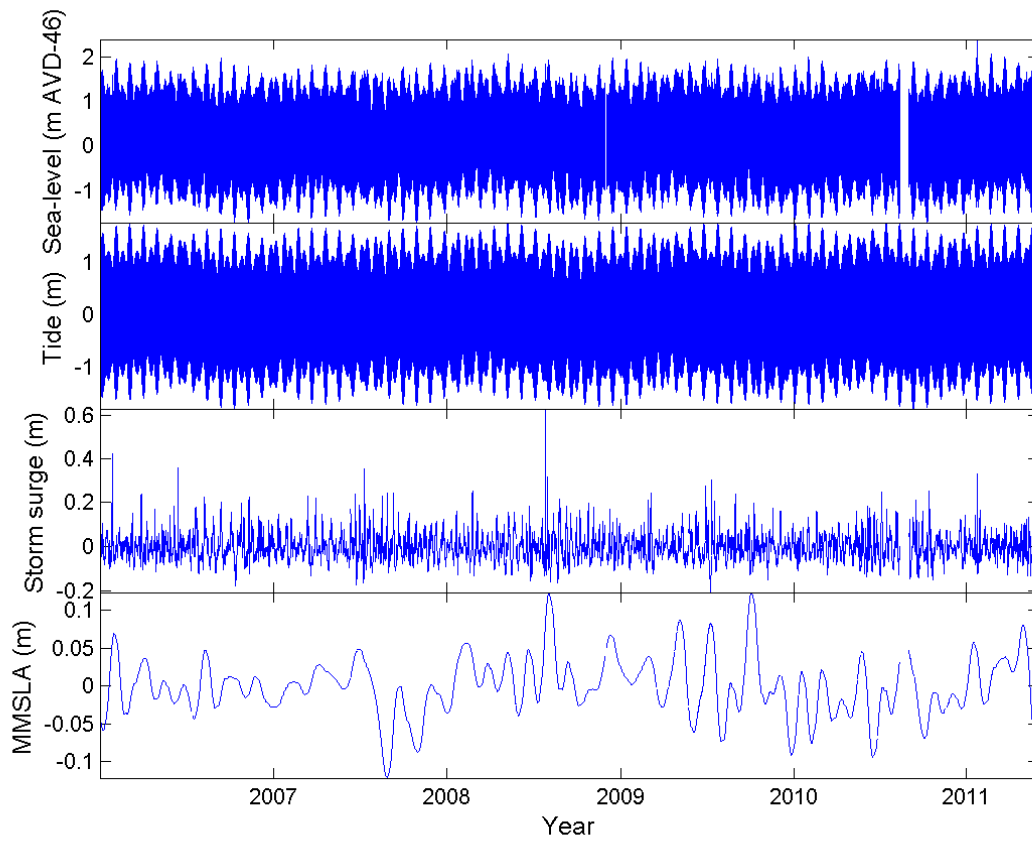
Figure 3-2: Decomposed Ports of Auckland Ltd tide-gauge sea-level record 2006–2011.
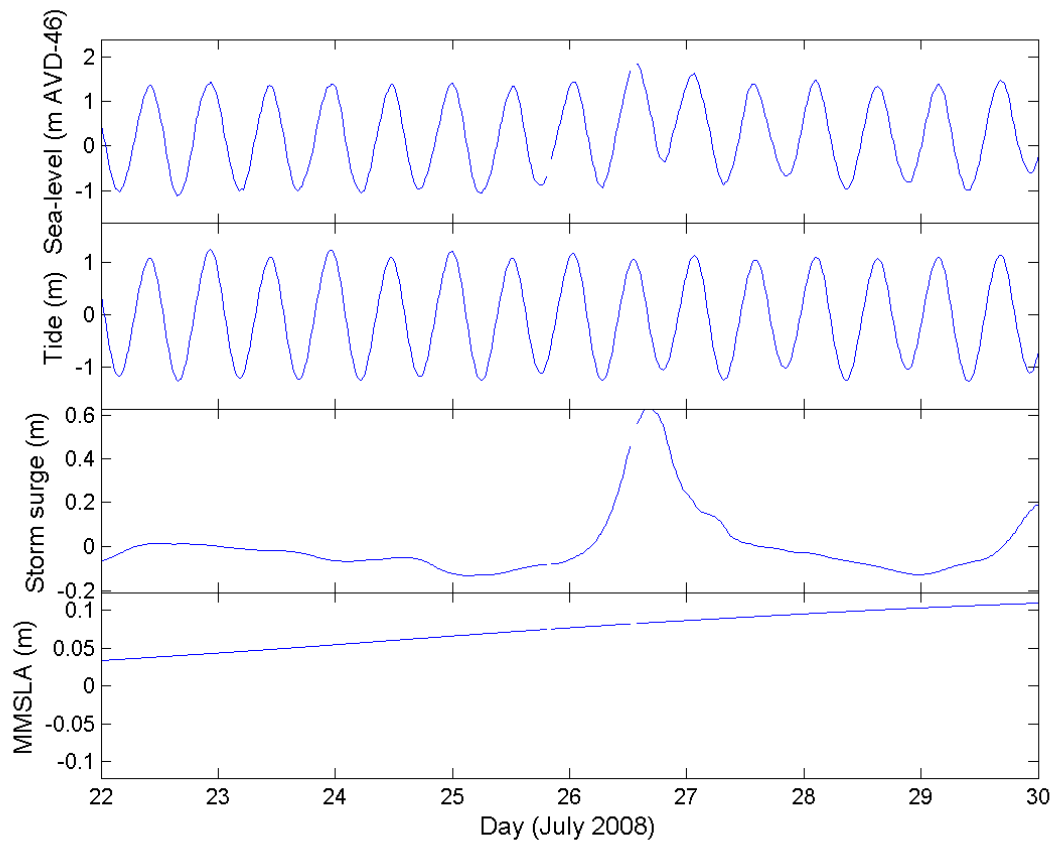
Figure 3-3: Decomposed Ports of Auckland Ltd tide-gauge sea-level record, 26 July 2008 storm surge.

Before undertaking extreme sea-level analyses, the raw sea-level time-series was detrended by removing a linear long-term sea-level rise trend of 1.5 mm/year (Hannah & Bell 2012). This was done using 2004 (1999–2008) as the pivot year, to make subsequent extreme-value analyses relative to present-day (1999–2008) MSL = +0.15 m AVD-46 (Table 2-1).

Table 3-1 shows the ten largest sea-level annual maxima, with their rank based on the de-trended sea-level time-series. This differs from Table 2-3 of Stephens et al. (2011c) owing to the more complete record available here. Interestingly, the large storm-surge event of 26 July 2008 (Figure 3-3) doesn't appear in the top-ten list of storm-tides because it only coincided with an average tide.

Table 3-1:   Ten largest sea-level annual maxima at Port of Auckland, in descending order.
Elevations are specified in AVD-46. Detrended annual maxima have been adjusted using a linear
long-term sea-level rise rate of 1.5 mm/year (Hannah & Bell 2012). Annual exceedance probabilities
(AEP) are provided by interpolating the event magnitudes onto the three extreme-sea-level curves
shown in Figure 3-4, using the Monte-Carlo joint-probability technique (MCJP), generalised Pareto
distribution (GPD) and generalised extreme-value distribution (GEV). These data differ by ±1 cm from
Table 2-3 of Stephens et al. (2011c) due to subtle differences in the processing of the datasets.

Year	Raw sea level (m AVD-46)	Detrended sea level (1.5 mm/year), adjusted to present-day MSL = +0.15 m AVD-46	AEP (MCJP)	AEP (GPD)	AEP (GEV)
23-Jan-11	2.38	2.41	0.007	0.008	0.005
26-Mar-36	2.27	2.41	0.006	0.008	0.005
14-Jul-95	2.15	2.20	0.069	0.079	0.083
4-Feb-04	2.14	2.33	0.018	0.019	0.018
7-Mar-54	2.13	2.25	0.044	0.048	0.053
14-Jul-56	2.13	2.24	0.045	0.05	0.054
14-Feb-18	2.11	2.28	0.03	0.037	0.037
20-Jun-47	2.11	2.24	0.049	0.056	0.06
11-Jul-26	2.09	2.25	0.044	0.048	0.052
27-Jul-38	2.07	2.21	0.069	0.078	0.083

Figure 3-4 shows results of three extreme sea-level analyses based on the Port of Auckland
gauge measurements. The peaks-over-threshold (POT) data are plotted using their
Gringorten (1963) plotting positions. If the empirical distribution of the data exactly matched
the Gumbel extreme-value distribution (similar to the GEV and GPD distributions), then they
would form a straight line when plotted in their Gringorten plotting positions. The GPD and
GEV distributions were fitted following (Coles 2001) using the *extRemes* software in *R*
(Stephenson & Gilleland 2006). A 1.915 m (AVD-46) threshold was used for the POT data,
selected using *extRemes* analysis tools. The MCJP technique was applied by Stephens et al.
(2011c) using data from only 2006–2011. A longer dataset from 1970–2000 was analysed in
this study to produce a storm surge comparison with the WASP storm surge hindcast for the
same time period. The inclusion of additional years of storm surge annual maxima makes the
MCJP more robust than the analysis by Stephens et al. (2011c) that used only 2006–2011
data.

The three techniques give similar results (Figure 3-4). The average recurrence interval for
the January 2011 event lies between 126 and 205 years, depending on the method used. It
is worth noting that the difference between a 100-year and a 200-year ARI event is only
6 cm, due to the rather flat extreme sea-level distribution. Thus small differences in the
extreme-value curves make considerable differences to the frequency estimates for these
large events. This illustrates that extreme-value modelling is not a precise science, and the
occurrence likelihoods for these large events are not precise estimates. However, the use of
a very robust dataset, three extreme sea-level modelling techniques, and the degree of
agreement between the models, provides confidence in the estimates.

The March 1936 storm-tide has a similar magnitude and exceedance probability to the 2011
event after removal of the sea-level trend. Following the Gringorten (1963) plotting position,

the 1936 event plots as a large outlier compared to the extreme sea-level models. This illustrates that if the empirical distribution of the annual maxima approximately conforms to an extreme-value distribution, then we would not expect to see, on average, two events as large as the 1936 and 2011 events within the 108-year observation period. This illustrates the concept that although the average recurrence interval (over a very long timeframe) might be considerable between the largest events, there is a (small) probability of more than one large storm-tide occurring at close intervals, as tides and storm surges randomly combine. The term annual exceedance probability conveys that (small) likelihood.
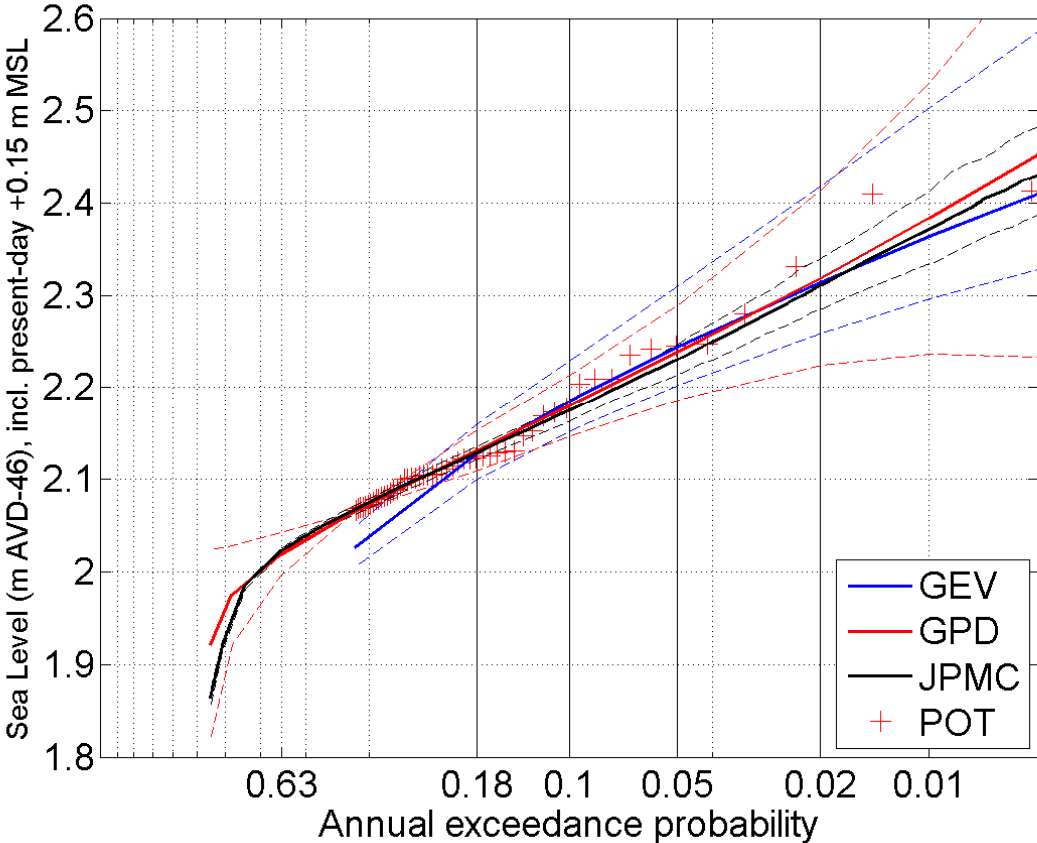
Figure 3-4: Extreme sea-level curves using Port of Auckland tide-gauge data. Three techniques were used: the Monte-Carlo joint-probability technique (MCJP), generalised Pareto distribution (GPD) fitted to peaks-over-threshold (POT) data and generalised extreme-value distribution (GEV) fitted to annual maxima (AM). Bold lines indicate central fit, dashed lines indicate 95% confidence intervals. The POT data have also been plotted using Gringorten (1963) plotting positions. Elevations are relative to AVD-46 including +0.15 m offset for baseline mean sea level (present-day estimate).

The extreme sea-level elevations from the three extreme sea-level models are given in Table 3-2. Elevations are specified relative to AVD-46 and include a +0.15 m offset for present-day MSL (Table 2-1).

Table 3-2:   Extreme sea-level at Port of Auckland tide-gauge.   Elevations are relative to AVD-46 including +0.15 m offset for baseline mean sea level (present-day estimate).

AEP	ARI	MCJP			POT/GPD			AM/GEV		
		Median	Lower 95th C.I.	Upper 95th C.I.	Median	Lower 95th C.I.	Upper 95th C.I.	Median	Lower 95th C.I.	Upper 95th C.I.
0.39	2	2.07	2.06	2.07	2.07	2.07	2.07	2.03	2	2.05
0.18	5	2.13	2.12	2.14	2.13	2.11	2.15	2.13	2.1	2.16
0.10	10	2.18	2.17	2.19	2.18	2.15	2.22	2.19	2.16	2.23
0.05	20	2.23	2.22	2.25	2.24	2.19	2.29	2.25	2.2	2.31
0.02	50	2.31	2.29	2.34	2.32	2.22	2.41	2.31	2.26	2.42
0.01	100	2.37	2.33	2.41	2.38	2.24	2.53	2.36	2.3	2.5
0.005	200	2.43	2.38	2.48	2.45	2.23	2.67	2.41	2.33	2.59

3.1.2 Hydrodynamic model

Simulations of tide and the wind-driven component of storm surge were undertaken using the DHI MIKE 3 FM modelling suite. The hydrodynamic model domain for the Waitemata Harbour is shown in Figure 3-5. This model was originally developed and calibrated as part of the Central Waitemata Contaminant Study (Oldman et al. 2007). The model was calibrated against sea-level measurements located at the entrance to the upper Waitemata, in the upper Whau River, the approach to the Whau River, the middle Waitemata, Shoal Bay and Watchman Island. The model closely reproduced the tidal wave at all sites, demonstrating accurate representation of tidal wave shoaling and amplification.

Tidal simulations for a full lunar month were forced at the open boundary using NIWA's New Zealand regional tide model (Stanton et al. 2001; Walters et al. 2001). The Waitemata Harbour model was also forced with winds of various speeds and directions to create wind response matrices. These results were used as discussed in Section 2.3.1.

A simulation of the 23 Jan 2011 storm-tide was forced at the open boundary using Port of Auckland tide gauge measurements with an appropriate phase-lag applied. Simulated storm-tide elevations on the 23 Jan 2011 were compared to predicted 100-year ARI storm-tide levels.
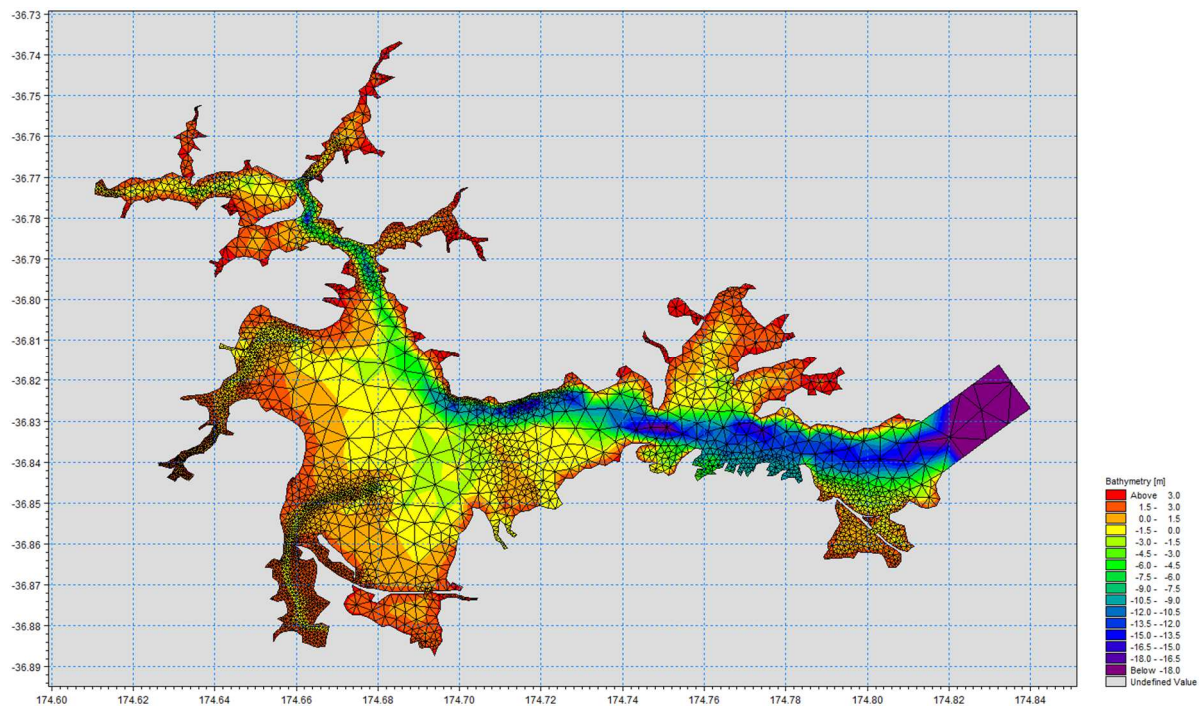
Figure 3-5: Waitemata Harbour MIKE-3 FM hydrodynamic model grid (Oldman et al. 2007).
Note: idealised channel created for eastern boundary condition.

3.1.3 Modelling storm surge

The Auckland Airport (located adjacent to the Manukau Harbour) wind and mean sea-level pressure records were obtained from 8 Nov 1965 – 11 May 2011. The isthmus between the Manukau and Waitemata Harbours is relatively flat so the airport weather station (located adjacent to the Manukau Harbour) should reasonably approximate the wind field in both Harbours. The wind-driven component of storm surge was calculated as described in Section 7.3 by using the wind record to interpolate storm surge from the simulated wind-surge response matrix from the hydrodynamic model. The wind-driven component of storm surge differs depending on the output location within the harbour due to the available wind fetch.

The inverse-barometer component of sea level arising from low-pressure weather systems was calculated as described in Section 7.3.1.

3.1.4 Modelling storm-tide

Storm-tide time-series were simulated using the methods described in Sections 2.3.1 and 7.3, at 114 locations within the Waitemata Harbour (Figure XX), for later extreme sea-level analysis.

The three sea-level components required for extreme sea-level analysis are tide + storm surge + monthly mean sea-level anomaly (MMSLA). The tide and storm surge are affected by harbour geography, but MMSLA is a slowly varying sea-level component that we assumed to be ubiquitous throughout the harbour. Simulated storm-tide time-series consisted of tide plus storm surge. A time-series of MMSLA derived from the Port of Auckland tide gauge was used in the Monte Carlo joint-probability extreme sea-level modelling. For each model-output location the tidal time-series, the storm surge time-series, and MMSLA time-series were input to the MCJP extreme sea-level analysis.

Tidal hysteresis was calculated from the hydrodynamic model using the mean sea-level over the simulated lunar month; enabling a mean-sea-level offset to be calculated for each location, relative to the Port of Auckland tide-gauge location. This mean sea-level offset due to tidal hysteresis was added to the extreme storm-tide distribution at each output location.

Figure 3-7 compares the extreme sea-level frequency–magnitude distributions derived from the Port of Auckland gauge data (Figure 3-1, Figure 3-4), and from simulated data at the gauge site, and, for comparison, at selected sites located further toward the upper Waitemata Harbour. Using the IB_{factor} as a calibration parameter (Section 7.3.1), the extreme sea-level distributions from both measured and simulated data were closely matched at the Port of Auckland tide-gauge site. The other curves demonstrate how the simulated extreme sea-level magnitudes magnify toward the estuary head, due to amplification of the tide and storm surge. Extreme storm-tide elevations for 114 locations in the Waitemata Harbour are presented in Table 3-3.
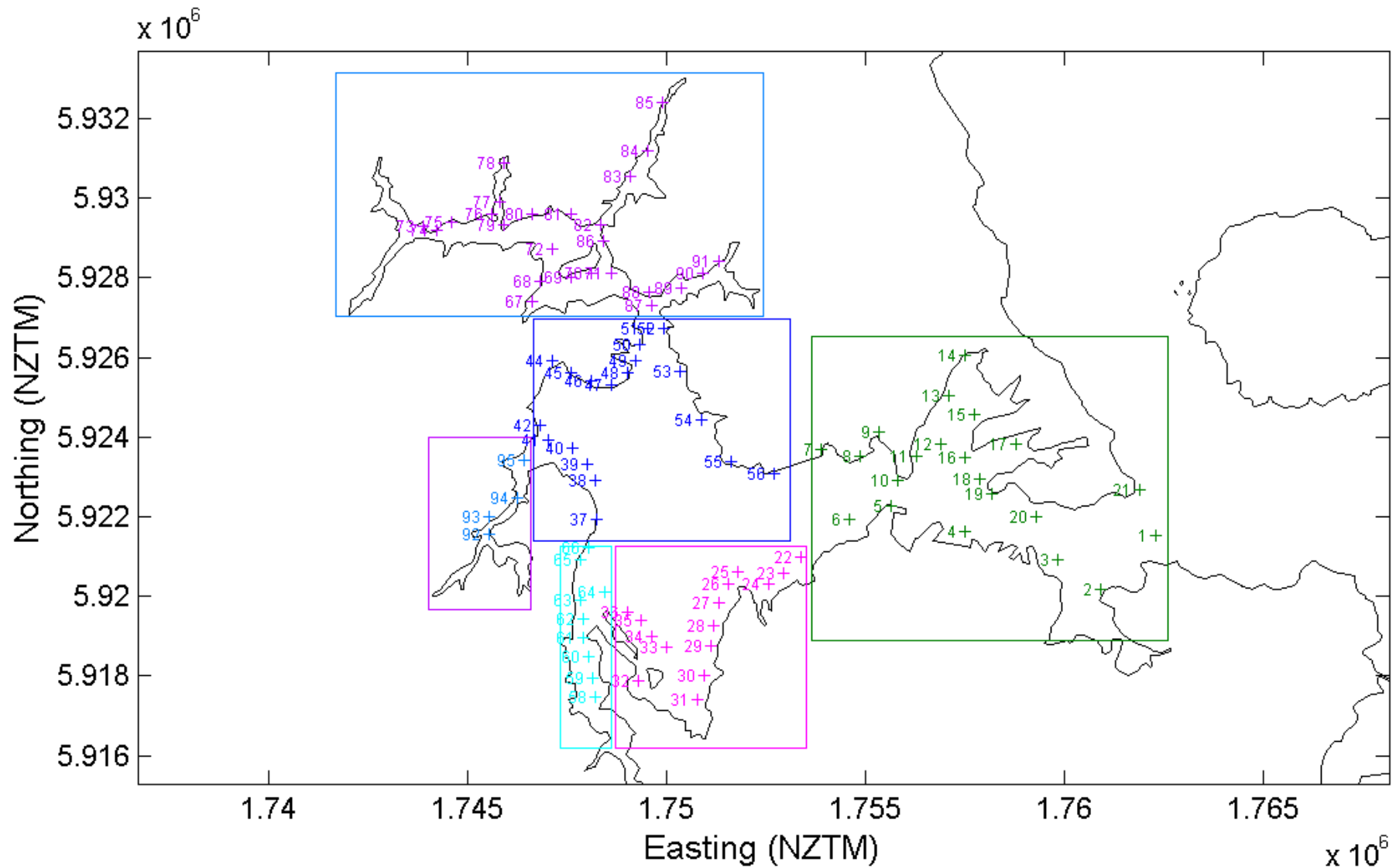
Figure 3-6: Locations of extreme storm-tide predictions in the Waitemata Harbour. Colour-coding corresponds to Table 3-3.

Coastal inundation by storm-tides and waves in the Auckland region
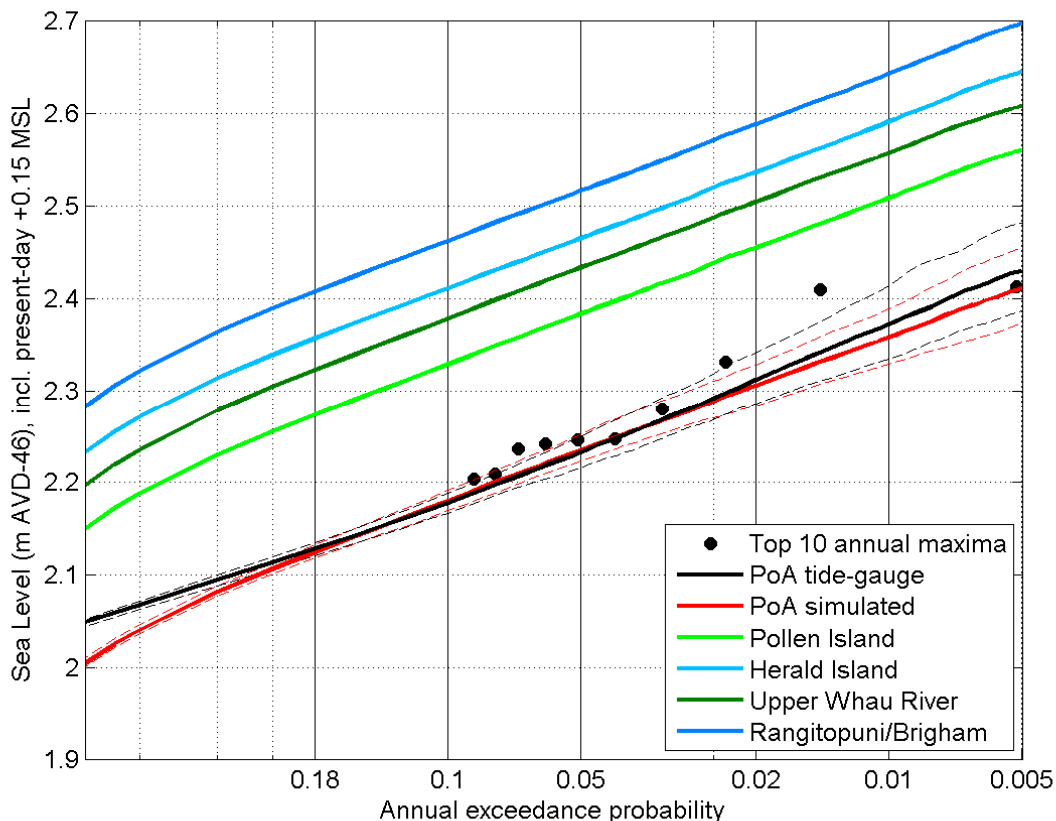
Figure 3-7: Simulated extreme storm-tide frequency-magnitude distributions in the Waitemata Harbour. Largest 10 annual maxima (Table 3-1) plotted in Gringorten plotting positions (rate of 10 events in 108-years). A selection of output locations plotted for comparison with Port of Auckland tide-gauge site. Elevations are relative to AVD-46 including +0.15 m offset for baseline mean sea level (present-day estimate).

Figure 3-8 and Figure 3-9 compare the simulated 100-year ARI storm-tide elevations to the simulation of the 23 January 2011 storm-tide. From extreme sea-level analyses at the Port of Auckland tide-gauge location we estimate that the average recurrence interval for the 23 January 2011 storm-tide was 88–205 years, and so the simulated elevations for 23 January 2011 are expected to lie close to, or a few cm above, the predicted 100-year ARI storm-tide levels (Figure 3-4). Figure 3-9 shows that this is generally the case at most locations throughout the harbour. The most noticeable discrepancy occurs at the three sites located behind the north-western motorway causeway near Pollen Island, where the 23 January 2011 storm-tide simulation is 17 cm above the predicted 100-year ARI levels. The bathymetric resolution of causeway channel in the hydrodynamic model was insufficient to correctly transfer tidal flow (on which the 100-year ARI elevations are based), whereas the combined influence of tide plus storm surge in the 23 January storm-tide simulation was sufficiently high to overcome this limitation in the simulation.

Further validation of the model was provided by the comparison of the simulated present-day 0.01 AEP inundation elevations and maps, against observed flooding during the 2011 storm-tide (Figure 8-9 – Figure 8-15).
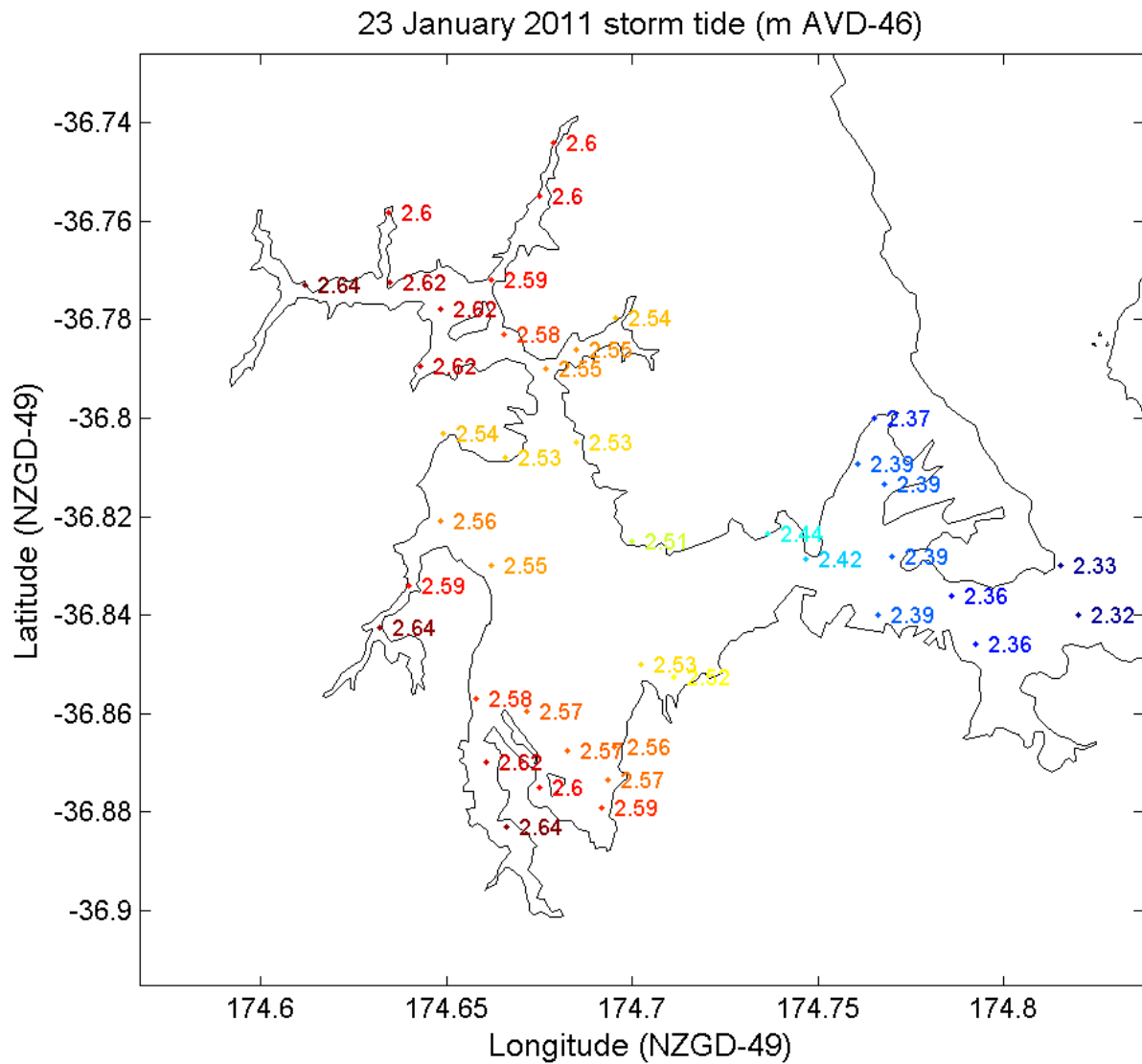
Figure 3-8: Storm-tide elevations in the Waitemata Harbour, simulated for 23 January 2011 storm-tide.   Elevations are relative to AVD-46 and include +0.15 m (present-day) offset for baseline mean-sea-level rise.
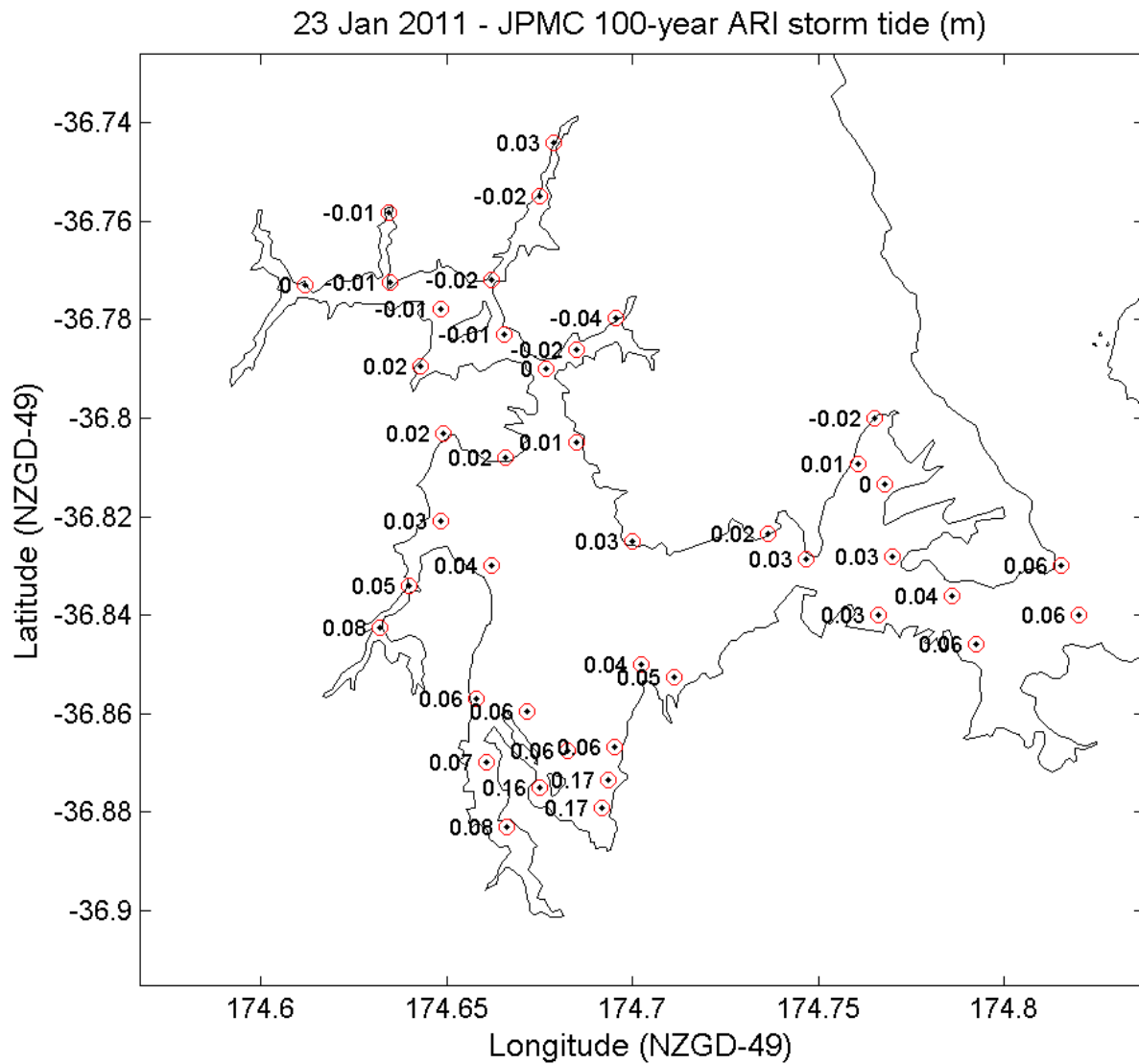
Figure 3-9: Elevation difference (cm) between 23 January 2011 storm-tide simulations and 100-year ARI estimates in the Waitemata Harbour. Positive values = 23 January 2011 storm-tide is above 100-year ARI storm-tide estimate, and vice versa.

**Table 3-3: Extreme sea-level in the Waitemata Harbour.** Elevations are relative to AVD-46 including +0.15 m offset for baseline mean sea level (present-day estimate). Elevations calculated from simulated data. Colour-coding corresponds to Figure 3-6.

Site	Easting (NZTM)	Northing (NZTM)	AEP: 0.39 ARI: 2 yr	AEP: 0.18 ARI: 5 yr	AEP: 0.1 ARI: 10 yr	AEP: 0.05 ARI: 20 yr	AEP: 0.02 ARI: 50 yr	AEP: 0.01 ARI: 100 yr	AEP: 0.005 ARI: 200 yr
1	1762303	5921531	1.94	2.03	2.08	2.14	2.21	2.26	2.31
2	1760922	5920192	1.98	2.06	2.12	2.17	2.24	2.30	2.35
3	1759830	5920934	1.99	2.07	2.13	2.18	2.25	2.30	2.35
4	1757487	5921632	2.04	2.12	2.18	2.23	2.31	2.36	2.41
5	1755640	5922256	2.08	2.16	2.22	2.27	2.34	2.40	2.45
6	1754603	5921918	2.11	2.19	2.25	2.30	2.37	2.43	2.48
7	1753867	5923685	2.12	2.20	2.26	2.31	2.38	2.44	2.49
8	1754872	5923511	2.10	2.18	2.24	2.29	2.36	2.42	2.47
9	1755321	5924125	2.10	2.18	2.23	2.29	2.36	2.41	2.46
10	1755798	5922917	2.08	2.16	2.22	2.27	2.34	2.40	2.45
11	1756273	5923530	2.06	2.15	2.20	2.26	2.33	2.38	2.43
12	1756876	5923808	2.06	2.14	2.20	2.25	2.32	2.38	2.43
13	1757077	5925036	2.07	2.15	2.20	2.26	2.33	2.38	2.43
14	1757480	5926061	2.07	2.15	2.21	2.26	2.33	2.39	2.44
15	1757720	5924558	2.07	2.15	2.20	2.26	2.33	2.38	2.43
16	1757504	5923474	2.05	2.13	2.19	2.24	2.31	2.37	2.42
17	1758777	5923817	2.05	2.13	2.19	2.24	2.32	2.37	2.42
18	1757869	5922946	2.04	2.13	2.18	2.24	2.31	2.36	2.41
19	1758183	5922574	2.03	2.12	2.17	2.23	2.30	2.35	2.40
20	1759279	5922009	2.01	2.09	2.14	2.20	2.27	2.32	2.37
21	1761896	5922670	1.95	2.03	2.09	2.14	2.21	2.26	2.31
22	1753394	5920977	2.14	2.22	2.28	2.33	2.41	2.46	2.51
23	1752927	5920576	2.15	2.23	2.29	2.34	2.41	2.47	2.52
24	1752568	5920305	2.16	2.24	2.30	2.35	2.42	2.47	2.52
25	1751774	5920613	2.17	2.25	2.31	2.36	2.43	2.49	2.54
26	1751548	5920296	2.17	2.26	2.31	2.37	2.44	2.49	2.54
27	1751319	5919843	2.18	2.26	2.32	2.37	2.44	2.50	2.55
28	1751176	5919250	2.18	2.27	2.32	2.38	2.45	2.50	2.55
29	1751101	5918756	2.19	2.27	2.33	2.38	2.45	2.51	2.56
30	1750937	5918027	2.08	2.16	2.22	2.27	2.34	2.40	2.45
31	1750777	5917400	2.10	2.19	2.24	2.30	2.37	2.42	2.47
32	1749304	5917884	2.12	2.20	2.26	2.31	2.39	2.44	2.49
33	1749997	5918709	2.19	2.27	2.33	2.38	2.45	2.51	2.56
34	1749646	5919012	2.19	2.27	2.33	2.38	2.45	2.51	2.56
35	1749355	5919387	2.19	2.27	2.33	2.38	2.45	2.51	2.56

Site	Easting (NZTM)	Northing (NZTM)	AEP: 0.39 ARI: 2 yr	0.18 5 yr	0.1 10 yr	0.05 20 yr	0.02 50 yr	0.01 100 yr	0.005 200 yr
36	1749031	5919620	2.19	2.27	2.33	2.38	2.45	2.51	2.56
37	1748233	5921920	2.19	2.27	2.33	2.38	2.45	2.51	2.56
38	1748224	5922919	2.19	2.27	2.33	2.38	2.46	2.51	2.56
39	1748025	5923311	2.19	2.28	2.33	2.39	2.46	2.51	2.57
40	1747622	5923718	2.20	2.28	2.34	2.39	2.46	2.52	2.57
41	1747028	5923917	2.20	2.29	2.34	2.40	2.47	2.52	2.58
42	1746820	5924309	2.20	2.29	2.34	2.40	2.47	2.52	2.58
43	1750882	5924426	2.18	2.26	2.32	2.37	2.44	2.50	2.55
44	1747124	5925913	2.20	2.28	2.34	2.39	2.46	2.52	2.57
45	1747619	5925615	2.20	2.28	2.34	2.39	2.46	2.52	2.57
46	1748124	5925418	2.20	2.28	2.34	2.39	2.46	2.52	2.57
47	1748622	5925321	2.19	2.28	2.33	2.39	2.46	2.51	2.57
48	1749020	5925613	2.20	2.28	2.34	2.39	2.46	2.52	2.57
49	1749222	5925920	2.21	2.29	2.35	2.40	2.47	2.53	2.58
50	1749318	5926318	2.22	2.30	2.35	2.41	2.48	2.53	2.59
51	1749521	5926714	2.23	2.31	2.37	2.42	2.49	2.55	2.60
52	1749923	5926718	2.23	2.31	2.37	2.42	2.49	2.54	2.60
53	1750332	5925635	2.20	2.28	2.34	2.39	2.46	2.52	2.57
54	1750882	5924426	2.18	2.26	2.32	2.37	2.44	2.50	2.55
55	1751631	5923392	2.16	2.24	2.30	2.35	2.42	2.48	2.53
56	1752696	5923084	2.14	2.22	2.28	2.33	2.40	2.45	2.51
57	1748140	5917965	2.23	2.32	2.37	2.43	2.50	2.55	2.60
58	1748221	5917482	2.23	2.32	2.38	2.43	2.50	2.55	2.60
59	1748140	5917965	2.23	2.32	2.37	2.43	2.50	2.55	2.60
60	1748031	5918485	2.23	2.31	2.37	2.42	2.49	2.55	2.60
61	1747920	5918968	2.22	2.31	2.36	2.42	2.49	2.54	2.59
62	1747898	5919449	2.21	2.29	2.35	2.41	2.48	2.53	2.58
63	1747833	5919919	2.20	2.28	2.34	2.39	2.47	2.52	2.57
64	1748434	5920119	2.19	2.28	2.33	2.39	2.46	2.51	2.56
65	1747832	5920917	2.19	2.28	2.33	2.39	2.46	2.51	2.56
66	1748033	5921213	2.19	2.27	2.33	2.38	2.46	2.51	2.56
67	1746620	5927412	2.28	2.36	2.42	2.47	2.54	2.60	2.65
68	1746820	5927915	2.28	2.36	2.42	2.47	2.54	2.60	2.65
69	1747616	5928013	2.27	2.36	2.42	2.47	2.54	2.59	2.64
70	1748118	5928115	2.27	2.36	2.41	2.47	2.54	2.59	2.64
71	1748618	5928117	2.27	2.35	2.41	2.46	2.53	2.59	2.64
72	1747119	5928709	2.30	2.39	2.44	2.50	2.57	2.62	2.68
73	1743880	5929297	2.32	2.41	2.46	2.52	2.59	2.64	2.70

| Site | Easting (NZTM) | Northing (NZTM) | AEP: 0.39 | 0.18 | 0.1 | 0.05 | 0.02 | 0.01 | 0.005 |
			ARI: 2 yr	5 yr	10 yr	20 yr	50 yr	100 yr	200 yr
74	1744235	5929180	2.32	2.41	2.46	2.52	2.59	2.64	2.70
75	1744613	5929407	2.32	2.41	2.46	2.51	2.59	2.64	2.69
76	1745617	5929612	2.32	2.40	2.46	2.51	2.58	2.64	2.69
77	1745809	5929908	2.29	2.38	2.43	2.49	2.56	2.62	2.67
78	1745909	5930885	2.30	2.38	2.44	2.49	2.56	2.61	2.66
79	1745915	5929318	2.31	2.40	2.45	2.51	2.58	2.63	2.69
80	1746617	5929606	2.31	2.39	2.45	2.50	2.57	2.63	2.68
81	1747617	5929611	2.30	2.38	2.44	2.49	2.56	2.62	2.67
82	1748344	5929332	2.29	2.37	2.43	2.48	2.55	2.61	2.66
83	1749079	5930540	2.31	2.39	2.45	2.50	2.57	2.62	2.68
84	1749537	5931198	2.31	2.40	2.45	2.50	2.57	2.63	2.68
85	1749907	5932412	2.25	2.33	2.39	2.44	2.51	2.56	2.61
86	1748417	5928920	2.28	2.37	2.42	2.47	2.55	2.60	2.65
87	1749621	5927312	2.24	2.32	2.38	2.43	2.50	2.56	2.61
88	1749565	5927646	2.24	2.33	2.38	2.44	2.51	2.56	2.61
89	1750370	5927743	2.25	2.34	2.39	2.44	2.52	2.57	2.62
90	1750923	5928128	2.26	2.34	2.40	2.45	2.52	2.58	2.63
91	1751319	5928425	2.26	2.35	2.40	2.45	2.52	2.58	2.63
92	1745533	5921567	2.24	2.32	2.38	2.43	2.50	2.56	2.61
93	1745541	5922011	2.23	2.32	2.37	2.43	2.50	2.55	2.60
94	1746262	5922487	2.22	2.31	2.36	2.42	2.49	2.54	2.59
95	1746430	5923416	2.21	2.30	2.35	2.41	2.48	2.53	2.59

3.2　Manukau Harbour

The methods used to simulate storm-tide time-series and frequency-magnitude distributions are explained in Section 7.3; this section provides information and examples specific to the application of those methods in the Manukau Harbour.

3.2.1　Tide-gauge

The modern digital Onehunga tide-gauge record (1 Jan 2001 – 31 May 2011) was used as the base dataset for storm-tide modelling in the Manukau Harbour (Figure 3-10). Note: this is much shorter than the lengthy record that was available for the Ports of Auckland Waitemata Harbour gauge, which will result in more uncertainty in upper extreme storm-tide values.

Fortunately, a historical analysis of the higher storm-tide levels measured at the Port of Onehunga is available (Auckland Harbour Board 1974) for the period 1926 to 1973.
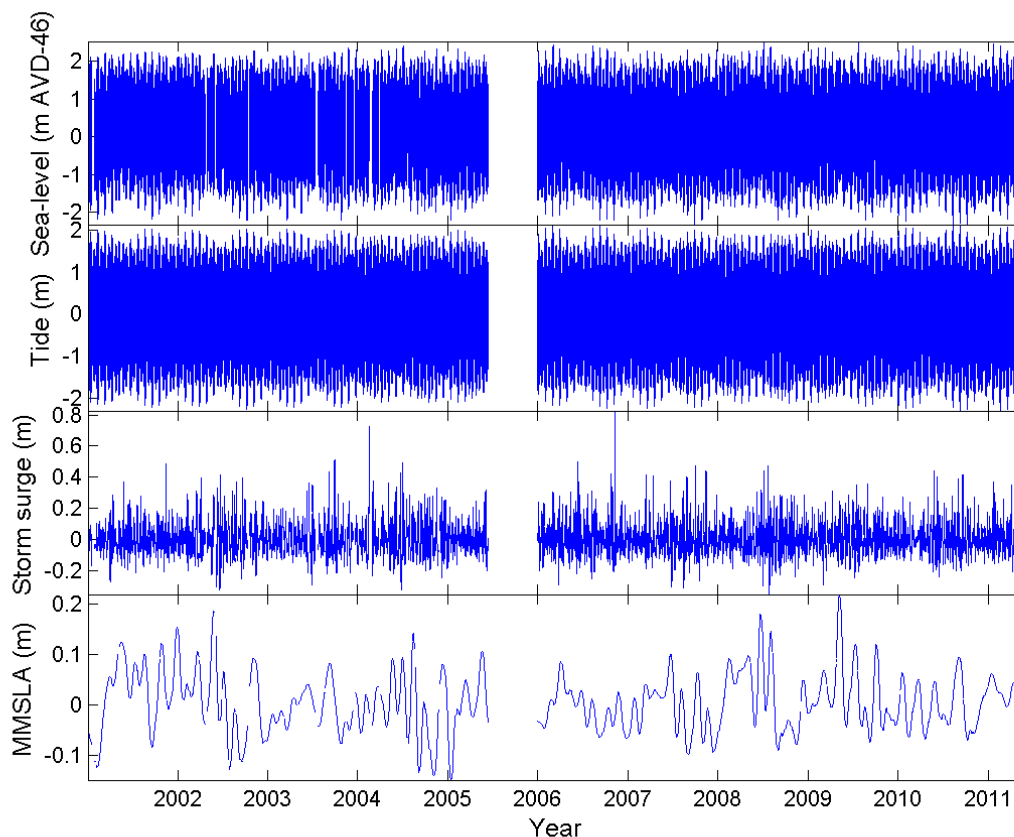
Figure 3-10: Onehunga sea-level record used for this study. The raw sea-level is plotted relative to AVD-46. Three sea-level components are also plotted: astronomical tide, storm surge and monthly mean sea-level anomaly (MMSLA). Source: measurements from Ports of Auckland Ltd.

3.2.2　Hydrodynamic model

An existing calibrated hydrodynamic model, Figure 3-11, Figure 3-12 (Reeve & Pritchard 2010) was used to simulate tides and the wind-driven component of storm surge in the Manukau Harbour. The bathymetry is much better resolved in the shallow upper reaches of the Manukau Harbour in this hydrodynamic model, compared to model used by Stephens et

al. (2011c). This, together with the simulation and scaling of tide over a full lunar month, means that the levels simulated here are considered to supersede those of Stephens et al. (2011c).

The hydrodynamic model was calibrated and validated against sea-level and current measurements at Onehunga Wharf, Paratutae Island, Waiuku, Papakura, Purakau and Wairopa Channels, Karore Bank, and Pahurehure Inlet. Water level calibrations indicated root-mean-square errors in the range 7–19 cm, relative-root-mean-square errors of ≤ 5% and bias of 1–9 cm, meaning that the model slightly over-predicted sea-level heights. This means that simulated storm-tide levels in the harbour will be conservatively high.
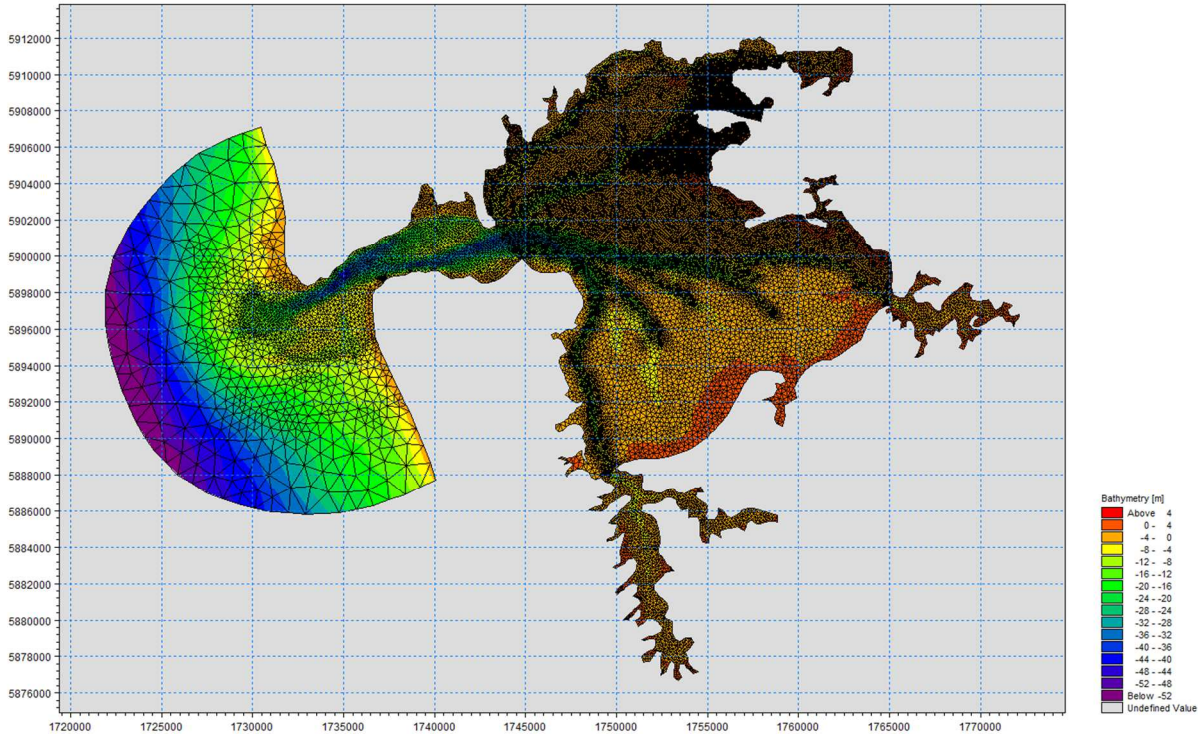
Figure 3-11: Hydrodynamic model MIKE3FM flexible mesh grid of the Manukau Harbour.
Colour scale indicates depth.
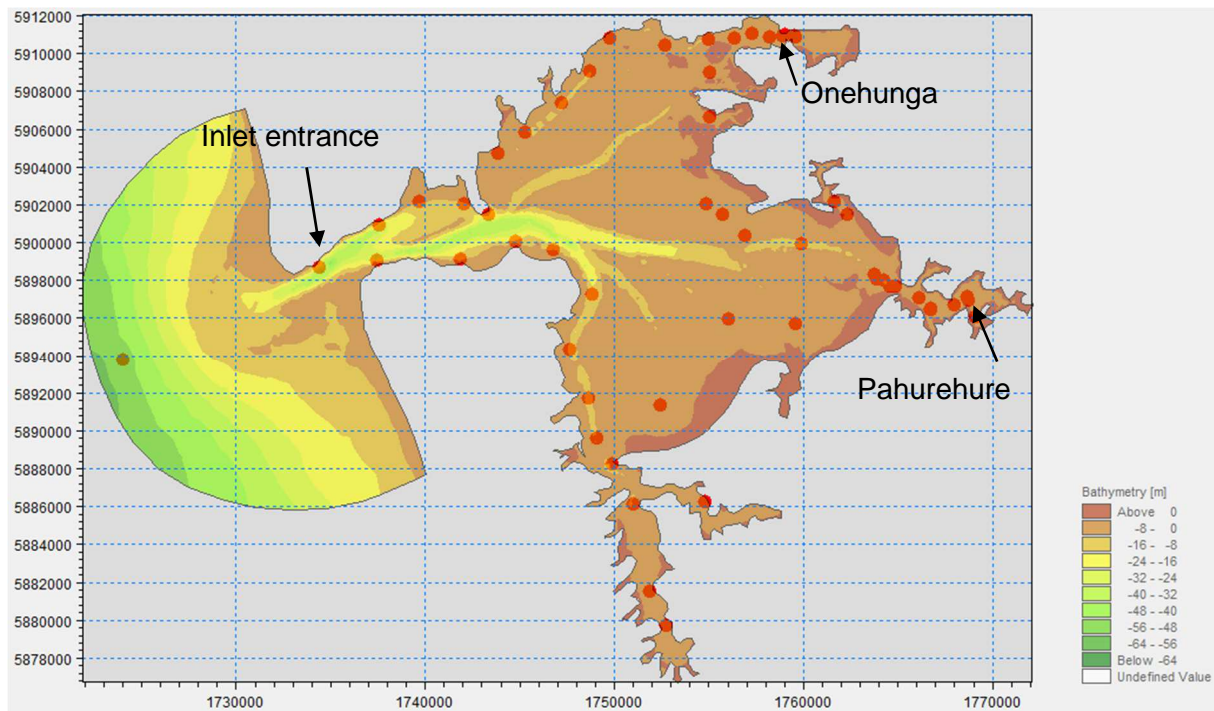
Figure 3-12: Hydrodynamic model bathymetry, with output locations marked.

3.2.3 Modelling storm surge

The Auckland Airport (located adjacent to the Manukau Harbour) wind and mean sea-level pressure records were obtained from 8 Nov 1965 – 11 May 2011. The wind-driven component of storm surge was calculated as described in Section 7.3 by using the wind record to interpolate storm surge from the simulated wind-surge response matrix from the hydrodynamic model. The wind-driven component of storm surge differs depending on the output location within the harbour due to the available wind fetch.

The inverse-barometer component of sea level was calculated as described in Section 7.3.1.

3.2.4 Modelling storm-tide

Storm-tide time-series were simulated using the methods described in Sections 2.3.1 and 7.3, at 68 locations within the Manukau Harbour (Figure 3-12), for later extreme sea-level analysis.

Time-series of monthly MMSLA were not simulated in the Manukau Harbour model, but the empirical cumulative exceedance distribution of MMSLA, derived from the Onehunga tide gauge (location in Figure 3-12), was included in the Monte Carlo joint-probability extreme sea-level modelling.

For each output location the tidal time-series were added to the storm surge time-series, and combined with MMSLA in a MCJP extreme sea-level analysis

Tidal hysteresis was calculated from the hydrodynamic model using the mean sea-level over the simulated lunar month; enabling a mean-sea-level offset to be calculated for each

location, relative to the Onehunga tide-gauge location. This mean sea-level offset due to tidal hysteresis was added to the extreme storm-tide distribution at each output location.

Figure 3-13 plots extreme storm-tide peaks and extreme sea-level distributions predicted for the Onehunga tide gauge. There are two extreme sea-level curves plotted – the MCJP curve is reliable, but the GPD fit to POT curve is unreliable, as follows:

Seven large historical events

The seven largest recorded historical storm-tides (Table 3-4) are plotted in their Gringorten potting positions, with six of these events from the analysis of 1926 to 1973 by the Auckland Harbour Board (1974). The Gringorten plotting positions assume that the empirical distribution of the data follows a Gumbel extreme-value distribution. An assumption has been made that these are the 7 largest storm tides in the 86 years since the earliest in 1926. However they could be the largest events in a longer timeframe, or there may have been sizeable events in the data gap between 1974 and the start of the modern record, and this would affect their plotting positions on Figure 3-13. Nevertheless, they provide a useful comparison for the fit of the two extreme-value models.

Unreliable GPD fit to modern digital data

A GPD model was fitted to the largest 5 storm-tides per year from the modern 2001–2011 digital record. The 2001–2011 record is not long enough (insufficient extreme events) to get reliable extreme sea-level estimates using the POT/GPD technique, hence the very flat distribution at low exceedance probabilities that under-predicts the historical storm-tide peak magnitudes.

Reliable MCJP fit to modern data

The extreme sea-level frequency–magnitude distribution from the MCJP technique, fitted using 2001–2011 data, is also plotted. The MCJP technique considers all possible combinations of tides, storm surges and MMSLA (even if the numerous possible combinations did not occur within the measured record), and so it compares better with the Gringorten estimates of the historical storm-tides. The MCJP technique is upward biased at higher AEPs (left side of Figure 3-13) by ≤ 5 cm.
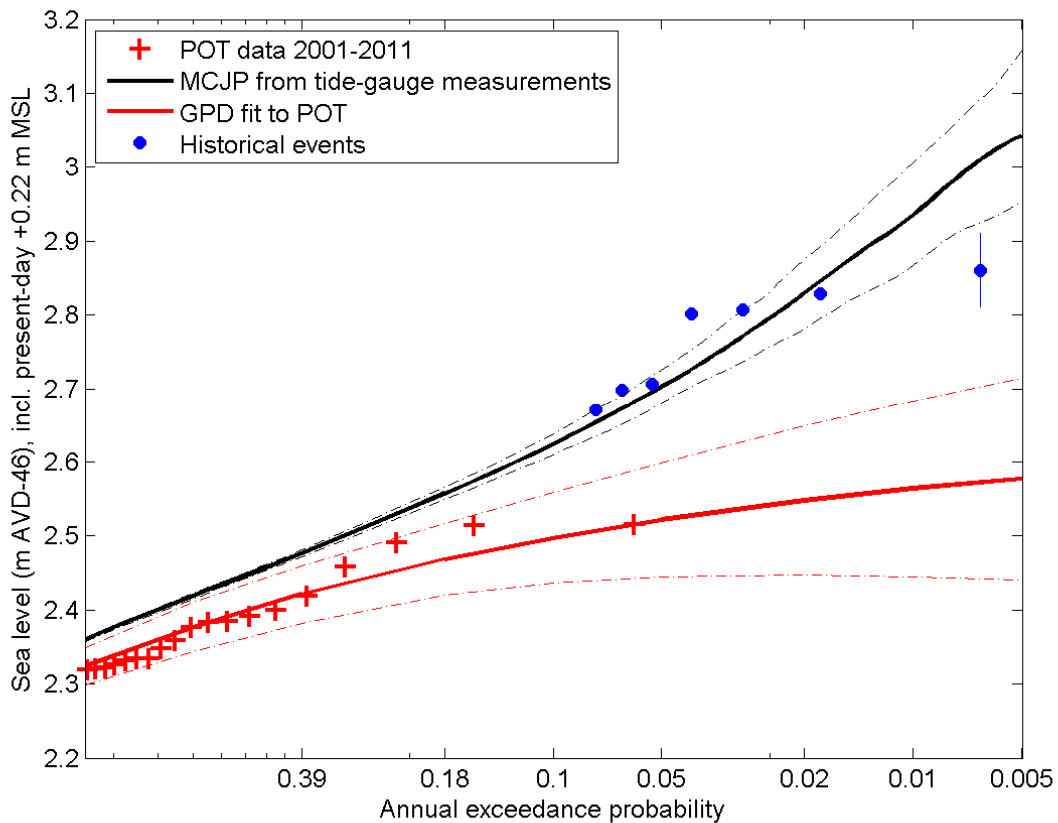
Figure 3-13: Extreme sea-level frequency–magnitude distribution at the Onehunga tide gauge in the Manukau Harbour. Elevations are relative to AVD-46 including +0.22 m offset for baseline mean sea level (present-day estimate). Historical events in Table 3-4.

Table 3-4: The seven largest storm-tide annual maxima since 1926 recorded at Onehunga.
Excludes a gap from 1974 to start of modern record in 2001.

Date	Metres above AVD-46; raw data with no sea-level rise adjustment	Metres above AVD-46 adjusted to present-day MSL = +0.22 m AVD-46, adjusted for 1.5mm/yr SLR
22-Jun-47	2.74	2.80
7-Sep-48	2.72	2.81
1949	2.62	2.71
1954	2.62	2.70
31-Aug-65	2.74	2.83
1972	2.62	2.67
17-Apr-99 (lower estimate)	2.80	2.81
17-Apr-99 (upper estimate)	2.90	2.91

Figure 3-14 compares the extreme sea-level frequency–magnitude distributions derived from the Onehunga gauge data (Figure 3-10), and from simulated data at the gauge site, and, for comparison, at sites located in the upper Pahurehure inlet and in the tidal inlet channel near the harbour entrance. Using the IB_{factor} as a calibration parameter, the extreme sea-level distributions from both measured and simulated data were closely matched at the Onehunga tide-gauge site. The other curves demonstrate how the simulated extreme sea-level magnitudes decrease toward the harbour entrance and increase toward the head of the harbour, due to amplification of the tide and storm surge. Note also how the slope of extreme sea-level curve steepens at lower frequencies. This represents a change in storm–tide characteristics between smaller and larger events. Although tides are the major component of all storm-tides, moderate to large storm surges play an increasingly important role in the very largest storm-tides. Traditional direct extreme-value techniques (POT/GPD, AM/GEV Table 7-4) cannot account for this change in storm-tide characteristics across all of the recorded storm-tides. Instead, a long enough data record is required that the direct techniques be fitted only to the largest storm-tide population (represented by the steeper, lower-frequency part of the MCJP curve). For short data records, where few or no large storm-tides are expected, the direct techniques fit to the smallest storm-tide population (represented by the shallower, lower, higher-frequency part of the MCJP curve), and a result is obtained like that shown in Figure 3-13.

Table 3-5 provides the estimated extreme sea-level frequency–magnitude relationship at Onehunga based on the MCJP technique applied to the Onehunga tide-gauge record. Table 3-6 provides the estimated extreme sea-level frequency–magnitude relationship at locations throughout the harbour.
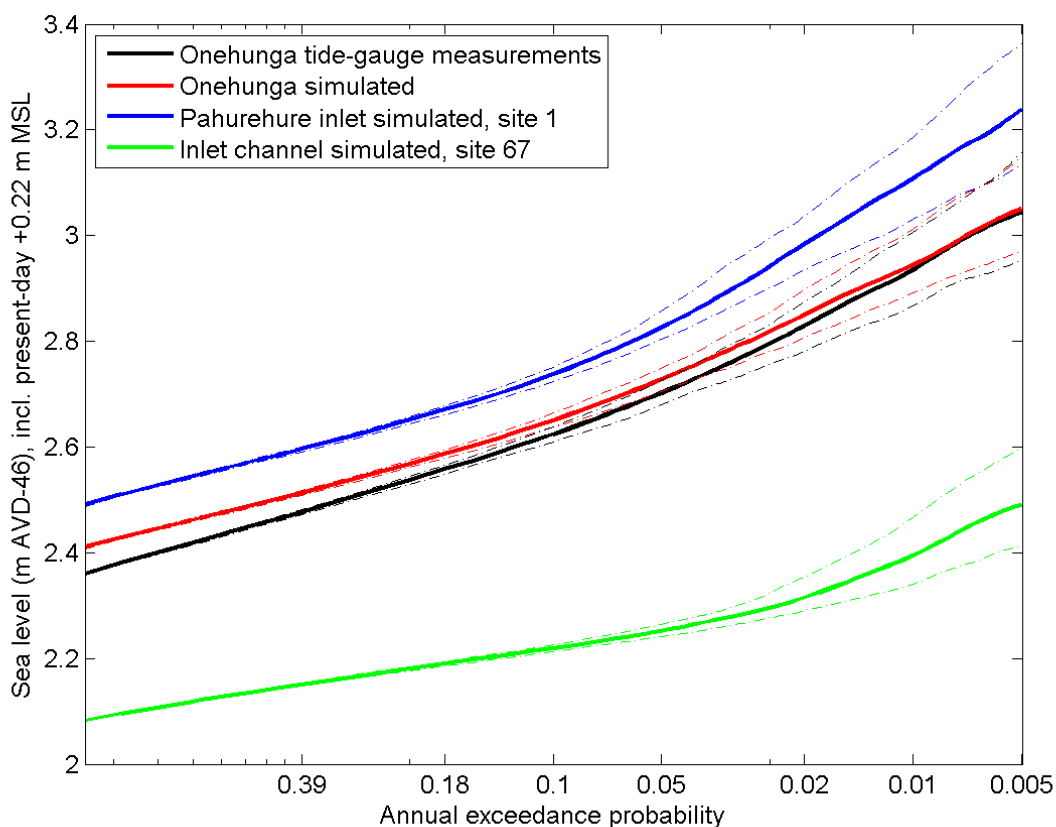
Figure 3-14: Extreme sea-level frequency–magnitude distribution at selected locations in the Manukau Harbour. Elevations are relative to AVD-46 including +0.22 m offset for baseline mean sea level (present-day estimate). The black line is identical to that in Figure 3-13.

Table 3-5: Extreme sea-level at Onehunga. Elevations are relative to AVD-46 including +0.22 m offset for baseline mean sea level (present-day estimate). C.I. = confidence interval. Elevations calculated from tide-gauge data.

AEP	0.39	0.18	0.10	0.05	0.02	0.01	0.005
ARI	2	5	10	20	50	100	200
Median	2.48	2.56	2.62	2.70	2.83	2.93	3.04
Lower 95th C.I.	2.47	2.55	2.61	2.68	2.78	2.87	2.95
Upper 95th C.I.	2.48	2.57	2.64	2.73	2.87	3.01	3.16
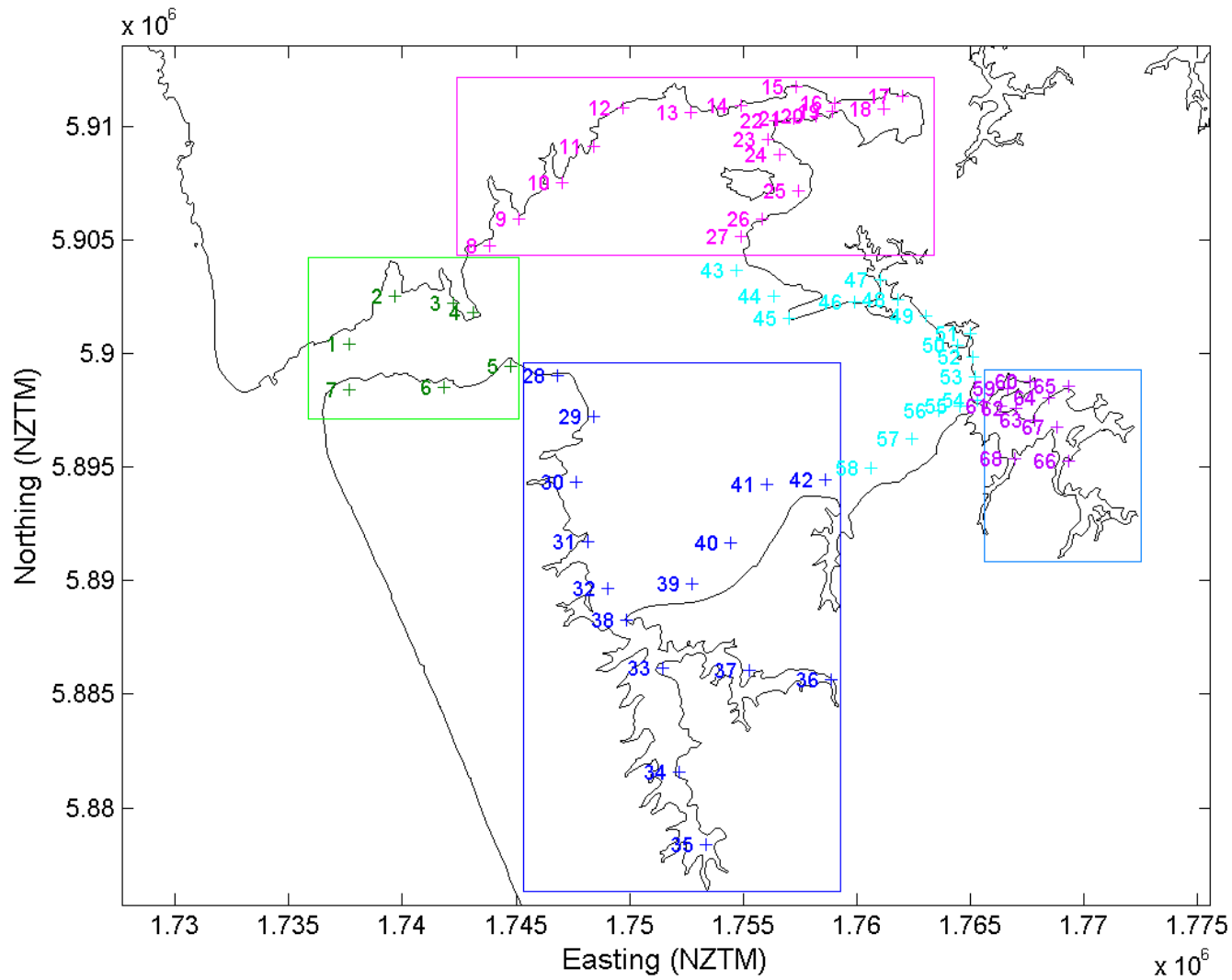
Figure 3-15: **Locations of extreme sea-level calculations in the Manukau Harbour.** Colour-coding corresponds to Table 3-6.

Table 3-6: Extreme sea-level in the Manukau Harbour. Elevations are relative to AVD-46 including +0.22 m offset for baseline mean sea level (present-day estimate). Elevations calculated from simulated data. Colour-coding corresponds to Figure 3-15.

Site	Easting (NZTM)	Northing (NZTM)	AEP: 0.39 ARI: 2 yr	0.18 5 yr	0.1 10 yr	0.05 20 yr	0.02 50 yr	0.01 100 yr	0.005 200 yr
1	1737645	5900426	2.15	2.18	2.21	2.25	2.31	2.39	2.48
2	1739641	5902530	2.23	2.27	2.31	2.34	2.40	2.47	2.55
3	1742241	5902235	2.20	2.24	2.27	2.31	2.38	2.47	2.56
4	1743142	5901836	2.34	2.39	2.42	2.46	2.52	2.57	2.64
5	1744746	5899440	2.28	2.32	2.35	2.39	2.46	2.55	2.65
6	1741848	5898534	2.19	2.23	2.26	2.30	2.36	2.45	2.55
7	1737649	5898426	2.13	2.17	2.21	2.24	2.30	2.37	2.46
8	1743836	5904737	2.29	2.33	2.36	2.40	2.47	2.56	2.65
9	1745134	5905940	2.33	2.37	2.40	2.44	2.51	2.60	2.69
10	1747030	5907543	2.34	2.39	2.42	2.46	2.54	2.63	2.73
11	1748427	5909146	2.35	2.40	2.43	2.48	2.57	2.66	2.75
12	1749723	5910848	2.39	2.44	2.49	2.54	2.63	2.71	2.79
13	1752724	5910654	2.42	2.48	2.53	2.60	2.69	2.77	2.85
14	1754923	5910958	2.47	2.53	2.59	2.66	2.76	2.84	2.93
15	1757321	5911763	2.50	2.57	2.63	2.71	2.83	2.92	3.02
16	1759022	5911066	2.54	2.62	2.68	2.76	2.88	2.97	3.08
17	1762021	5911372	2.56	2.64	2.72	2.80	2.92	3.00	3.09
18	1761223	5910771	2.51	2.58	2.66	2.76	2.91	3.02	3.12
19	1758923	5910666	2.54	2.61	2.67	2.75	2.87	2.97	3.07
20	1758223	5910465	2.52	2.59	2.65	2.73	2.85	2.95	3.05
21	1757224	5910363	2.50	2.57	2.63	2.71	2.83	2.93	3.03
22	1756424	5910261	2.50	2.57	2.63	2.70	2.82	2.92	3.02
23	1756126	5909461	2.48	2.55	2.61	2.69	2.82	2.91	3.02
24	1756627	5908762	2.48	2.55	2.62	2.70	2.83	2.92	3.03
25	1757430	5907164	2.45	2.52	2.58	2.67	2.81	2.91	3.03
26	1755832	5905960	2.43	2.49	2.54	2.62	2.77	2.88	2.99
27	1754934	5905159	2.42	2.48	2.53	2.61	2.75	2.86	2.97
28	1746847	5899044	2.32	2.36	2.39	2.43	2.51	2.61	2.71
29	1748450	5897247	2.37	2.41	2.45	2.49	2.58	2.68	2.78
30	1747655	5894346	2.38	2.42	2.46	2.50	2.60	2.71	2.82
31	1748160	5891747	2.44	2.48	2.53	2.58	2.71	2.83	2.95
32	1749064	5889649	2.49	2.55	2.61	2.68	2.83	2.95	3.08
33	1751470	5886154	2.53	2.58	2.63	2.72	2.89	3.03	3.17
34	1752179	5881555	2.63	2.70	2.77	2.86	3.04	3.18	3.32
35	1753385	5878358	2.67	2.74	2.82	2.93	3.12	3.26	3.42

Site	Easting (NZTM)	Northing (NZTM)	AEP: 0.39 / ARI: 2 yr	0.18 / 5 yr	0.1 / 10 yr	0.05 / 20 yr	0.02 / 50 yr	0.01 / 100 yr	0.005 / 200 yr
36	1758871	5885667	2.68	2.75	2.82	2.93	3.12	3.26	3.41
37	1755270	5886061	2.67	2.72	2.78	2.88	3.05	3.20	3.34
38	1749867	5888251	2.49	2.54	2.59	2.67	2.84	2.97	3.11
39	1752763	5889856	2.44	2.49	2.55	2.64	2.81	2.95	3.08
40	1754460	5891659	2.45	2.50	2.56	2.65	2.82	2.95	3.09
41	1756055	5894262	2.43	2.48	2.54	2.62	2.79	2.93	3.06
42	1758654	5894467	2.43	2.49	2.55	2.64	2.82	2.95	3.09
43	1754737	5903659	2.41	2.46	2.51	2.56	2.65	2.73	2.82
44	1756339	5902562	2.42	2.48	2.52	2.58	2.67	2.76	2.86
45	1757041	5901563	2.43	2.48	2.52	2.57	2.68	2.77	2.87
46	1759939	5902269	2.49	2.55	2.60	2.66	2.77	2.87	2.96
47	1761037	5903271	2.55	2.61	2.66	2.72	2.83	2.92	3.02
48	1761839	5902372	2.55	2.61	2.67	2.73	2.85	2.95	3.05
49	1763040	5901675	2.54	2.61	2.67	2.74	2.87	2.97	3.07
50	1764443	5900377	2.56	2.62	2.69	2.77	2.90	3.01	3.12
51	1765042	5900879	2.57	2.64	2.71	2.79	2.92	3.02	3.13
52	1765144	5899879	2.56	2.63	2.69	2.78	2.92	3.03	3.14
53	1765246	5898979	2.56	2.62	2.69	2.77	2.92	3.05	3.17
54	1765347	5897979	2.55	2.62	2.68	2.77	2.92	3.05	3.18
55	1764548	5897678	2.55	2.61	2.67	2.75	2.91	3.03	3.17
56	1763648	5897476	2.54	2.60	2.66	2.75	2.90	3.03	3.16
57	1762451	5896274	2.53	2.59	2.65	2.74	2.91	3.04	3.18
58	1760653	5894970	2.46	2.52	2.58	2.68	2.85	2.98	3.12
59	1766646	5898482	2.59	2.66	2.72	2.81	2.97	3.09	3.22
60	1767646	5898784	2.60	2.67	2.73	2.82	2.98	3.11	3.22
61	1766348	5897681	2.59	2.66	2.72	2.81	2.97	3.10	3.22
62	1767048	5897583	2.61	2.68	2.74	2.83	2.98	3.12	3.25
63	1767849	5897084	2.63	2.70	2.77	2.86	3.02	3.15	3.27
64	1768447	5898085	2.64	2.71	2.78	2.87	3.02	3.15	3.28
65	1769346	5898587	2.65	2.72	2.79	2.88	3.04	3.16	3.29
66	1769353	5895287	2.95	3.03	3.10	3.20	3.37	3.51	3.66
67	1768850	5896786	2.64	2.71	2.78	2.87	3.03	3.16	3.30
68	1766952	5895382	2.60	2.67	2.73	2.83	2.99	3.13	3.27

3.3 Kaipara Harbour

The methods used to simulate storm-tide time-series and frequency-magnitude distributions are explained in Section 7.3; this section provides information and examples specific to the application of those methods in the Kaipara Harbour.

3.3.1 Tide-gauge analysis

The Pouto Point sea-level record from 18 April 2001 to 1 September 2012 is plotted in Figure 3-16. The Pouto Point sea-level gauge is located on a wave-exposed sandy shoreline inside the Kaipara Harbour. Occasionally, sand waves bury the bubbler orifice, affecting the tide-gauge readings for several months. For example, a burial occurred beginning around the start of September 2012. In 2011 the bubbler orifice had broken free of its mooring block (Dale Hansen, Northland Regional Council, *pers. comm.*), so those data have been omitted from our analysis. As outlined in Section 2.2, we suspect that the relationship between tide-gauge zero and One-Tree-Point 1964 datum needs re-surveying. Despite these difficulties, the gauge record is invaluable as a reference point for hydrodynamic modelling, for tidal harmonic analysis, and for extreme sea-level modelling. Although too short for extreme sea-level analysis using direct techniques (Table 7-4), it is suitable for analysis using the indirect MCJP technique.
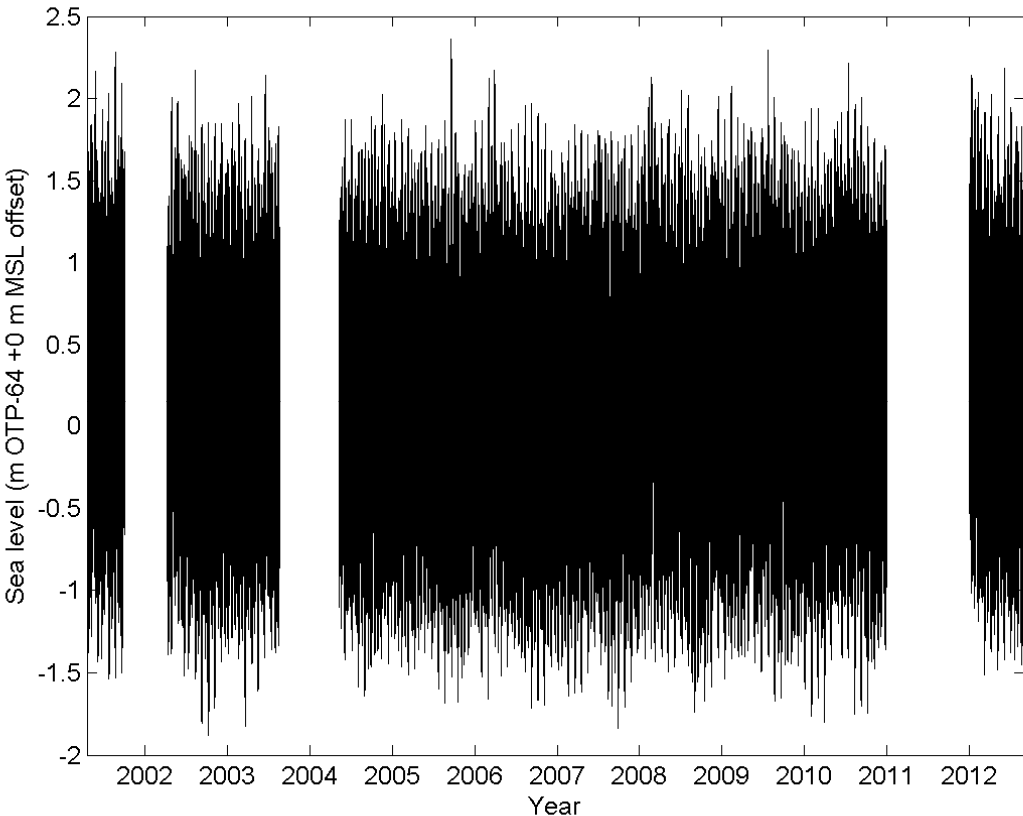
Figure 3-16: Pouto Point sea-level record 2001-2012. Source: Northland Regional Council.

3.3.2 Hydrodynamic model

A Deltares Delft3d 2-dimensional depth averaged hydrodynamic model was developed for the Kaipara Harbour during a previous study for Auckland Council (Pritchard et al. 2012). Three curvi-linear model grids that covered the Northern, Central and Southern areas of the harbour were designed to be online coupled (dynamically nested) and simultaneously run to resolve tidal elevations and hydrodynamic flows through the entire Kaipara Harbour (Figure 3-17). New and archived depth survey data were used to construct the bathymetric grid for the model. The model grid resolved the deeper sub-tidal channels and inter-tidal flats that interact with currents to control the hydrodynamics of the harbour.

A series of calibration and validation simulations were undertaken for a fortnight in March 2011 that coincided with the timing of observations of sea surface elevation and current flow measured around the harbour during an extensive fieldwork program in 2011 and additional bathymetric surveys, Figure 3-18 (Stephens et al. 2011a).The model was driven at an offshore open boundary by tidal sea-level elevations and a wind stress was imposed at the sea surface.

The predicted values were then compared to observational data. The error between predicted and observed data was then assessed using several statistical skill tests. The skill tests for predicted sea surface heights indicated root mean square errors of 10–20 cm, relative root mean square errors ~5%, and bias 1–2 cm indicating excellent agreement with observations. The generation of over-tide harmonics in the model demonstrated that the shallow water effects within the model domain are predicted.

Inclusion of surface wind stress in simulations showed that there was less than 5% improvement introduced by the wind across all skill measures, when compared to the tide-only simulations.
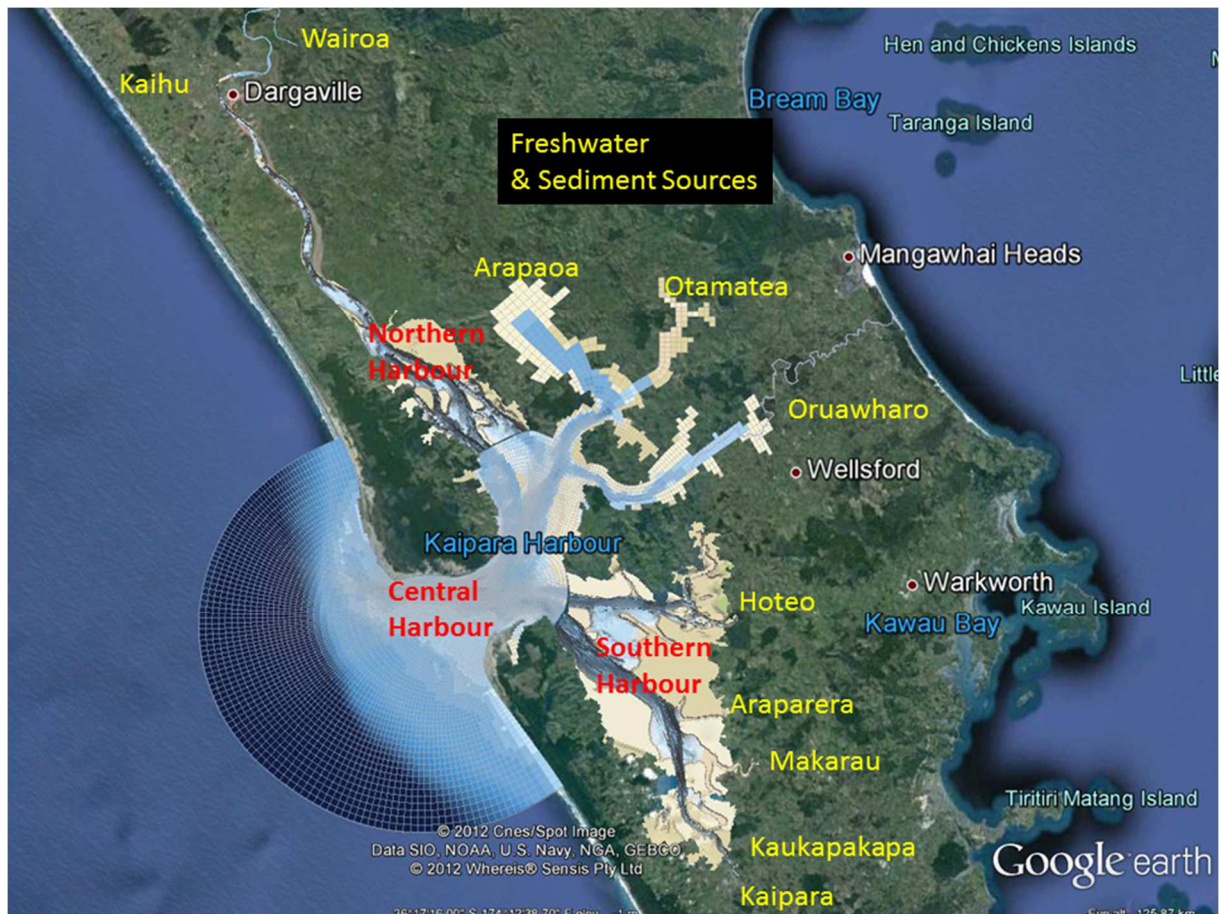
Figure 3-17: Aerial photo of the Kaipara Harbour and tidal inlet with Delft3d model grid overlaid. The three coupled model domains are labelled in red. The freshwater sources are labelled in yellow.
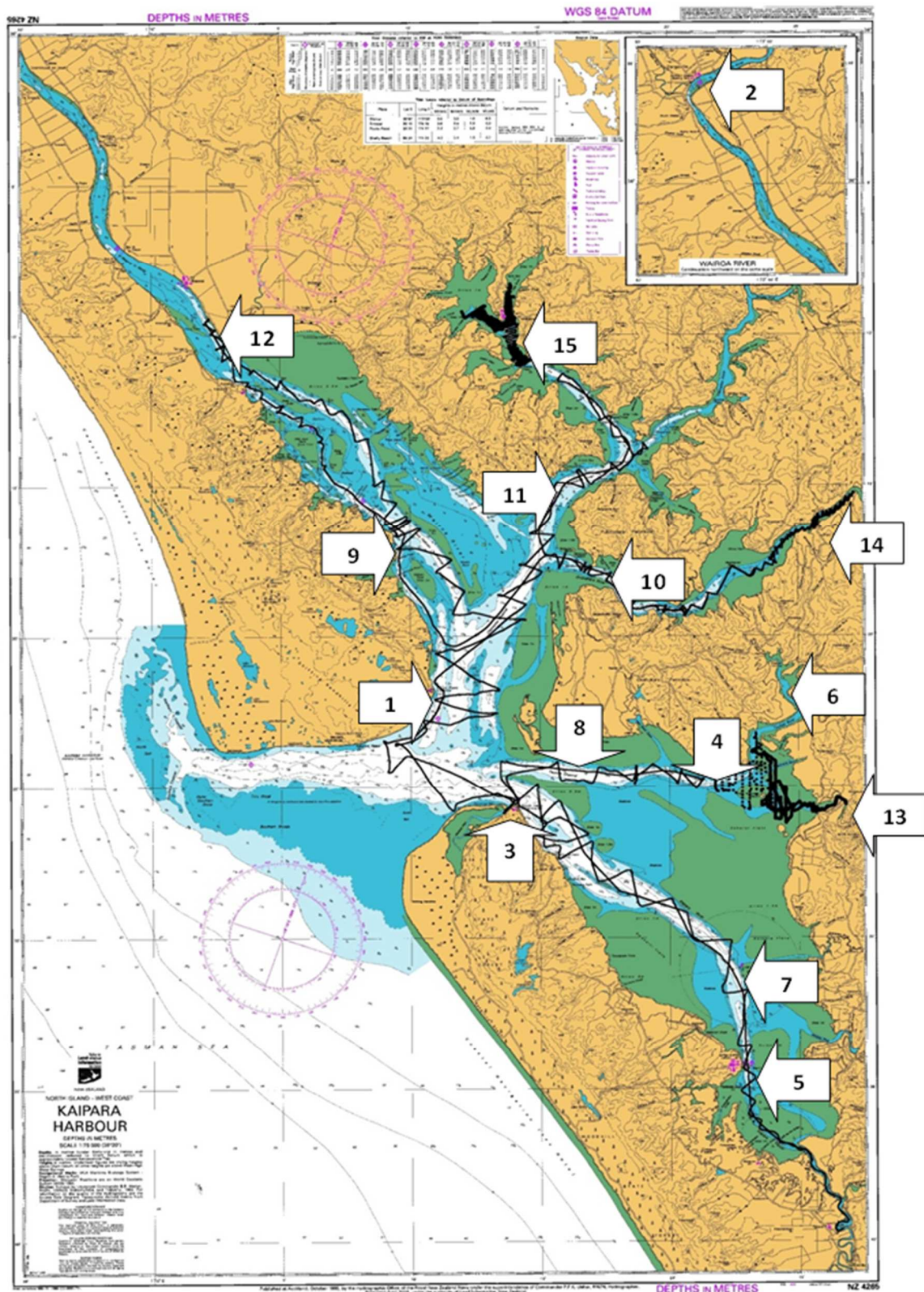
Figure 3-18: Location of sea-level records and bathymetry collection (black lines) in 2011 for hydrodynamic model calibration.

3.3.3 Meteorological record

There are no long-term wind records located directly adjacent to the Kaipara Harbour. A representative wind record for modelling wind-driven storm surge in the Kaipara Harbour was reconstructed from several wind records (Table 3-7).

Table 3-7: Wind records used for Kaipara Harbour wind-driven storm surge modelling.

Name	Agent and Network Number	Latitude, Longitude	Record Start	Record Finish	Record used in reconstruction	Scaling factor
Kaipara South Head N.Z.F.S.	1368, A64422	-36.459, 174.256	1 Jun 1966	30 Apr 1968	Not used	× 1
Auckland, Whenuapai Aero	1410, A64761	-36.793, 174.624	1 Jan 1960	22 Jul 2007	1 Jan 1960 – 31 Mar 1997	× 1.26
Whangarei Aero AWS	1287, A54737	-35.769, 174.364	1 Jan 1994	1 Jan 2013	1 Apr 1997 – 30 May 2005	× 1.73
Auckland, Whenuapai AWS	23976,A64762	-36.793, 174.624	30 May 2005	1 Jan 2013	30 May 2005 – 8 Jun 2010	× 1.26

The Kaipara South Head wind record was perfectly located to represent wind near the Kaipara Harbour entrance, but the 1966–68 record is too short to use for reconstructing wind-driven storm surge over the ~30 years required. Instead, the Kaipara South Head record was used to scale the Whenuapai wind speeds, from a linear comparison between the overlapping parts of the record. The scaling factor was Whenuapai wind speed × 1.26. The 1960–2007 Whenuapai record has significant gaps after 1997, so the Whangarei record was used to fill the gap between 1997 and the modern Whenuapai record beginning in 2005 (Table 3-7). The reconstructed time-series are plotted in Figure 3-19 and a wind rose in Figure 3-20. The highest frequency of winds is from the south-west quadrant.
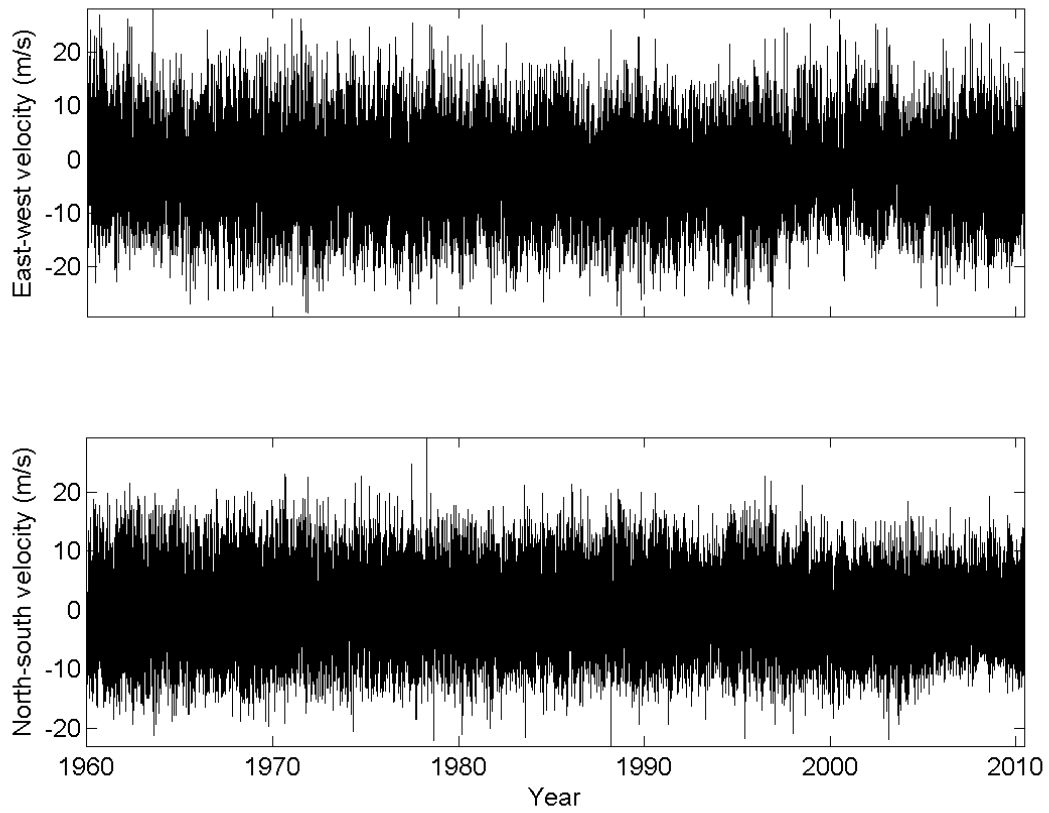
Figure 3-19: Reconstructed wind time-series used for modelling of wind-driven storm surge in the Kaipara Harbour.

Coastal inundation by storm-tides and waves in the Auckland region
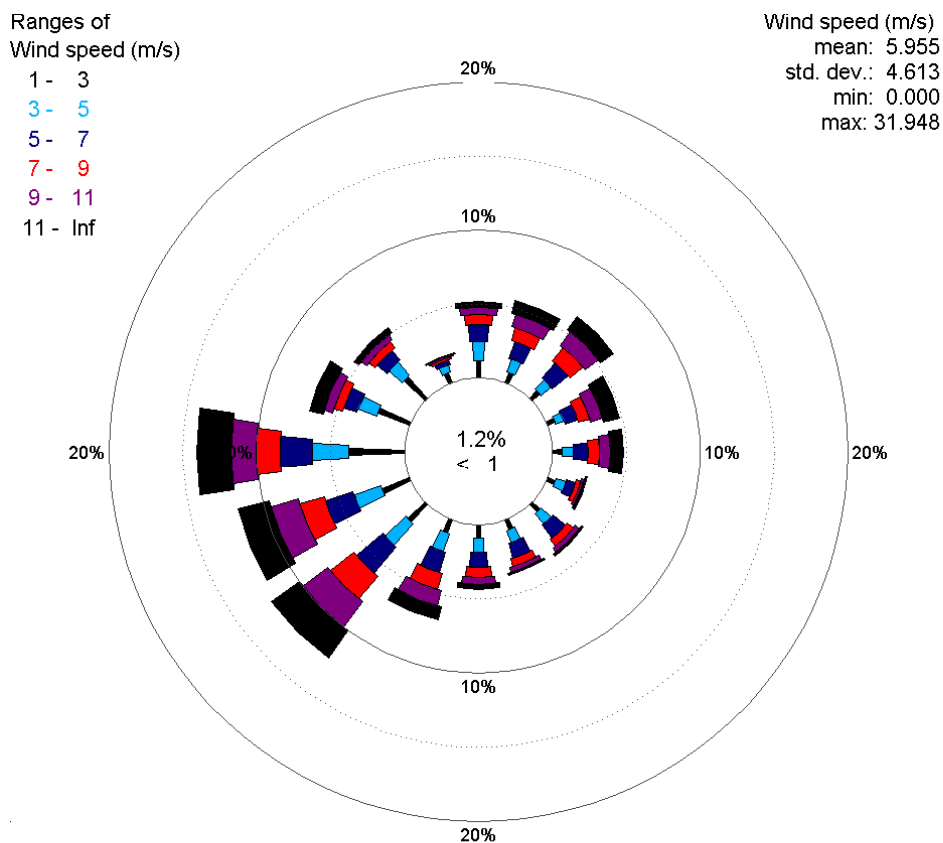
Figure 3-20: Rose plot of reconstructed wind series used for modelling of wind-driven storm surge in the Kaipara Harbour. Wind direction relates to where wind blows <u>from</u>.

3.3.4 Modelling storm-tide

Storm-tide time-series were simulated at 27 locations within the central and southern Kaipara Harbour, for later extreme sea-level analysis (Figure 3-21). The three sea-level components required are tide + storm surge + monthly mean sea-level anomaly. Time-series of monthly MMSLA were not simulated, but the empirical cumulative exceedance distribution of MMSLA, derived from tide gauges, was included in the extreme sea-level analysis.

The hydrodynamic model was used to predict tide elevations at these locations for a full perigean lunar cycle (1-month). The 1-month tidal time-series were each compared to the Pouto Point tide-gauge location (Site 7, Figure 3-21), and scaling factors were derived for each location, for the full range of the tide. Tidal time-series were then predicted for the duration of the available meteorological record. For example, Figure 3-22 shows the tide predictions for the Pouto Point tide-gauge location, and site 16 at the Kaipara River entrance. Tidal amplification occurs due to topographic constriction of the tidal wave and due to the generation of compound over tides inside the shallowing estuary basins.

Tidal hysteresis was calculated from the hydrodynamic model using the mean sea-level over the simulated lunar month; enabling a mean-sea-level offset to be calculated for each location, relative to a location outside the harbour entrance. This mean sea-level offset due to tidal hysteresis was added to the extreme storm-tide distribution at each output location.

The wind-driven component of storm surge was calculated as described in Sections 2.3.1 and 7.3 by using the wind record to interpolate storm surge from the simulated wind-surge response matrix. The wind-driven component of storm surge differs depending on the output location within the harbour due to the available wind fetch.

The inverse-barometer component of sea level was calculated using the Whenuapai mean sea-level pressure record (Figure 3-23) and Equation 7-1. The inverse-barometer component of sea level was calculated as described in Section 7.3.1, and is shown in Figure 3-23.
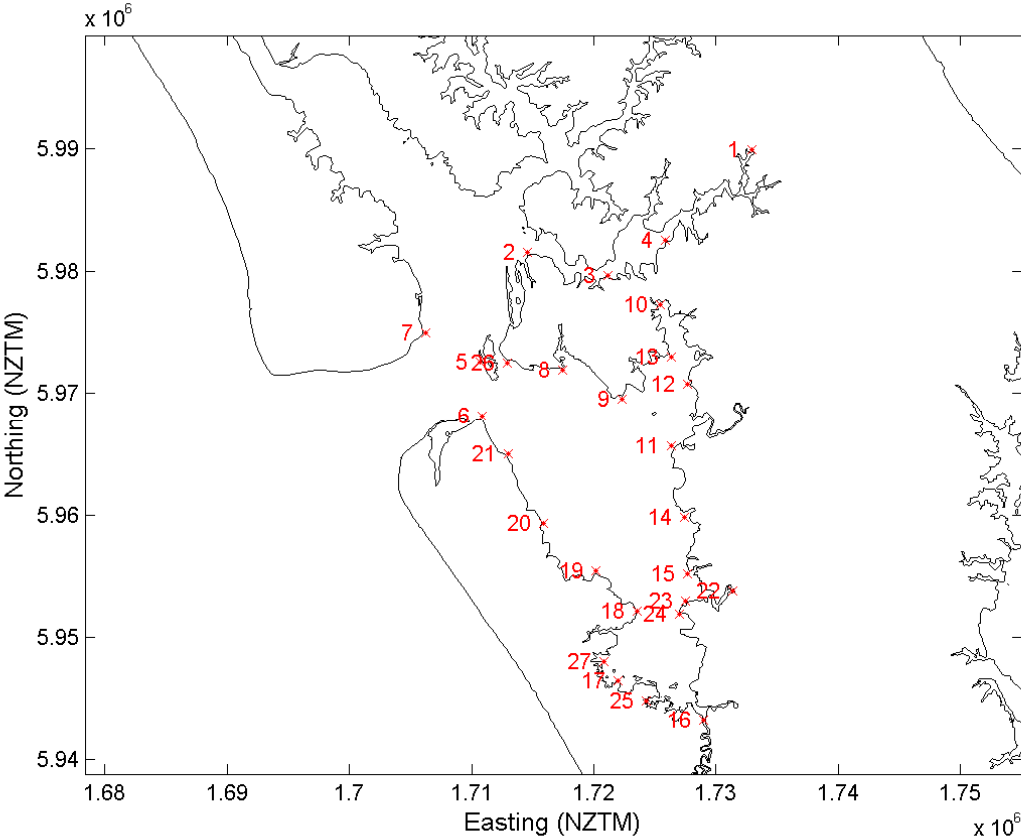
Figure 3-21: Locations of storm-tide model output from the central and southern Kaipara Harbour. The northern Harbour lies within the Northland region.
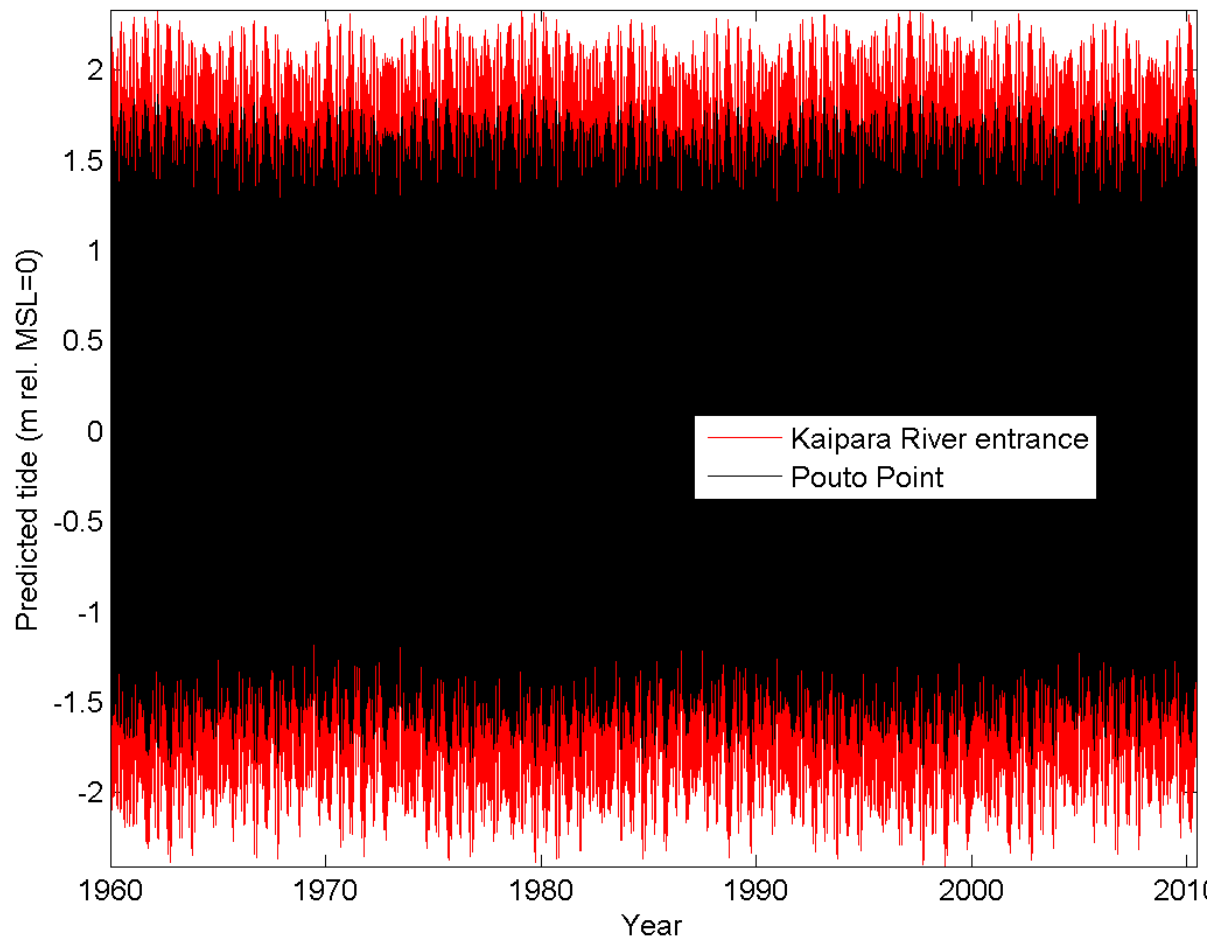
Figure 3-22: Predicted tide at Pouto Point and Kaipara River entrance. Pouto Point tide, site 7 is predicted directly from harmonic analysis of Pouto Point tide-gauge measurements. Tides at Kaipara River entrance, site 16 (and other locations not shown) were predicted by scaling the Pouto Point predictions using hydrodynamic model results. Tides were predicted for the duration of the available wind record.
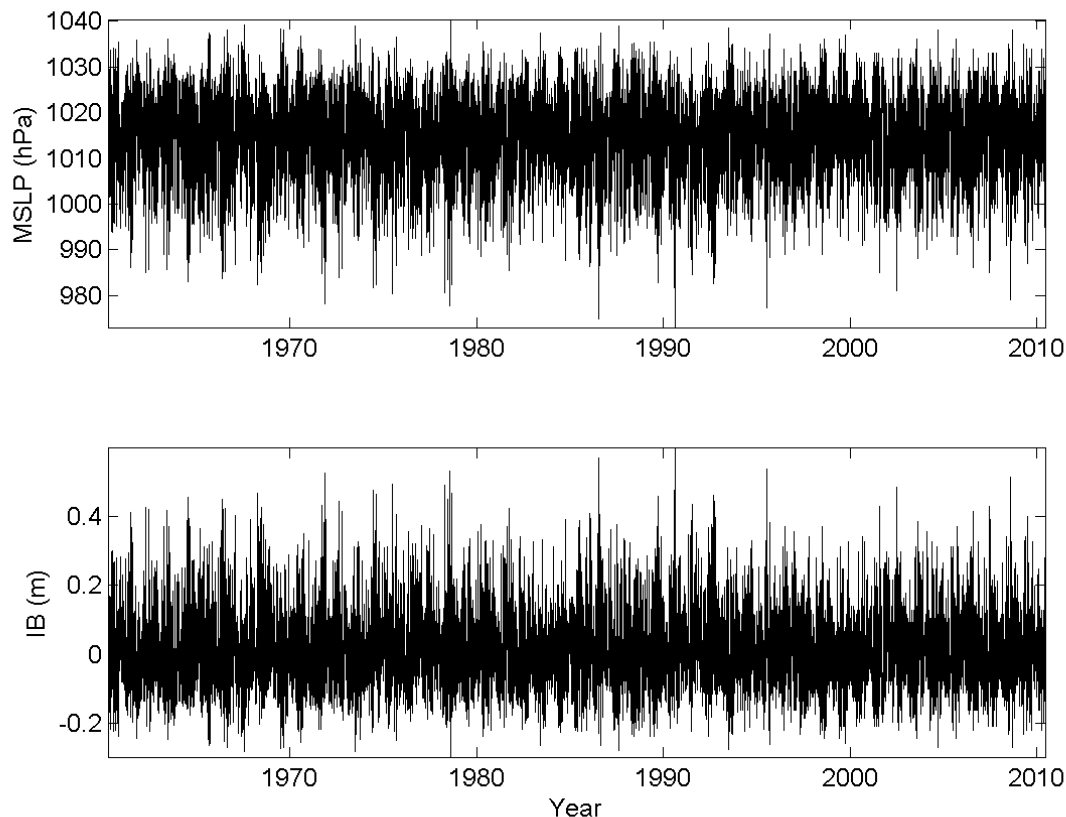
Figure 3-23: Kaipara mean sea-level pressure record and calculated inverse-barometer sea level. MSLP = mean sea-level pressure measured at Whenuapai. IB = inverse-barometer sea level.

Storm-tide time-series were simulated using the methods described in Sections 2.3.1 and 7.3, at 27 locations within the Kaipara Harbour (Figure 3-21), for later extreme sea-level analysis.

Three extreme sea-level frequency–magnitude distributions are shown in Figure 3-24 for Pouto Point and one for the Kaipara River mouth. The black and red lines compare the extreme sea-level distributions calculated using the Pouto Point tide-gauge measurements, using the Monte-Carlo joint-probability (MCJP) technique and a peaks-over-threshold (POT/GPD) technique (see Section 7.2 for more information about these techniques). The record is not long enough (not enough extreme events) to get reliable extreme sea-level estimates using the POT/GPD technique, hence the very flat distribution at low exceedance probabilities; the POT/GPD is shown for comparison purposes.

The black and green lines compare extreme sea-level distributions at Pouto Point derived from measured and simulated data. The IB_{factor} was used as a calibration parameter to ensure that the modelled extreme storm-tide distribution matched that derived from the tide-gauge. The technique was then applied to other locations in the harbour (Figure 3-21). An example is shown in Figure 3-24 (blue line) for the Kaipara River mouth (site 16; Figure 3-21). This demonstrates the significant increase in extreme storm-tide magnitude higher in the estuary arms, due primarily to topographic amplification of the tide (e.g., Figure 3-22), but also to storm surge amplification.

Coastal inundation by storm-tides and waves in the Auckland region

Table 3-8 provides the estimated extreme sea-level frequency–magnitude relationship at Pouto Point based on the MCJP technique applied to the Pouto Point tide-gauge record. Table 3-9 provides the estimated extreme sea-level frequency–magnitude relationship at locations throughout the southern arm of the harbour.

The MCJP technique randomly samples from several sea-level component time-series and empirical cumulative exceedance distributions. In most tide-gauge records, the monthly mean sea-level anomaly is normally distributed. However, the Pouto Point tide-gauge record had a positively skewed MMSLA distribution, which we attribute to the episodic burial of the bubbler orifice by sand for several months on occasion. The sand burial increases the back-pressure in the bubbler tube, causing the gauge to read higher than normal pressures, and this affects the MMSLA component of sea level. As a workaround, we instead used the (normally-distributed) empirical cumulative exceedance distribution of MMSLA from the open-west-coast gauge record located at Anawhata, located 58 km south of the Kaipara Harbour entrance.
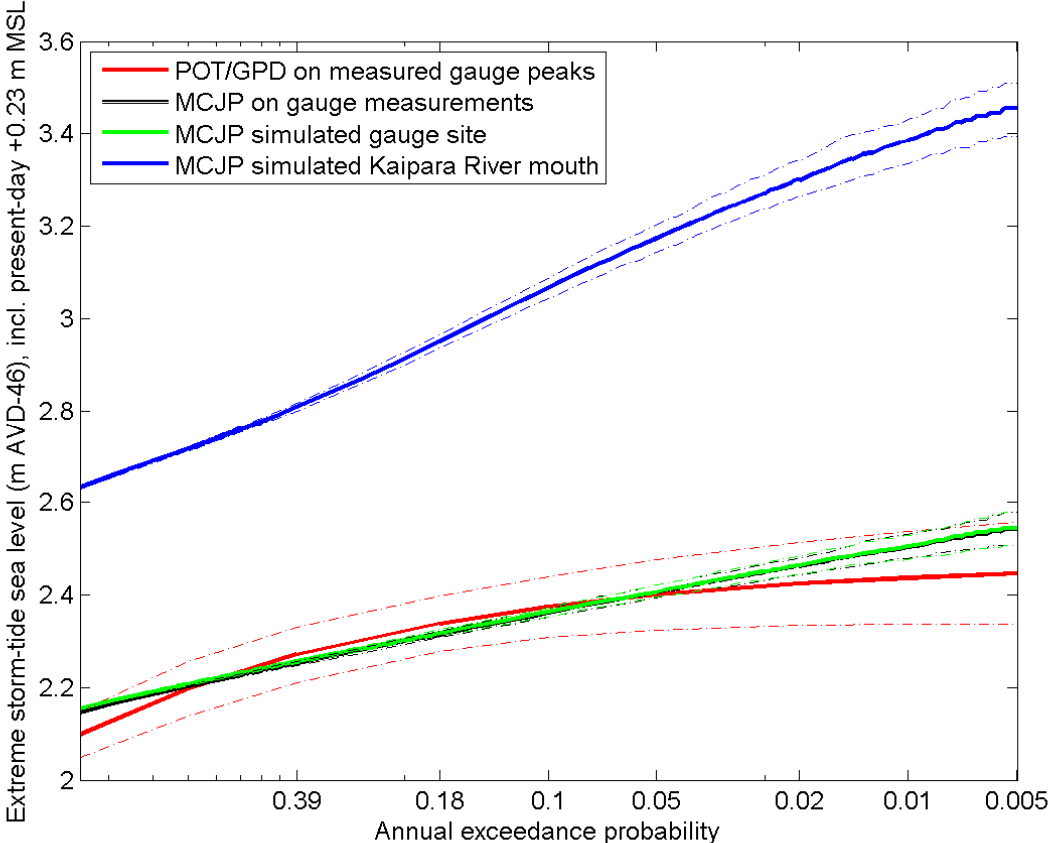
Figure 3-24: Extreme sea-level curves for Pouto Point tide-gauge. Elevations are relative to AVD-46 including +0.23 m offset for baseline mean sea level (present-day estimate). Bold lines marks median values, dashed lines mark 95th percentile confidence intervals.

Table 3-8: Extreme sea-level at Pouto Point. Elevations are relative to AVD-46 including +0.23 m offset for baseline mean sea level (present-day estimate). C.I. = confidence interval. Elevations calculated from tide-gauge data.

AEP	0.39	0.18	0.10	0.05	0.02	0.01	0.005
ARI	2	5	10	20	50	100	200
Median	2.25	2.31	2.36	2.41	2.46	2.50	2.54
Lower 95th C.I.	2.25	2.31	2.35	2.39	2.44	2.48	2.51
Upper 95th C.I.	2.26	2.32	2.37	2.42	2.48	2.53	2.58

Table 3-9: Extreme sea-level in the Kaipara Harbour. Elevations are relative to AVD-46 including +0.23 m offset for baseline mean sea level (present-day estimate). Elevations calculated from simulated data. Locations given in Figure 3-21.

		AEP:	0.39	0.18	0.10	0.05	0.02	0.01	0.005
		ARI:	2 yr	5 yr	10 yr	20 yr	50 yr	100 yr	200 yr
Site number	Easting (NZTM)	Northing (NZTM)							
1	1732914	5989908	2.80	2.87	2.92	2.98	3.04	3.09	3.14
2	1714569	5981549	2.35	2.41	2.45	2.50	2.56	2.60	2.64
3	1721187	5979670	2.53	2.60	2.64	2.69	2.75	2.79	2.84
4	1725821	5982551	2.65	2.72	2.77	2.82	2.88	2.92	2.97
5	1710704	5972533	2.24	2.30	2.34	2.39	2.44	2.49	2.52
6	1710904	5968074	2.28	2.34	2.39	2.43	2.49	2.53	2.57
7	1706237	5974952	2.28	2.34	2.38	2.43	2.48	2.52	2.56
8	1717470	5971893	2.41	2.47	2.51	2.56	2.62	2.66	2.70
9	1722273	5969479	2.50	2.56	2.61	2.66	2.72	2.76	2.81
10	1725440	5977226	2.55	2.62	2.68	2.74	2.82	2.89	2.95
11	1726302	5965647	2.59	2.66	2.72	2.78	2.86	2.91	2.97
12	1727640	5970779	2.59	2.66	2.72	2.77	2.85	2.90	2.96
13	1726306	5972938	2.64	2.71	2.76	2.81	2.88	2.93	2.99
14	1727398	5959766	2.65	2.73	2.79	2.86	2.95	3.01	3.07
15	1727676	5955207	2.72	2.81	2.88	2.96	3.05	3.12	3.19
16	1728962	5943240	2.95	3.10	3.21	3.32	3.44	3.53	3.60
17	1721949	5946471	2.85	2.95	3.03	3.11	3.22	3.29	3.36
18	1723547	5952115	2.76	2.84	2.91	2.98	3.07	3.14	3.20
19	1720204	5955418	2.65	2.72	2.78	2.83	2.91	2.96	3.01
20	1715889	5959302	2.55	2.62	2.67	2.71	2.77	2.82	2.86
21	1712991	5965012	2.38	2.45	2.49	2.54	2.59	2.64	2.68
22	1731343	5953771	2.75	2.86	2.96	3.05	3.16	3.24	3.31
23	1727503	5952984	2.73	2.83	2.91	2.99	3.10	3.17	3.23
24	1727028	5951911	2.78	2.87	2.95	3.04	3.14	3.22	3.28
25	1724252	5944778	2.86	2.97	3.06	3.15	3.27	3.34	3.41

| Site number | Easting (NZTM) | Northing (NZTM) | AEP: 0.39 | 0.18 | 0.10 | 0.05 | 0.02 | 0.01 | 0.005 |
			ARI: 2 yr	5 yr	10 yr	20 yr	50 yr	100 yr	200 yr
26	1712894	5972482	2.34	2.40	2.45	2.49	2.55	2.59	2.63
27	1720787	5948055	2.83	2.91	2.98	3.05	3.15	3.21	3.28

4 Extreme sea-level elevations from storm-tides and waves on the open coasts of the Auckland region

In this section we provide location-specific information, such as data and models, required to explain how the methods from Section 2 were applied to the open coastlines in the Auckland region.

4.1 The open east coast

Section 7.4 outlines the general procedure for calculating extreme sea-level elevations for open-coast locations. To briefly recap, both wave and storm-tide conditions were simulated for the 1970–2000 period, at 37 locations along the eastern open-coast (Figure 4-1). A joint-probability analysis was undertaken (Section 7.2.5) to calculate the likelihood of various coincident storm-tide and wave combinations. Wave setup was then calculated and added to storm-tide elevations to calculate the total combined storm-tide plus wave setup elevation.
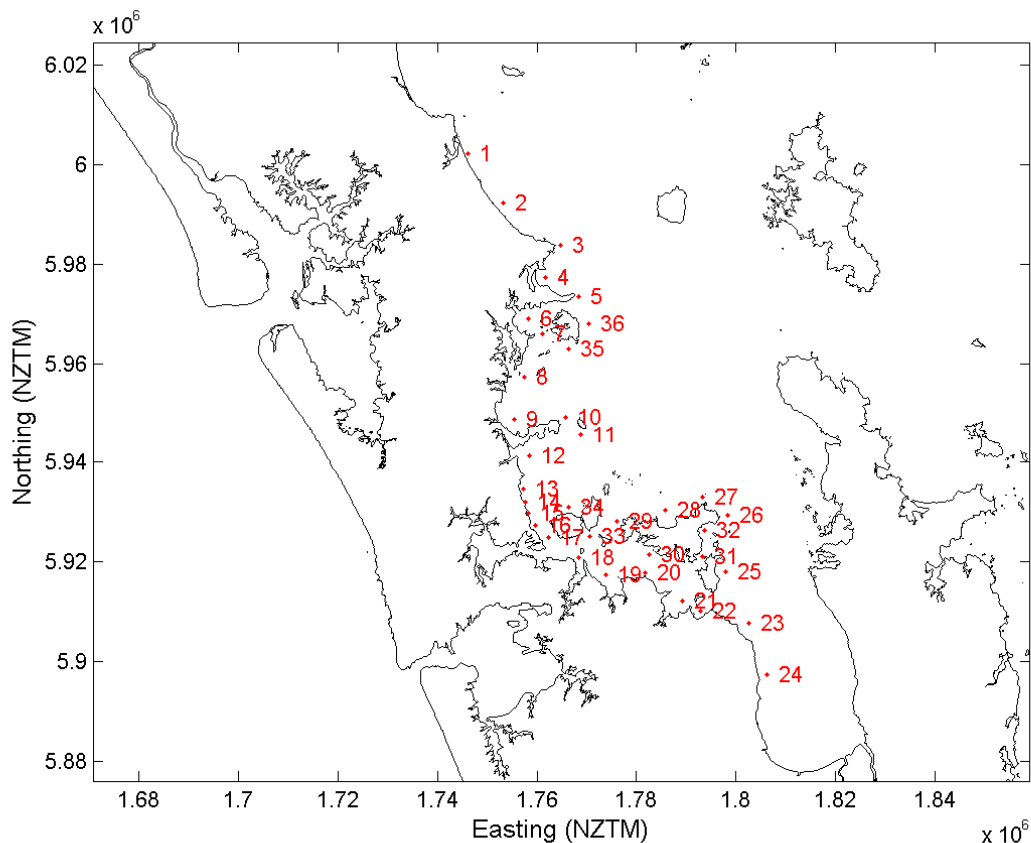
Figure 4-1: Locations of storm-tide and wave simulation output along the east open coast of the Auckland region.

4.1.1 Storm-tide on the eastern open-coast

Time-series of storm-tide sea-level for 1970–2000 were estimated by adding the following three sea-level components:

- Astronomical tide – predicted using NIWA's New Zealand tide model (Stanton et al. 2001; Walters et al. 2001).

- Storm surge – hindcast by the WASP models (http://wrenz.niwa.co.nz/webmodel/coastal).

- Monthly mean sea-level anomaly – derived from the Port of Auckland (Waitemata) tide gauge (e.g., Figure 3-2, Figure 3-3).

Figure 4-2 shows an example of the WASP storm surge prediction at the Port of Auckland tide-gauge location[10], compared to that derived from the tide-gauge measurements. Although not an exact match, it can be seen that the WASP model generally reproduced the magnitude and timing of the storm surges. Figure 4-3 shows the scatter between the measured and modelled storm surges at the tide-gauge location. While there is considerable scatter (at times), the quantile-quantile[11] relationship lies close to the 1:1 line, indicating that the probability distributions of the measured and modelled storm surges are similar. For example, the magnitude of the largest modelled storm surges matches those of the largest measured storm surges.

From the re-constructed storm-tide time-series (tide + storm surge), extreme storm-tide distributions were calculated using the MCJP technique (Table 7-4) for each location, and the distribution of these is shown in Figure 4-4. Storm-tide elevations are shown in Table 4-1.

---

[10] Output from the WASP project is available on NIWA's Coastal Explorer website, at locations along the ~50 m contour around New Zealand. However, storm-surges were simulated over the entire coastal region, including right into the coast during the WASP project, and we have used those inshore results for the present study.
[11] Quantile-quantile, or Q-Q plots are a graphical method of showing how the frequencies or probabilities of two distributions (e.g., model versus measured) compare (e.g., Figure 4-3). If the distributions are similar, then the points will tend to lie on a straight 1:1 line.
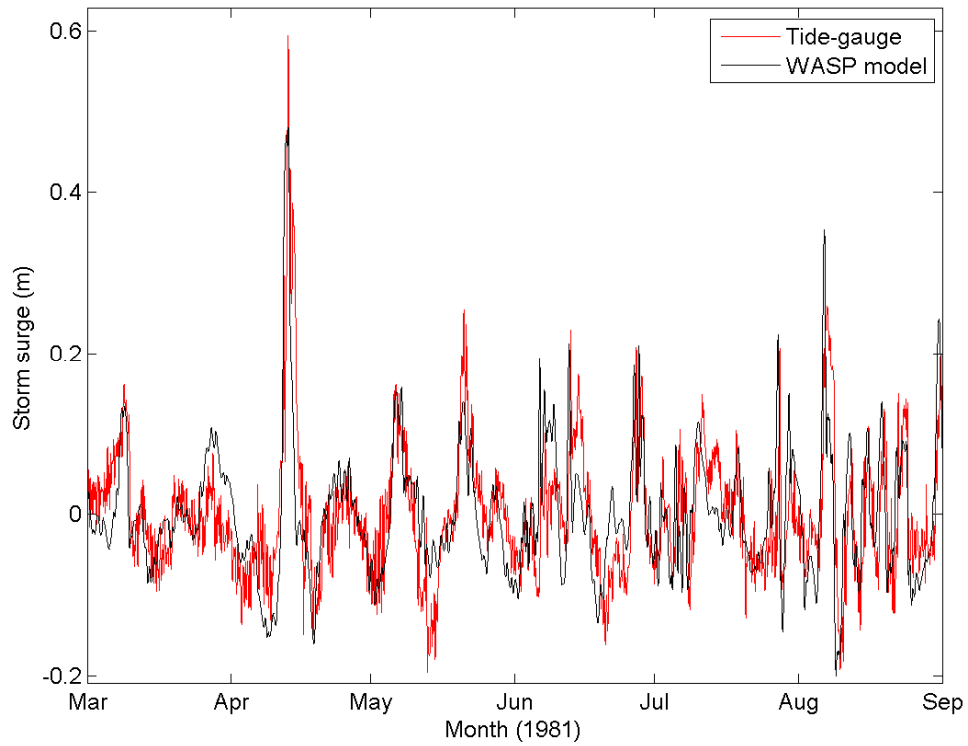
Figure 4-2: Time-series of storm surge at Port of Auckland from tide gauge and WASP model.
Selection chosen to include a large storm surge (in April 1981).
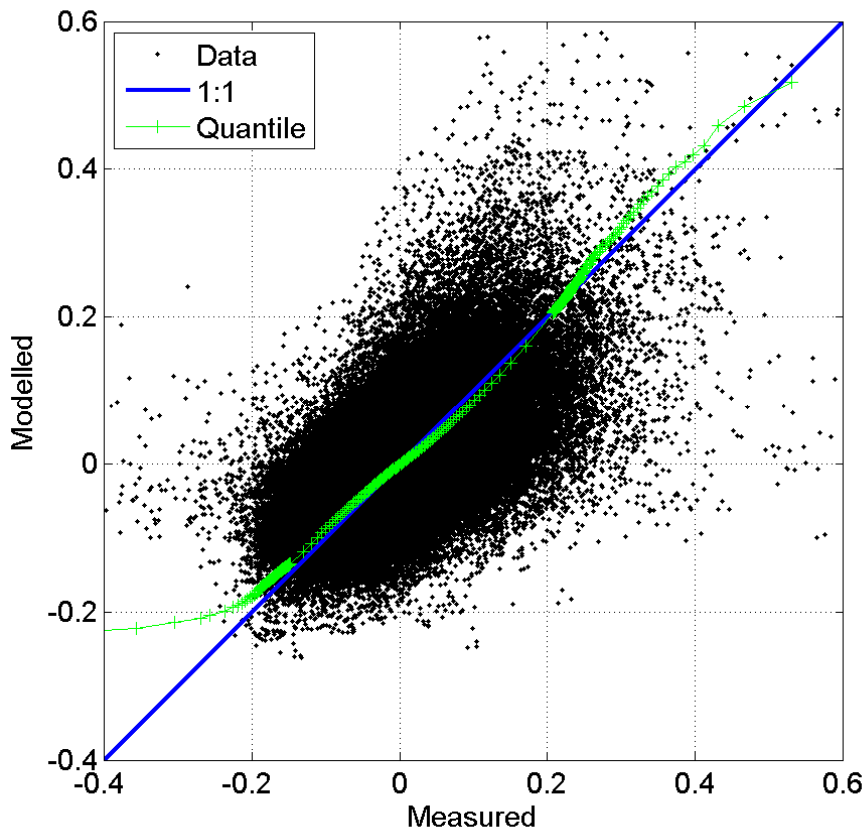
Figure 4-3: Scatter plot of measured (tide gauge) and modelled (WASP) storm surge at Port of Auckland (Waitemata), with quantile-quantile comparison. Values in metres.
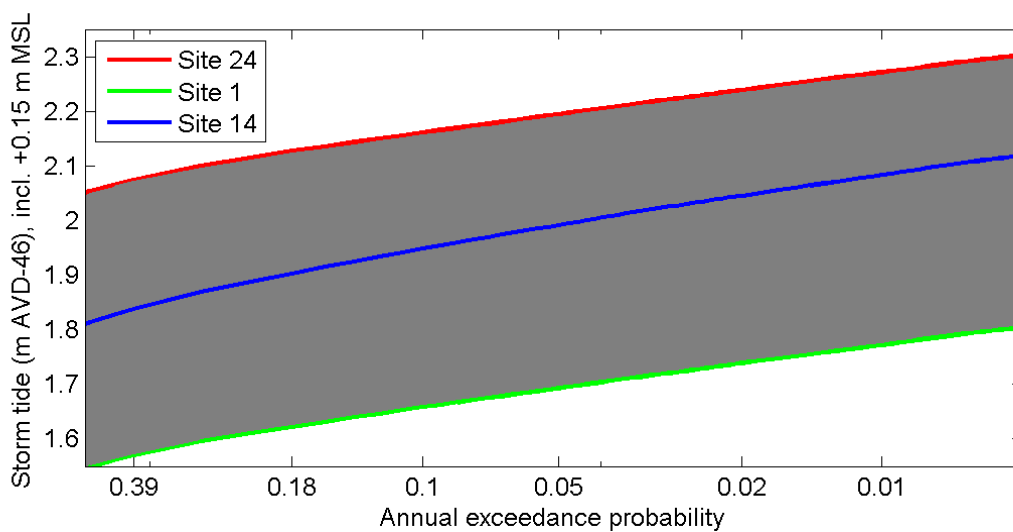
Figure 4-4: Distribution of extreme storm-tides on the open-coast of the Auckland region. Shaded area represents the range of elevations between the 37 sites. Examples given for individual sites 1, 14 and 24 (Figure 4-1).

Table 4-1: Storm-tide elevations on the eastern open-coast. Elevations are relative to AVD-46 including +0.15 m offset for baseline mean sea level (present-day estimate). Sites shown in Figure 4-1.

Site	Easting (NZTM)	Northing (NZTM)	AEP: 0.39 ARI: 2 yr	0.18 5 yr	0.10 10 yr	0.05 20 yr	0.02 50 yr	0.01 100 yr	0.005 200 yr
1	1746045	6002166	1.57	1.62	1.65	1.68	1.72	1.76	1.78
2	1753102	5992291	1.59	1.64	1.67	1.70	1.74	1.77	1.80
3	1764823	5983832	1.62	1.67	1.70	1.73	1.76	1.79	1.81
4	1761674	5977388	1.66	1.71	1.74	1.78	1.82	1.85	1.88
5	1768344	5973565	1.68	1.72	1.76	1.78	1.82	1.84	1.87
6	1758271	5968983	1.78	1.84	1.88	1.92	1.98	2.01	2.05
7	1760994	5965903	1.77	1.82	1.86	1.89	1.94	1.97	2.00
8	1757358	5957292	1.76	1.81	1.85	1.88	1.92	1.95	1.98
9	1755351	5948872	1.76	1.82	1.86	1.89	1.93	1.97	2.00
10	1765782	5949110	1.76	1.81	1.84	1.87	1.91	1.94	1.96
11	1768729	5945579	1.77	1.82	1.85	1.88	1.91	1.94	1.96
12	1758449	5941213	1.81	1.86	1.90	1.93	1.98	2.01	2.04
13	1757328	5934697	1.83	1.89	1.93	1.96	2.01	2.04	2.07
14	1757600	5931984	1.84	1.90	1.94	1.98	2.03	2.06	2.09
15	1758282	5929752	1.85	1.91	1.95	1.99	2.04	2.07	2.10
16	1759748	5927428	1.86	1.93	1.97	2.01	2.06	2.10	2.12
17	1762306	5924882	1.89	1.96	2.00	2.04	2.10	2.13	2.15
18	1768474	5920856	1.93	2.00	2.04	2.09	2.14	2.18	2.20
19	1773944	5917482	1.94	2.00	2.05	2.09	2.14	2.18	2.20
20	1781649	5917865	1.96	2.01	2.05	2.09	2.14	2.17	2.19
21	1789299	5912170	2.00	2.06	2.10	2.14	2.20	2.23	2.26
22	1792968	5910034	2.00	2.06	2.10	2.15	2.20	2.24	2.26
23	1802591	5907745	1.99	2.04	2.07	2.10	2.14	2.17	2.19
24	1806261	5897453	2.07	2.12	2.16	2.19	2.23	2.25	2.28
25	1798030	5918077	1.94	1.98	2.01	2.04	2.07	2.10	2.12
26	1798292	5929361	1.85	1.90	1.93	1.95	1.98	2.00	2.02
27	1793282	5932939	1.81	1.85	1.88	1.91	1.94	1.96	1.98
28	1785826	5930285	1.80	1.84	1.87	1.90	1.93	1.95	1.98
29	1776063	5928106	1.84	1.89	1.93	1.96	1.99	2.02	2.05
30	1782627	5921463	1.94	1.99	2.03	2.06	2.10	2.13	2.15
31	1793244	5921007	1.95	2.00	2.03	2.06	2.10	2.12	2.14
32	1793594	5926216	1.90	1.94	1.97	2.00	2.03	2.06	2.08
33	1770683	5925185	1.90	1.96	2.00	2.04	2.09	2.12	2.14

Site	Easting (NZTM)	Northing (NZTM)	AEP: 0.39 ARI: 2 yr	AEP: 0.18 ARI: 5 yr	AEP: 0.10 ARI: 10 yr	AEP: 0.05 ARI: 20 yr	AEP: 0.02 ARI: 50 yr	AEP: 0.01 ARI: 100 yr	AEP: 0.005 ARI: 200 yr
34	1766404	5930907	1.82	1.87	1.90	1.94	1.97	2.00	2.02
35	1766328	5963017	1.76	1.81	1.84	1.87	1.90	1.93	1.95
36	1770378	5967921	1.71	1.75	1.78	1.81	1.85	1.87	1.89

4.1.2 Waves on the eastern open-coast

Time-series of wave statistics (e.g., height, period and direction) were also derived from WASP hindcasts. There are many islands offshore from Auckland's east coast that affect the wave climate through wave refraction and sheltering, and the spatial resolution of the New Zealand-regional-scale WASP models was too coarse to resolve these features. Therefore, the WASP hindcast was used to drive a nested SWAN wave model with sufficient spatial resolution to translate the WASP wave predictions from offshore in deep water to the Auckland coastline.

Wave modelling methods

The SWAN model (Booij et al. 1999; Ris et al. 1999) is a spectral wave model intended for shallow water applications in coastal and estuarine environments. It computes the evolution of the wave energy spectrum in position (*x, y*) and time (*t*), explicitly taking into account the various physical processes acting on waves in shallow water. The model can incorporate boundary conditions representing waves arriving from outside the model domain.

For the present study, an outer Hauraki Gulf grid ("outer_hauraki") was established at 750 m resolution in both *X* and *Y*, at 0° orientation. The grid origin was located at New Zealand Transverse Mercator (NZTM) coordinates (2640375E, 6437875N). The 130 × 240 cell grid extends for 96.75 km eastward, and 179.25 km northward from the origin. This places the northern limit near Whangarei, and the eastward limit at approximately 175.5°E, to include the western coast of Great Barrier Island (Figure 4-5).

The spectral grid consisted of 33 wave frequencies between 0.0418 Hz and 0.8018 Hz (or periods of 1.2–24 s) geometrically spaced, so that successive frequencies were in the ratio f_{n+1} / f_n = 1.125, while 24 wave direction bins of 15° width were used. The shallow water effects of depth-limited breaking, bed friction and triad nonlinear interactions were activated, with default parameterisations for SWAN Version 40.85 (SWAN 2011) used.

In order to simulate wave development in a given region, it is necessary to specify the winds blowing over the region. Waves entering the region through any open boundaries also need to be included, while the effects of changing water levels and currents can also be accounted for if these can be provided. In general all of these inputs vary both in space and time. The SWAN model performs interpolation of input wind, sea level and current fields to the required spatial and temporal resolution of the nearshore model.

These wave and wind forcings were derived from larger scale simulations (approximately 30 km resolution) carried out by NIWA under the Waves and Storm surge Projections (WASP) programme, described below.

The NIWA tidal model is based on an unstructured mesh that provides much finer resolution in coastal waters than the 9 km regular grid used for wave and wind inputs. Hence for the present study, tidal currents and sea levels were input on a 1 km resolution regular grid (AKLTIDE-1) covering the Auckland region, at 15 minute time intervals.
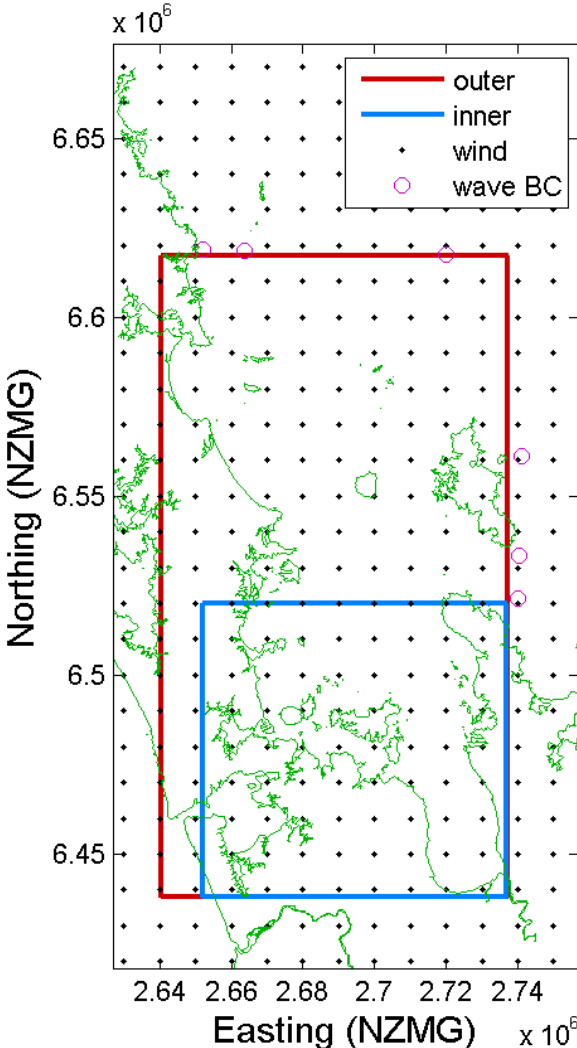
Figure 4-5: Outer and inner SWAN wave model grids of the Hauraki Gulf. Dots mark wind input locations on 9 km grid. Circles mark wave boundary conditions from the WASP project.

WASP wave hindcasts

At a global level, the hindcasts in the WASP programme were based on inputs from the ERA-40 Reanalysis dataset (Uppala et al. 2005) from the European Centre for Medium Range Weather Forecasts (ECMWF), which provided wind and pressure fields over a 45-year period, from October 1957 - September 2002, on a global domain at 1.125 x 1.125 degree resolution in longitude and latitude (125 km at the equator).

To provide wave hindcasts, the Wavewatch III™ model (Tolman, H. L. 1991; Tolman, Hendrik L. 2007) was first run on a global grid ('era40gw_125') matching the input ERA40 grid (see Uppala et al. 2005) except for being reduced to the latitude range -81° to +81°. To provide more detailed outputs at a New Zealand regional scale, two different nested hindcasts were then run. The first of these ('waspnzw_10'), run on a nested subdomain covering waters around New Zealand at 0.125° x 0.09375° resolution (approximately 10 km), used the same (low resolution) wind inputs as the global wave model, so the finer resolution served only to interpolate wave conditions into nearshore locations. A second regional hindcast ('rcm_9_era') was run for the years 1970-2000, nested in the same global wave simulation. For this, ERA40 winds had been downscaled by a Regional Climate Model. These wind fields were interpolated to a regular latitude/longitude regional grid ('rcm_9') at approximately 9 km resolution for wave model simulations. No air-sea temperature difference fields were available, so no stability corrections were made to the wind input term for this simulation.

The latter ('rcm_era') hindcast was used in the present work to provide both wind and wave inputs for the Hauraki Gulf SWAN model. Wave boundary conditions were specified as directional spectra on the open boundaries of the outer Hauraki Gulf SWAN grid.

Verification

The model was tested against data from two wave buoy deployments, both in the northern part of the Gulf – no suitable records were available for the more protected inner Gulf. The first was a Waverider buoy deployed by the then Auckland Regional Council between 15 May 1998 and 10 June 2004 at (36.8833°S, 175.0833°E) near the Mokohinau Islands. The second was from a NIWA wave buoy located at (36.8833°S, 175.0833°E) near Mangawhai Beach from 1 September 1996 to 30 November 1996.

Figure 4-6 – Figure 4-11 compare data and model in the form of colour-scaled plots of the joint occurrence distribution of measured and modelled values of each wave parameter (significant height H_{m0}, peak period T_{peak}, and peak direction $θ_{peak}$), for all measurement times within the simulation period. Figure 4-6–Figure 4-8 cover the comparison for the Mokohinau Islands buoy site and Figure 4-9–Figure 4-11 the Mangawhai buoy site. Quantile-quantile plots of the same collocated measured and modelled values of significant wave height and peak period are overlaid (red lines). Additionally, percentile values of modelled parameters were derived for the full simulation period, along with corresponding percentile values derived from the full measurement record, seasonally-adjusted to give equal weight to each month. These are compared in the green quantile-quantile lines: this is a comparison that can be made for non-overlapping records, though it is not needed in this case.

At both locations the model gave some over prediction of wave heights in moderate conditions but show good agreement in more energetic conditions, with quantile-quantile plots remaining close to the equivalence line. Peak wave period tends to be underestimated by the model. Peak wave directions at the Mokohinau site predominantly lie in the northeast quadrant (0–90°) and the north (340–360°), open to the Pacific Ocean, with waves from the southwest quadrant (180–270°) of secondary importance. Agreement between measured and modelled directions is generally good, although there is a population of events in which the model expects peak waves from the south-west while the measured waves are predominantly from the north east.

These results suggest that the model is overemphasising local generation relative to oceanic swell, possibly through input wind speeds being overestimated, at least during south-westerly conditions. A more detailed treatment of local wind fields over the Hauraki Gulf may be needed to improve this. For locations with open-ocean exposure, this will be of less importance in the most energetic conditions, which generally involve north-easterly winds acting over much longer fetches.
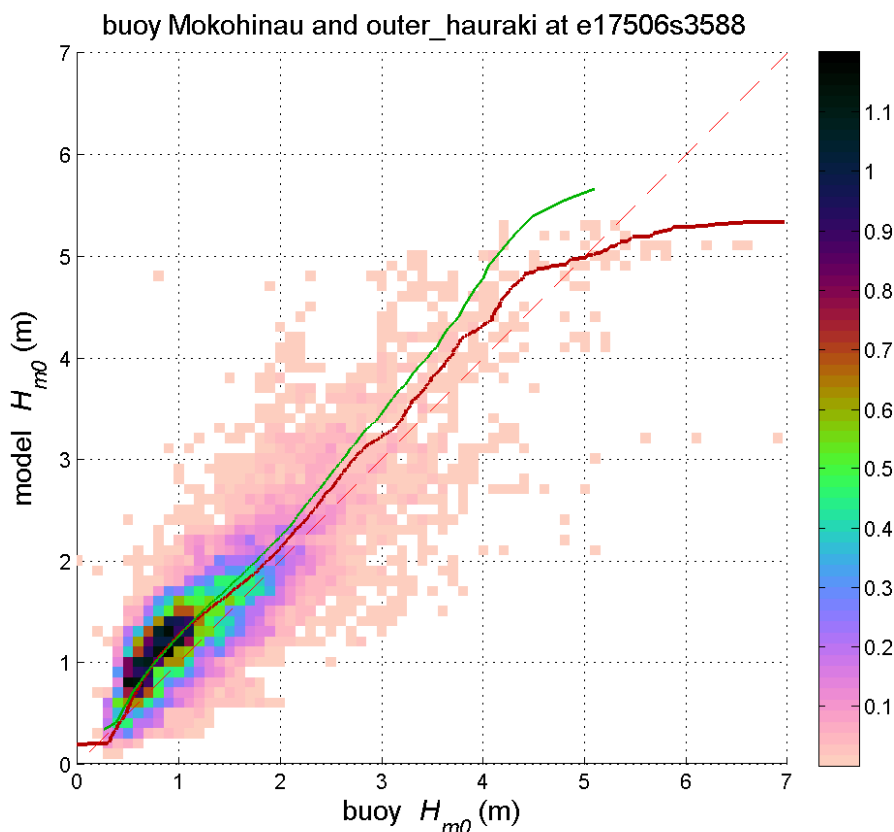
Figure 4-6: Comparison of significant wave height (H_{m0}) values predicted by the outer Hauraki Gulf SWAN model with measurements from the Mokohinau Islands Waverider buoy. The colour scale shows the joint occurrence distribution of measured and predicted wave heights, while the solid lines show quantile-quantile plots, either using coincident records (red line), or seasonally-adjusted statistics derived from all records (green line).
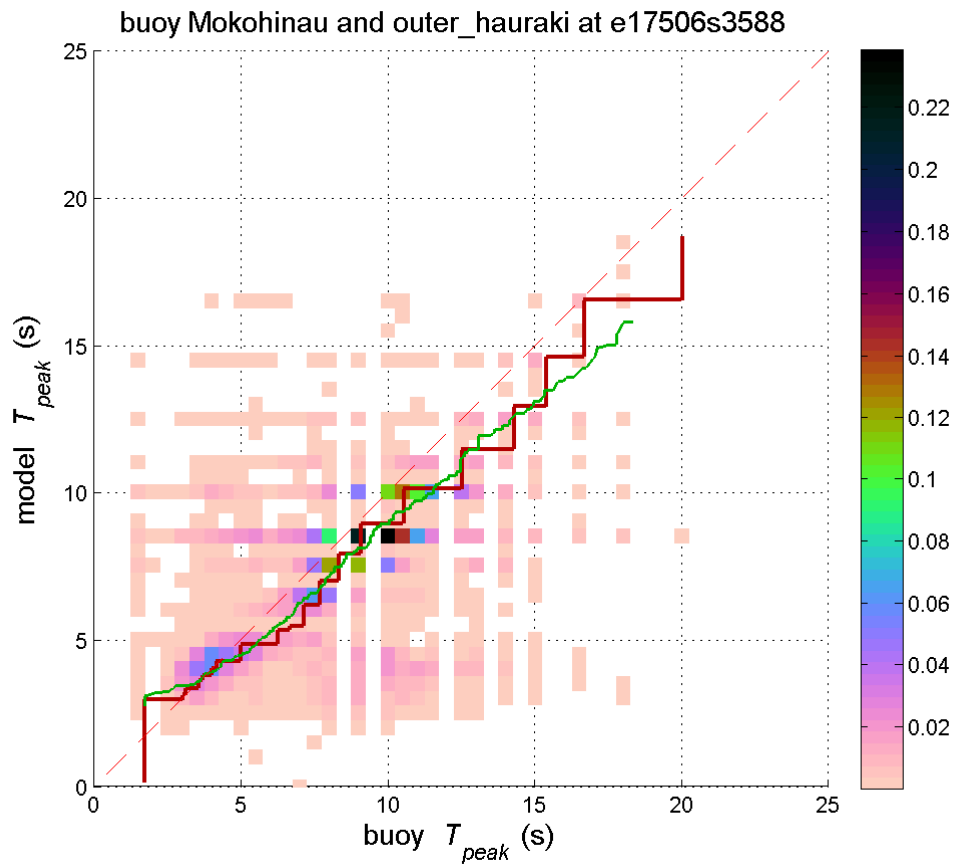
Figure 4-7: Comparison of peak wave period (T_{peak}) values predicted by the outer Hauraki Gulf SWAN model with measurements from the Mokohinau Islands Waverider buoy. The colour scale shows the joint occurrence distribution of measured and predicted wave heights, while the solid lines show quantile-quantile plots, either using coincident records (red line), or seasonally-adjusted statistics derived from all records (green line).
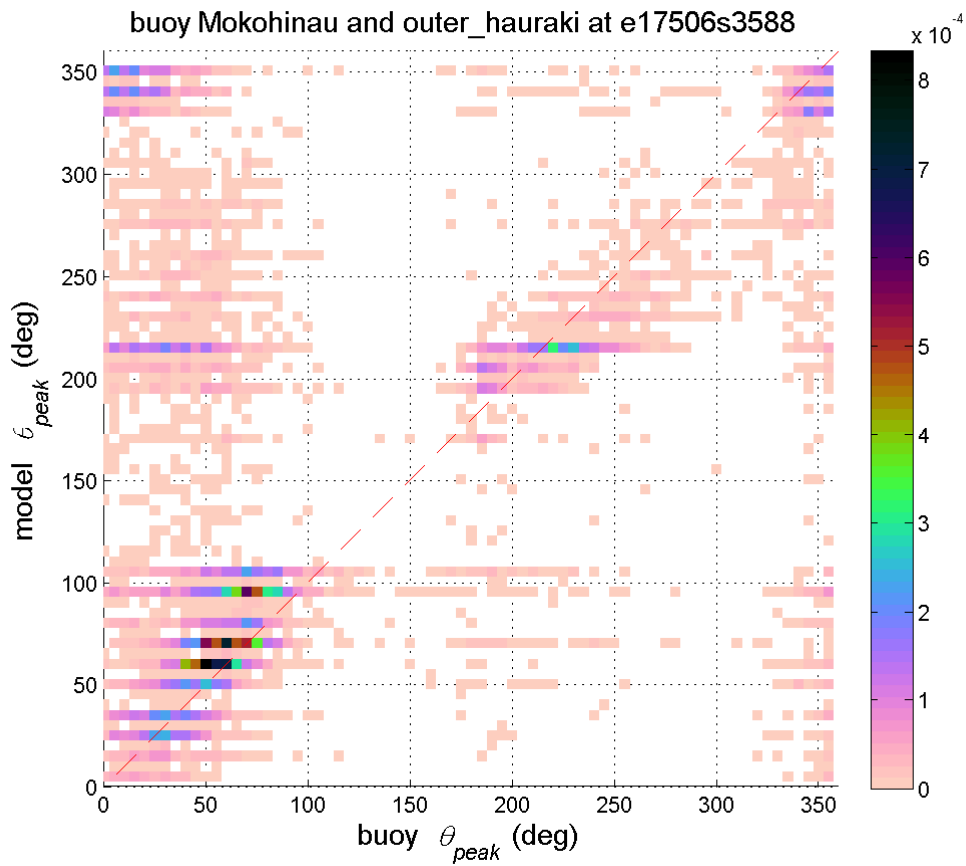
Figure 4-8: Comparison of peak wave direction (θ_{peak}) values predicted by the outer Hauraki Gulf SWAN model with measurements from the Mokohinau Islands Waverider buoy. The colour scale shows the joint occurrence distribution of measured and predicted wave heights.
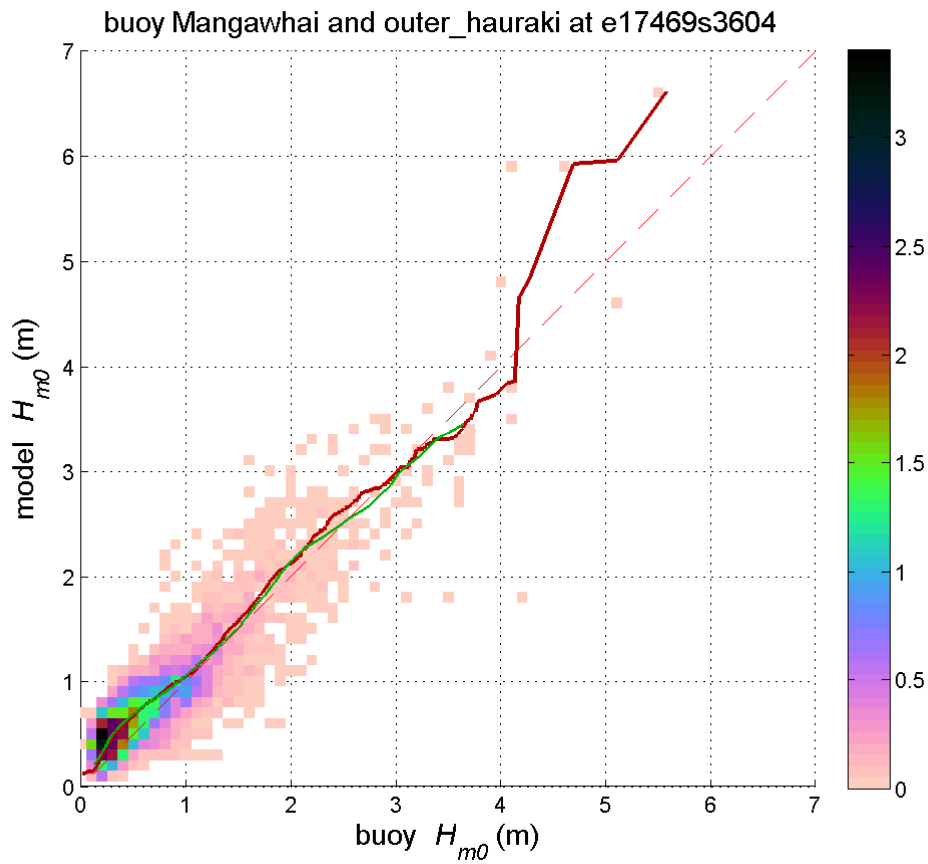
Figure 4-9: Comparison of significant wave height (H_{m0}) values predicted by the outer Hauraki Gulf SWAN model with measurements from the Mangawhai wave buoy. The colour scale shows the joint occurrence distribution of measured and predicted wave heights, while the solid lines show quantile-quantile plots, either using coincident records (red line), or seasonally-adjusted statistics derived from all records (green line).
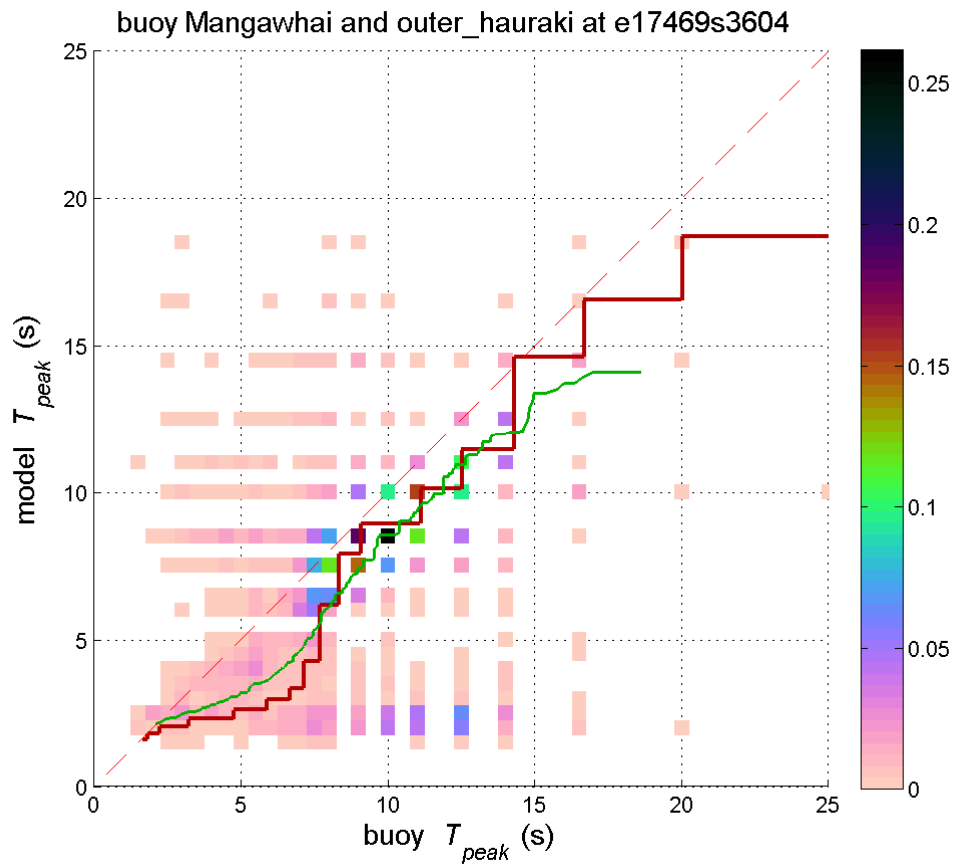
Figure 4-10: Comparison of peak wave period (T_{peak}) values predicted by the outer Hauraki Gulf SWAN model with measurements from the Mangawhai wave buoy. The colour scale shows the joint occurrence distribution of measured and predicted wave heights, while the solid lines show quantile-quantile plots, either using coincident records (red line), or seasonally-adjusted statistics derived from all records (green line).
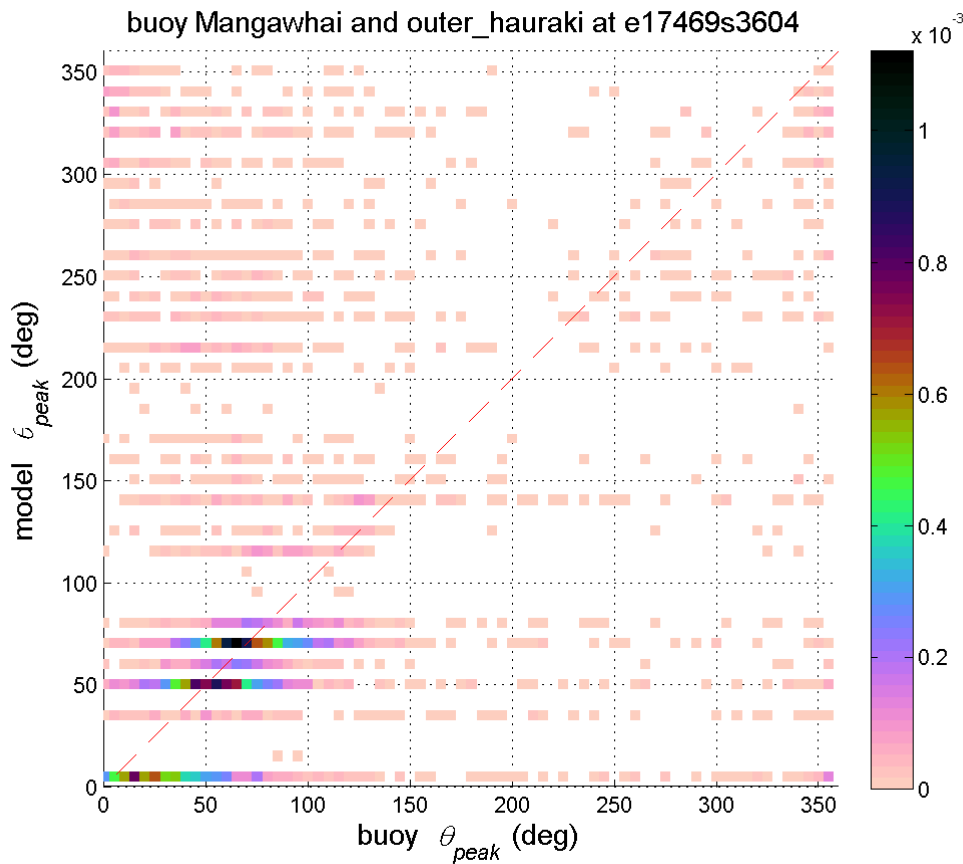
Figure 4-11: Comparison of peak wave direction (θ_{peak}) values predicted by the outer Hauraki Gulf SWAN model with measurements from the Mangawhai wave buoy. The colour scale shows the joint occurrence distribution of measured and predicted wave heights.

Extreme wave analysis

The generalised Pareto distribution (GPD) was fitted to peaks-over-threshold (POT) wave data to predict the likelihood of extreme wave heights. The GPD was fitted to the largest 5% of significant wave height peaks, with peaks separated by at least three days to be classified as separate events.

As a cautionary note, regional-scale wave models such as used here are known for under-predicting the very largest waves, because they often don't have sufficient temporal and spatial resolution and accuracy of the wind-fields in the strongest storms. Although good comparisons were obtained with the available buoy records, the buoy records are short and it is likely that the wave hindcast used here is similarly affected. The buoy records themselves are too short to conduct reliable extreme-wave analyses. As a sensitivity analysis Equation 2-1 was evaluated for all 100-year ARI significant wave heights (Table 4-2), using a 1:7 beach slope and 10 s wave period. The effect of increasing the significant wave height by 50% was to increase wave setup by 0.12–0.37 m, with a medium of 0.27 m. This sensitivity has not been added to the calculated storm-tide plus wave setup elevations, but the user may wish to include an allowance for this in an additional freeboard factor.
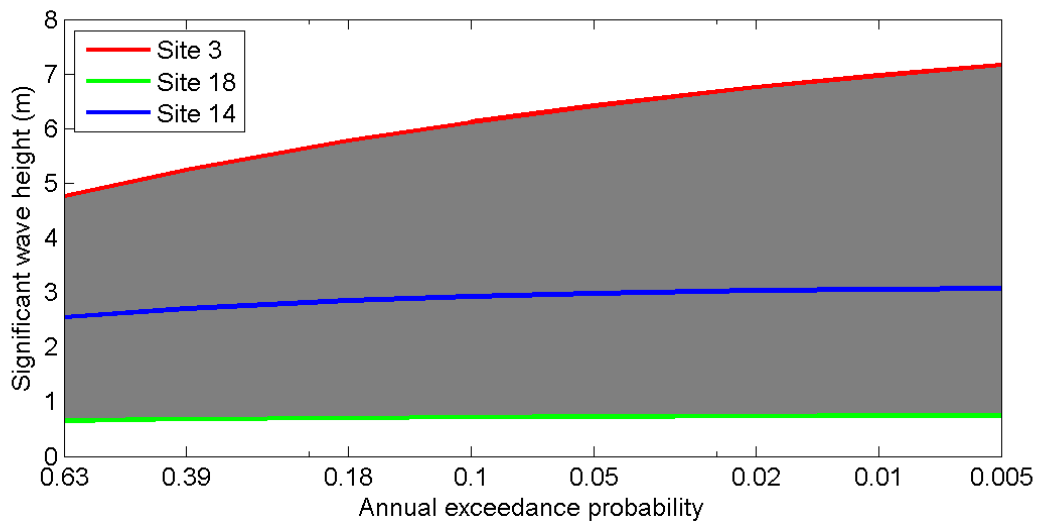
Figure 4-12: Distribution of extreme significant wave height on the eastern open-coast of the Auckland region. Shaded area represents the range of elevations between the 37 sites. Examples given for individual sites 3, 14 and 18 (Figure 4-1).

Table 4-2: Extreme significant wave heights offshore from the eastern open coast at same sites as Table 4-1 and Figure 4-1. Extremes calculated from 1970–2000 wave hindcast data.

Site	Easting (NZTM)	Northing (NZTM)	AEP: 0.39 ARI: 2 yr	AEP: 0.18 ARI: 5 yr	AEP: 0.10 ARI: 10 yr	AEP: 0.05 ARI: 20 yr	AEP: 0.02 ARI: 50 yr	AEP: 0.01 ARI: 100 yr	AEP: 0.005 ARI: 200 yr
1	1746045	6002166	4.57	5.08	5.40	5.69	6.01	6.21	6.39
2	1753102	5992291	4.87	5.42	5.77	6.09	6.45	6.68	6.89
3	1764823	5983832	5.24	5.77	6.12	6.42	6.76	6.97	7.16
4	1761674	5977388	4.14	4.56	4.83	5.06	5.31	5.47	5.61
5	1768344	5973565	4.88	5.34	5.62	5.87	6.14	6.31	6.45
6	1758271	5968983	1.62	1.79	1.91	2.02	2.16	2.25	2.33
7	1760994	5965903	1.64	1.82	1.95	2.07	2.22	2.33	2.44
8	1757358	5957292	3.27	3.63	3.87	4.07	4.30	4.45	4.58
9	1755351	5948872	3.01	3.27	3.43	3.56	3.70	3.78	3.85
10	1765782	5949110	3.56	3.89	4.09	4.28	4.48	4.61	4.73
11	1768729	5945579	3.29	3.66	3.90	4.12	4.37	4.53	4.68
12	1758449	5941213	3.02	3.35	3.57	3.76	3.97	4.11	4.23
13	1757328	5934697	2.89	3.14	3.29	3.42	3.56	3.65	3.72
14	1757600	5931984	2.71	2.85	2.93	2.98	3.03	3.06	3.07
15	1758282	5929752	2.76	2.93	3.02	3.09	3.15	3.19	3.22
16	1759748	5927428	2.54	2.71	2.81	2.89	2.98	3.03	3.07
17	1762306	5924882	2.11	2.26	2.35	2.44	2.53	2.58	2.63
18	1768474	5920856	0.68	0.70	0.72	0.73	0.74	0.74	0.75

Site	Easting (NZTM)	Northing (NZTM)	AEP: 0.39 / ARI: 2 yr	AEP: 0.18 / ARI: 5 yr	AEP: 0.10 / ARI: 10 yr	AEP: 0.05 / ARI: 20 yr	AEP: 0.02 / ARI: 50 yr	AEP: 0.01 / ARI: 100 yr	AEP: 0.005 / ARI: 200 yr
19	1773944	5917482	1.71	1.81	1.87	1.92	1.98	2.01	2.04
20	1781649	5917865	1.49	1.58	1.64	1.69	1.75	1.79	1.82
21	1789299	5912170	1.26	1.31	1.33	1.35	1.37	1.38	1.39
22	1792968	5910034	0.78	0.79	0.80	0.80	0.80	0.80	0.81
23	1802591	5907745	3.09	3.31	3.45	3.57	3.70	3.78	3.85
24	1806261	5897453	2.64	2.79	2.89	2.97	3.05	3.10	3.14
25	1798030	5918077	3.11	3.33	3.47	3.58	3.71	3.79	3.86
26	1798292	5929361	4.04	4.39	4.63	4.83	5.07	5.22	5.36
27	1793282	5932939	4.25	4.65	4.91	5.14	5.41	5.58	5.74
28	1785826	5930285	4.12	4.53	4.82	5.08	5.39	5.61	5.81
29	1776063	5928106	2.07	2.15	2.19	2.22	2.26	2.28	2.30
30	1782627	5921463	1.06	1.11	1.13	1.15	1.17	1.19	1.20
31	1793244	5921007	1.13	1.19	1.23	1.26	1.30	1.32	1.34
32	1793594	5926216	2.09	2.34	2.50	2.64	2.80	2.91	3.01
33	1770683	5925185	0.85	0.88	0.89	0.90	0.90	0.91	0.91
34	1766404	5930907	3.15	3.45	3.65	3.82	4.02	4.16	4.27
35	1766328	5963017	3.87	4.35	4.67	4.96	5.30	5.53	5.74
36	1770378	5967921	4.82	5.26	5.54	5.77	6.03	6.20	6.34

4.1.3 Combined storm-tide plus wave setup on the eastern open coast

Joint-probability analyses of both extreme storm-tides and waves were undertaken using coinciding significant wave height, wave period, and storm-tide sampled at each high tide. A joint-probability analysis of storm-tides and waves describes the combined likelihood of a high storm-tide and large wave event occurring at the same time (Figure 7-1).

At each location, the highest combined storm-tide plus wave setup elevation was determined for each annual exceedance probability, as described in Section 7.4. These values are presented in Table 4-3. A map of the 0.01 AEP storm-tide plus wave setup elevations is shown in Figure 4-13, and the contribution of wave setup above the storm-tide alone is shown in Figure 4-14. As expected, this shows the largest contribution of wave setup (~0.8 m) to the 0.01 AEP combined storm-tide plus wave setup elevations on the more wave exposed locations, relative to wave-sheltered beaches in the inner Hauraki Gulf such as Karaka Bay (~0.1 m).

Table 4-3: Maximum storm-tide plus wave setup elevations along the eastern open-coast.
Elevations are relative to AVD-46 and include a +0.15 m mean-sea-level offset (1999–2008).

		Joint AEP:	0.39	0.18	0.10	0.05	0.02	0.01	0.005
		Joint ARI:	2 yr	5 yr	10 yr	20 yr	50 yr	100 yr	200 yr
Site	Easting (NZTM)	Northing (NZTM)							
1	1746045	6002166	2.07	2.23	2.30	2.39	2.48	2.54	2.66
2	1753102	5992291	2.12	2.28	2.38	2.48	2.60	2.64	2.75
3	1764823	5983832	2.15	2.29	2.40	2.49	2.60	2.68	2.76
4	1761674	5977388	2.00	2.13	2.21	2.28	2.37	2.46	2.50
5	1768344	5973565	2.32	2.47	2.57	2.67	2.78	2.84	2.90
6	1758271	5968983	1.83	1.89	1.94	2.00	2.06	2.11	2.15
7	1760994	5965903	1.86	1.91	1.95	2.01	2.08	2.13	2.19
8	1757358	5957292	2.04	2.18	2.26	2.33	2.45	2.50	2.56
9	1755351	5948872	2.05	2.17	2.26	2.35	2.42	2.50	2.57
10	1765782	5949110	2.19	2.32	2.41	2.49	2.62	2.68	2.74
11	1768729	5945579	2.08	2.20	2.28	2.37	2.45	2.51	2.60
12	1758449	5941213	2.05	2.17	2.25	2.35	2.43	2.52	2.57
13	1757328	5934697	2.08	2.20	2.28	2.35	2.46	2.52	2.56
14	1757600	5931984	2.07	2.16	2.24	2.32	2.40	2.44	2.50
15	1758282	5929752	2.07	2.17	2.25	2.31	2.41	2.46	2.55
16	1759748	5927428	2.15	2.27	2.33	2.40	2.50	2.55	2.60
17	1762306	5924882	2.02	2.14	2.21	2.29	2.37	2.40	2.46
18	1768474	5920856	2.00	2.08	2.13	2.18	2.24	2.28	2.31
19	1773944	5917482	2.07	2.18	2.25	2.31	2.39	2.44	2.48
20	1781649	5917865	2.07	2.16	2.22	2.29	2.35	2.39	2.43
21	1789299	5912170	2.09	2.18	2.25	2.31	2.37	2.42	2.46
22	1792968	5910034	2.05	2.15	2.21	2.26	2.32	2.35	2.38
23	1802591	5907745	2.38	2.50	2.58	2.65	2.75	2.83	2.87
24	1806261	5897453	2.32	2.43	2.50	2.56	2.65	2.70	2.75
25	1798030	5918077	2.34	2.46	2.54	2.63	2.72	2.78	2.83
26	1798292	5929361	2.33	2.45	2.53	2.61	2.71	2.78	2.91
27	1793282	5932939	2.28	2.42	2.50	2.61	2.73	2.81	2.90
28	1785826	5930285	2.29	2.44	2.56	2.65	2.78	2.86	2.96
29	1776063	5928106	2.25	2.35	2.41	2.48	2.56	2.61	2.66
30	1782627	5921463	2.00	2.08	2.12	2.17	2.23	2.26	2.29
31	1793244	5921007	2.00	2.05	2.09	2.14	2.20	2.24	2.28
32	1793594	5926216	2.07	2.16	2.24	2.31	2.39	2.46	2.52
33	1770683	5925185	2.04	2.13	2.18	2.23	2.29	2.31	2.34
34	1766404	5930907	2.13	2.25	2.32	2.40	2.50	2.57	2.63
35	1766328	5963017	2.15	2.30	2.42	2.52	2.65	2.75	2.77
36	1770378	5967921	2.32	2.47	2.58	2.68	2.77	2.87	2.93

Figure 4-13:1% annual exceedance probability storm-tide plus wave setup elevations on the eastern open-coast. Elevations are relative to AVD-46 and include +0.15 m mean sea-level offset (1999–2008).
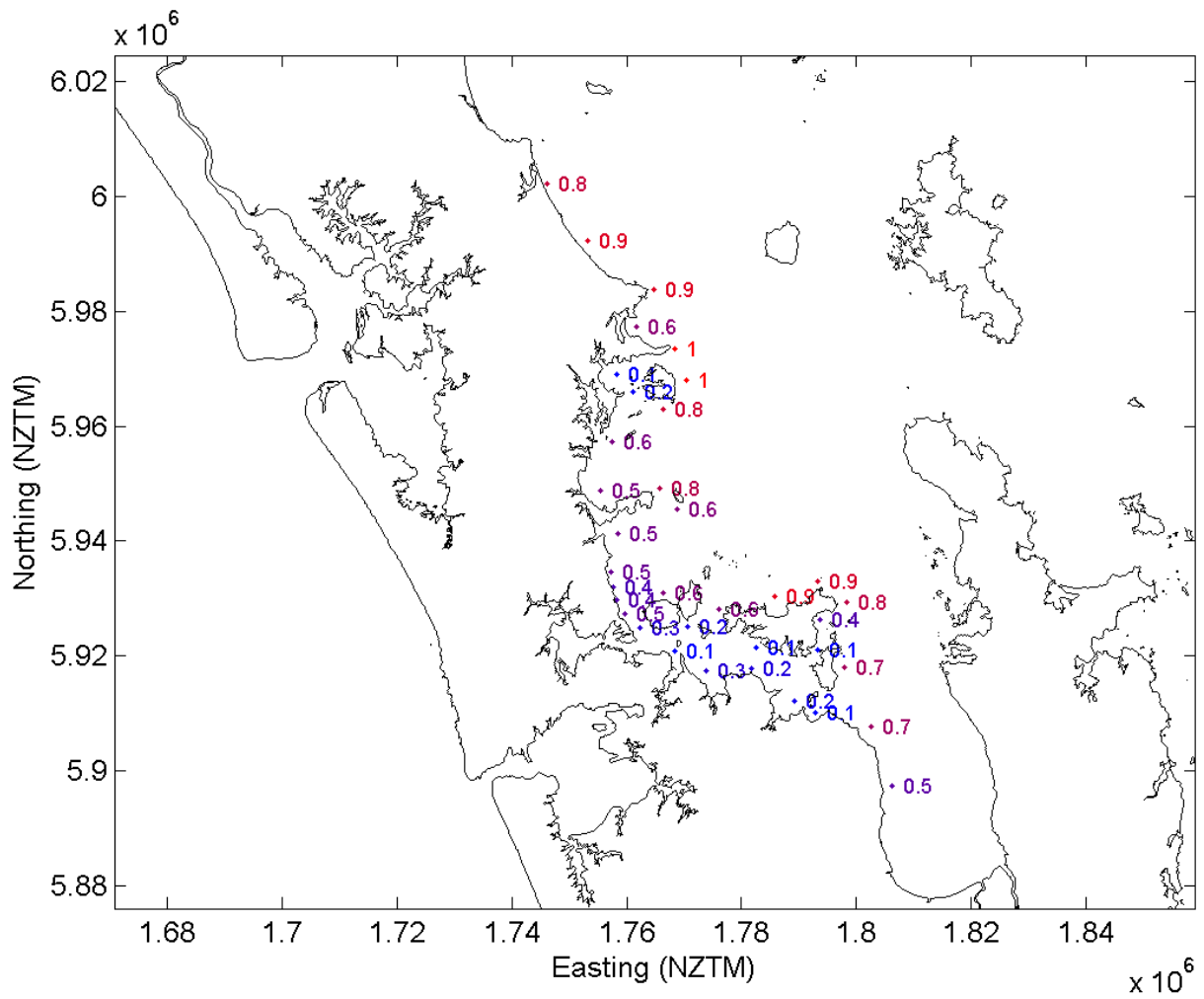
Figure 4-14: Difference between 1% annual exceedance probability storm-tide plus wave setup and storm-tide-only elevations on the eastern open-coast. Elevations in metres.

Coastal inundation by storm-tides and waves in the Auckland region

4.2 East-coast estuaries

Storm-tide elevations in the numerous relatively small east-coast harbours and estuaries were calculated as follows:

- The maximum storm-tide plus wave setup elevations calculated for the open east coast were applied to the harbour entrances.

- The storm-tide component is expected to amplify inside the harbours. An amplification factor that increased with distance from the harbour entrance was applied to the storm-tide component.

The calculated elevations are shown in Table 4-4.

Table 4-4: Maximum storm-tide plus wave setup elevations in small east-coast estuaries.
Elevations are relative to AVD-46 and include a +0.15 m mean-sea-level offset (1999–2008).

Site	Easting (NZTM)	Northing (NZTM)	Joint AEP: 0.39 / Joint ARI: 2 yr	0.18 / 5 yr	0.10 / 10 yr	0.05 / 20 yr	0.02 / 50 yr	0.01 / 100 yr	0.005 / 200 yr
Mangawhai Harbour	1742349	6001359	2.11	2.27	2.35	2.44	2.52	2.59	2.70
Whangateau Harbour	1759163	5974912	2.05	2.17	2.25	2.33	2.42	2.52	2.55
Whangateau Harbour	1758250	5978697	2.02	2.15	2.23	2.31	2.39	2.49	2.52
Omaha R. (Whangateau Hbr)	1756538	5977574	2.04	2.16	2.24	2.32	2.41	2.51	2.54
Matakana River estuary	1753842	5971395	1.85	1.92	1.97	2.03	2.09	2.14	2.18
Matakana River estuary	1754603	5971927	1.85	1.91	1.96	2.02	2.08	2.13	2.17
Matakana River estuary	1754432	5974837	1.87	1.93	1.98	2.04	2.10	2.15	2.20
Matakana River estuary	1755060	5972536	1.85	1.91	1.96	2.02	2.08	2.13	2.18
Matakana River estuary	1755269	5974476	1.87	1.93	1.98	2.04	2.10	2.15	2.19
Pukapuka Inlet (Mahurangi)	1750849	5961126	2.09	2.23	2.31	2.38	2.50	2.56	2.61
Mahurangi Harbour	1753626	5960575	2.07	2.22	2.29	2.36	2.48	2.54	2.59
Mahurangi Harbour	1751686	5968031	2.13	2.27	2.35	2.42	2.54	2.60	2.66
Mahurangi Harbour	1754615	5960537	2.07	2.21	2.29	2.36	2.48	2.53	2.59
Te Kapa R. (Mahurangi)	1756099	5963200	2.09	2.23	2.31	2.38	2.50	2.56	2.61
Mahurangi Harbour	1753210	5958010	2.05	2.20	2.27	2.34	2.46	2.52	2.57
Puhoi River estuary	1750338	5956222	2.07	2.21	2.29	2.36	2.48	2.53	2.59
Waiwera River estuary	1750889	5954757	2.06	2.21	2.28	2.35	2.47	2.53	2.58
Orewa River estuary	1749727	5948635	2.07	2.19	2.29	2.37	2.44	2.53	2.59
Weiti River	1751800	5946524	2.10	2.22	2.30	2.40	2.48	2.57	2.62
Karepiro Bay	1754558	5942016	2.06	2.19	2.26	2.36	2.45	2.53	2.58
Okura River	1752751	5939753	2.08	2.21	2.28	2.38	2.47	2.55	2.61
Tamaki Estuary	1765514	5913666	2.06	2.15	2.20	2.25	2.32	2.35	2.38
Tamaki Estuary	1766408	5911555	2.13	2.23	2.28	2.33	2.39	2.42	2.45
Pakuranga Creek (Tamaki)	1769431	5912063	2.14	2.24	2.29	2.34	2.40	2.43	2.46

Site	Easting (NZTM)	Northing (NZTM)	Joint AEP: 0.39	0.18	0.10	0.05	0.02	0.01	0.005
			Joint ARI: 2 yr	5 yr	10 yr	20 yr	50 yr	100 yr	200 yr
Tamaki Estuary	1764589	5907948	2.17	2.27	2.32	2.37	2.43	2.46	2.49
Mangamangaroa Creek	1772868	5912475	2.08	2.20	2.26	2.32	2.40	2.46	2.49
Turanga Creek	1775337	5910030	2.10	2.21	2.27	2.33	2.42	2.47	2.51
Waikopua Creek	1777927	5912838	2.08	2.20	2.26	2.32	2.40	2.46	2.49
Wairoa River estuary	1784026	5907369	2.12	2.21	2.28	2.34	2.40	2.46	2.49
Wairoa River estuary	1784970	5907950	2.11	2.20	2.27	2.33	2.39	2.45	2.48
Wairoa River estuary	1785600	5907417	2.12	2.21	2.28	2.34	2.41	2.46	2.50

4.3   The open west coast

The 1970–2000 WASP hindcasts of storm surge and waves were also used to calculate the frequency and magnitude of combined storm-tide plus wave setup elevations on the western open-coast of the Auckland region. Figure 4-15 marks the five selected output locations along the coastline, plus the locations of model hindcast data available from the WASP modelling project (http://wrenz.niwa.co.nz/webmodel/coastal).
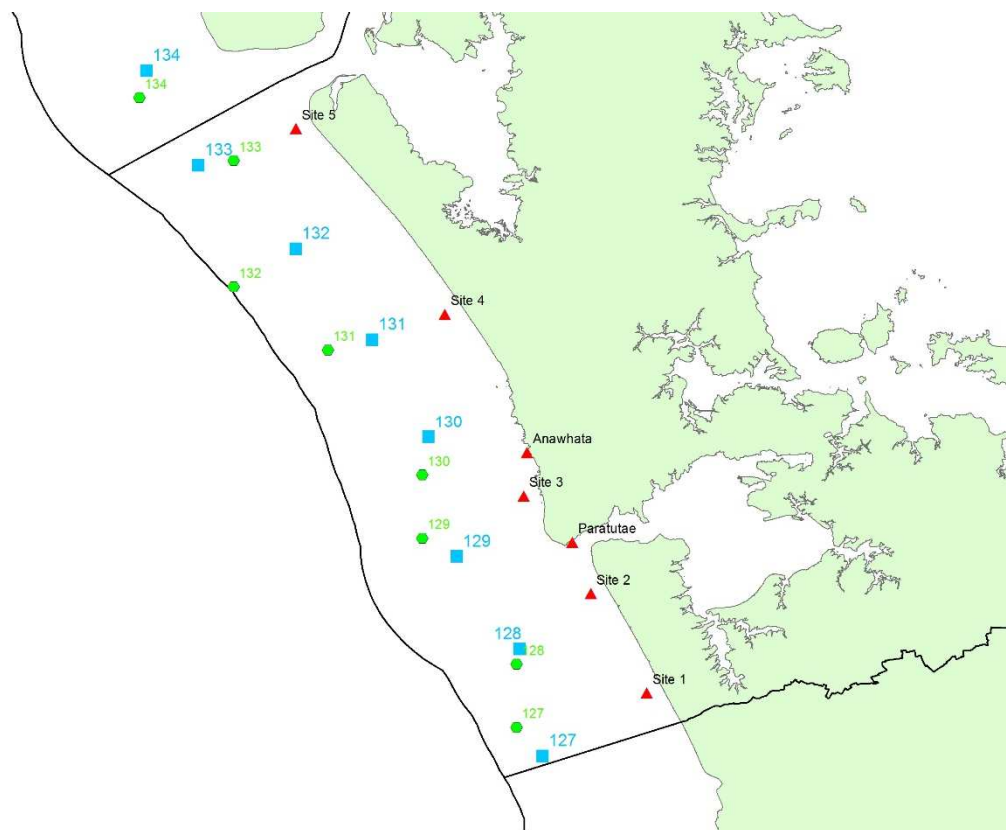
Figure 4-15: Location of combined storm-tide plus wave setup elevation calculations along the western open-coast. Blue squares mark the nominal WASP output locations on the 50 m isobath; green circles mark the centres of the wave model grid cells from which the wave outputs for each site were actually taken; red triangles mark output locations for coastal extreme water levels, and the location of the Anawhata tide gauge.

4.3.1 Storm-tide on the western open-coast

Storm-tide was simulated at the five output locations (Figure 4-15) by summing:

1.   Predicted tide from NIWA's tide model (12 constituents) with minor bias correction for amplitude and phase for the M2, S2 and N2 main tidal constituents to align better with the Anawhata sea level gauge measurements.

2.   Storm surge from the WASP models extracted from the nearest location to each output location (Figure 4-15) using a wavelet filter that isolates periods of 1-16 days. The WASP storm surge was checked against measured storm surge from the Anawhata tide gauge using a quantile-quantile comparison. The quantile-quantile comparison

used all available data from the gauge (1999-2011) that included two years (1999 & 2000) of data that overlapped the WASP simulation (1970–2000). The comparison revealed that the WASP model under-predicted the measured storm surge at the Anawhata gauge site (Figure 4-16), probably due to shoaling effects of the storm-surge wave and the presence of some wave setup in the coastal gauge at Anawhata. By assuming a similar under-prediction at all five output locations the WASP storm surge was scaled using the Anawhata comparison, by adjusting each quantile in the modelled storm surge to match that from the Anawhata gauge (1:1 equivalence).

3. Monthly mean sea-level anomaly from the WASP models extracted from the nearest location to each output location (Figure 4-15) using a low-pass wavelet filter to extract sea-level variability with periods of ≥ 32 days (1 month). This is the same way that MMSLA is extracted from the non-tidal sea-level component of the tide-gauge record. Note, however, that WASP simulated storm surge and did not explicitly simulate MMSLA. The MMSLA derived from the WASP storm-surge time-series is actually a low-pass component of simulated storm-surge. The modelled and measured MMSLA were compared using a quantile-quantile comparison. The model under-predicted the Anawhata gauge measurements, as expected (since MMSLA was not explicitly simulated). As there were large quantile-quantile deviations from the equivalence line at very high and low quantiles, and the remaining data exhibited an approximately linear trend, the modelled MMSLA was adjusted by a linear factor of 1.8 (Figure 4-17). This scaling factor was applied to simulated MMSLA for all five output locations.

The extreme storm-tide frequency–magnitude distributions calculated from measured and simulated data were compared (Figure 4-18). The simulated median extreme storm-tide distribution was under-predicting the measurement-based best-fit by ~8 cm at 0.01 AEP, although it lay well inside the 95% confidence intervals for the measurement-based model. For conservatism, it was decided to scale the extreme storm-tide distributions at all five locations, using relative scaling for each AEP of interest, based on the Anawhata comparisons; the resulting extreme storm-tide distributions are compared to the measurement-based distribution in Figure 4-19, and tabled in Table 4-5. The differences between the 5 sites relate mainly to tide range differences. Note that the large outlier in Figure 4-18 is the storm-tide of 17 April 1999, when a broad and deepening trough was preceded by strong north-westerly flows and followed by colder south-westerlies. A major front occurred within the trough. It brought gale force winds over the North Island, contributing to sea flooding along the west coast.
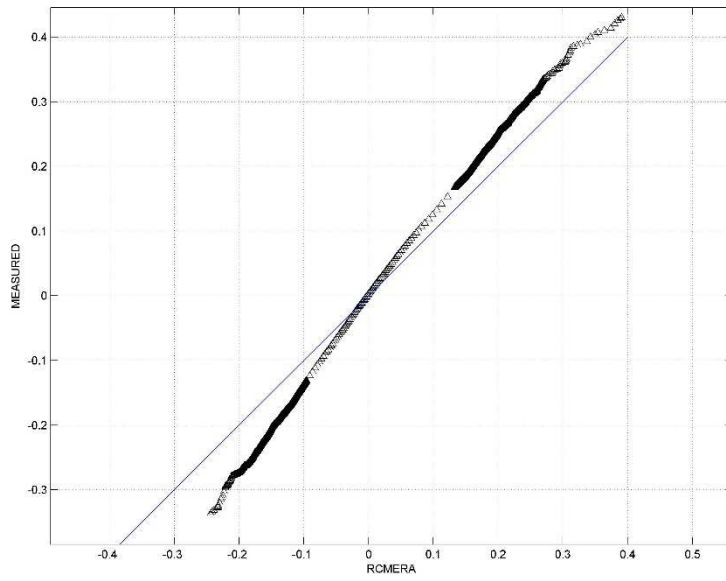
Figure 4-16: Quantile-quantile comparison of storm surge derived from the Anawhata tide gauge and the WASP model. RCMERA = WASP model; Measured = Anawhata tide gauge.
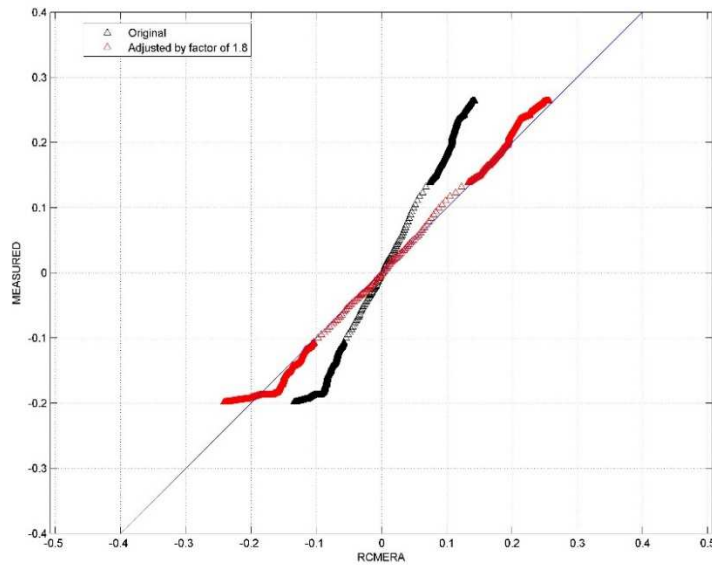
Figure 4-17: Quantile-quantile comparison of monthly mean sea-level anomaly derived from the Anawhata tide gauge and the WASP model. RCMERA = low-pass filtered storm-surge from WASP model; Measured = MMSLA from the Anawhata tide gauge. The adjusted distribution is plotted in red.
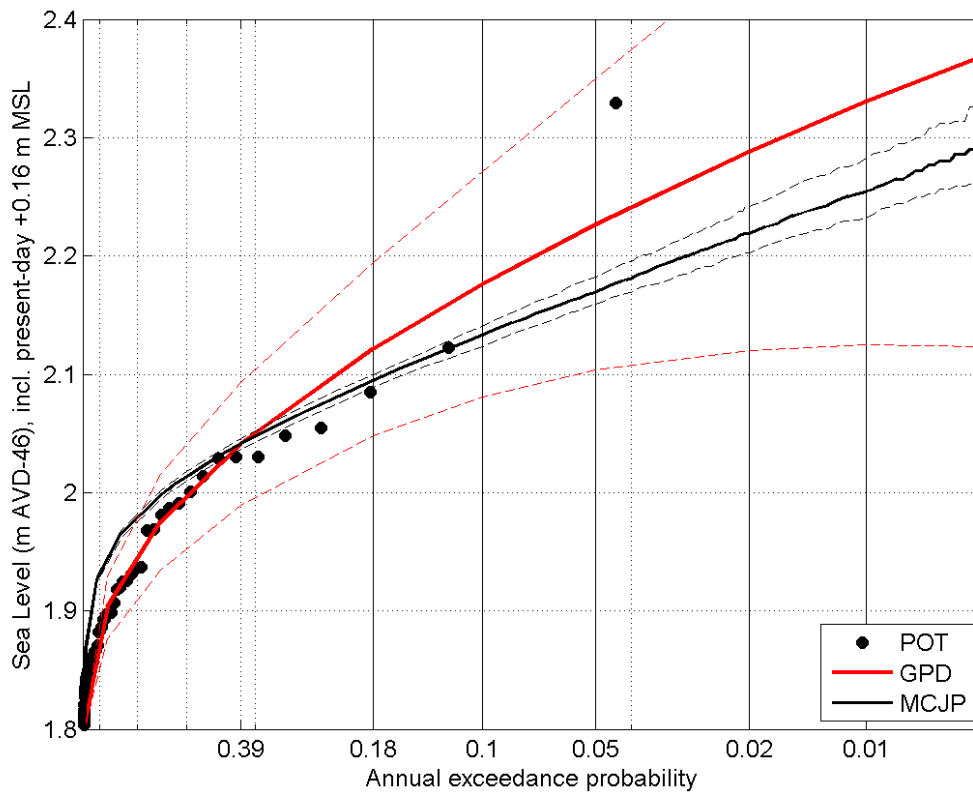
Figure 4-18: Extreme storm-tide distributions at Anawhata. Elevations are relative to AVD-46 including +0.16 m offset for baseline mean sea level (present-day estimate). POT = peaks-over-threshold data; GPD = generalised Pareto model fit to POT data; MCJP = Monte Carlo joint-probability model of simulated storm-tide.
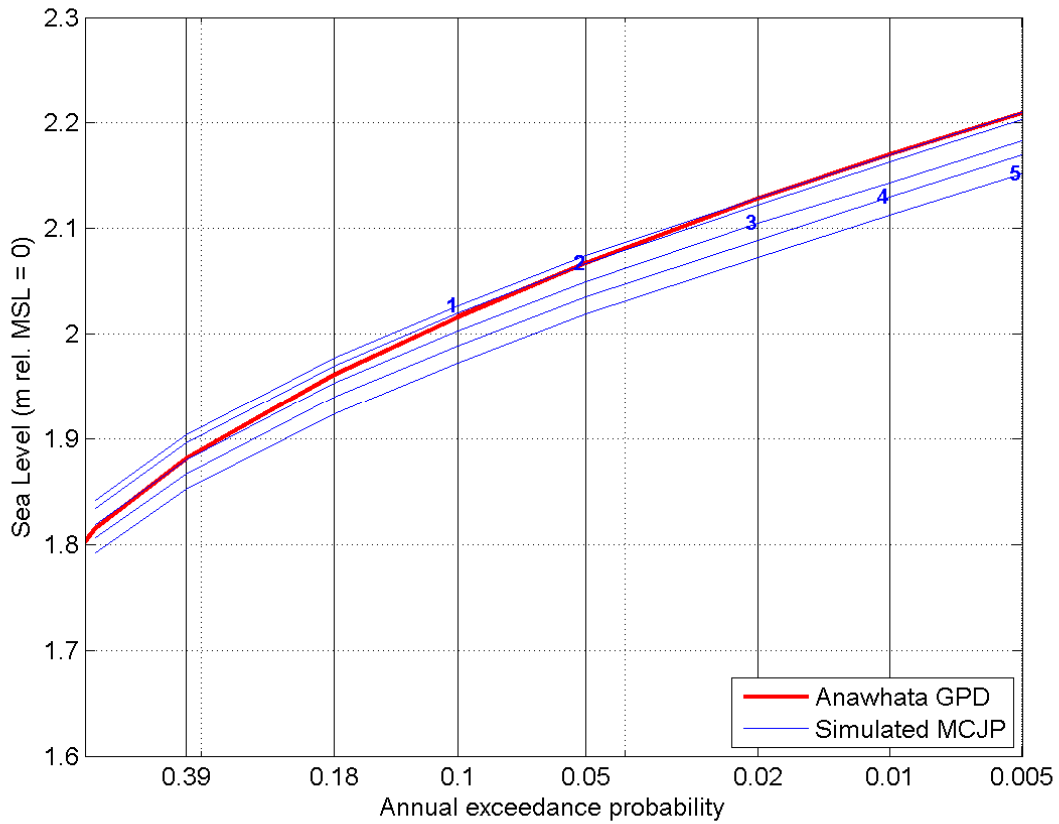
Figure 4-19: Storm-tide frequency–magnitude distributions along western open-coast. Number represents site locations as in Figure 4-15. The curves show relative changes; no MSL offset is applied.

Table 4-5: Storm-tide elevations along the western open-coast. Elevations are relative to AVD-46 and include a +0.16 m mean-sea-level offset.

Site	Easting (NZTM)	Northing (NZTM)	AEP: 0.39 / ARI: 2 yr	0.18 / 5 yr	0.10 / 10 yr	0.05 / 20 yr	0.02 / 50 yr	0.01 / 100 yr	0.005 / 200 yr
1	1742786	5876179	2.00	2.06	2.14	2.19	2.23	2.29	2.33
2	1736812	5890706	1.99	2.06	2.13	2.18	2.23	2.28	2.32
3	1729036	5905254	1.98	2.04	2.11	2.16	2.21	2.26	2.30
4	1719636	5933133	1.97	2.03	2.10	2.15	2.19	2.25	2.29
5	1702991	5959977	1.95	2.01	2.08	2.13	2.18	2.23	2.27

4.3.2 Waves on the western open-coast

The WASP wave simulations (1970-2001) were used directly for the open west coast without undergoing any rescaling. Comparisons of the WASP simulation with the nearest wave buoy data are plotted in Figure 4-20 (Taharoa wave buoy) and Figure 4-21 (Hokianga wave buoy). The dark red lines are quantile-quantile plots using the buoy-model overlap period. The green lines are quantile-quantile plots using the full records of both model and buoy, with the latter seasonally adjusted to correct for the record not being a whole number of years, and hence having, for example, more January than June data. This can be done even with no data overlap, e.g., with the Hokianga wave buoy data (June 2006 – July 2007).

The nearest WASP wave output locations was assigned to each of the five output sites as shown in the Figure 4-15.

A GPD was fitted to the 30-year simulated wave data record from WASP from each site and used to scale the marginal extremes of the joint probability data. The extreme significant wave height data are plotted in Figure 4-22 and tabled in Table 4-6.
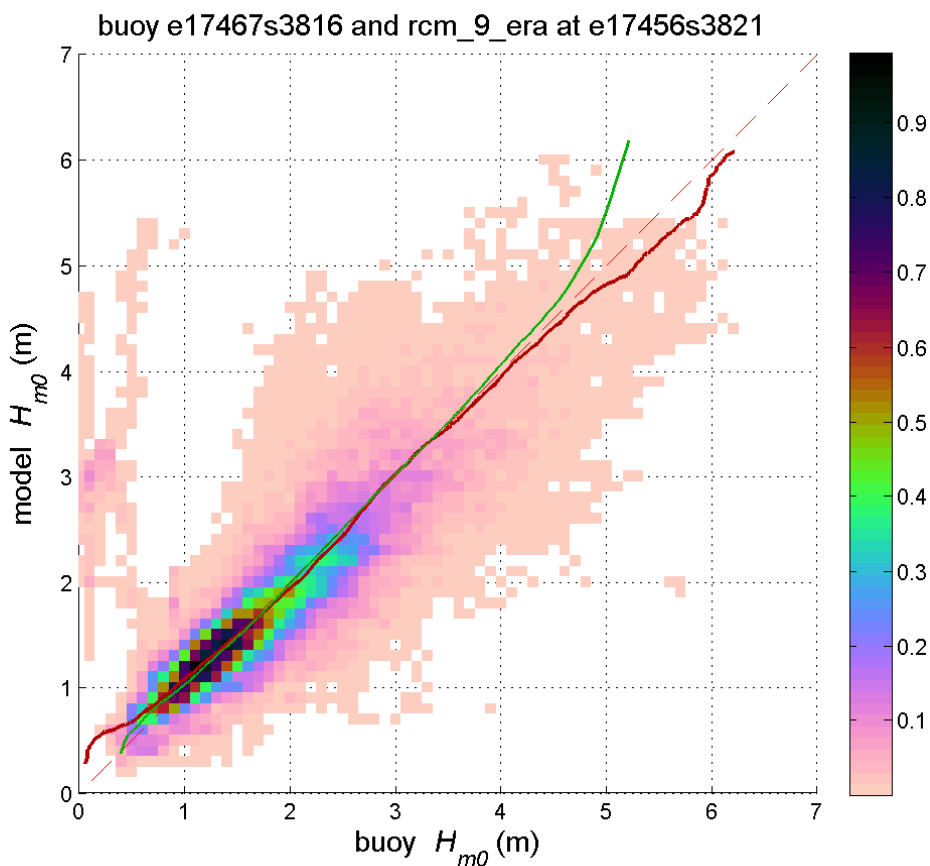
Figure 4-20: Comparison of significant wave height values predicted by the WASP rcm_9_era model with measurements from the Taharoa wave buoy. The colour scale shows the joint occurrence distribution of measured and predicted wave heights, while the solid lines show quantile-quantile plots, either using coincident records (red line), or seasonally-adjusted statistics derived from all records (green line).
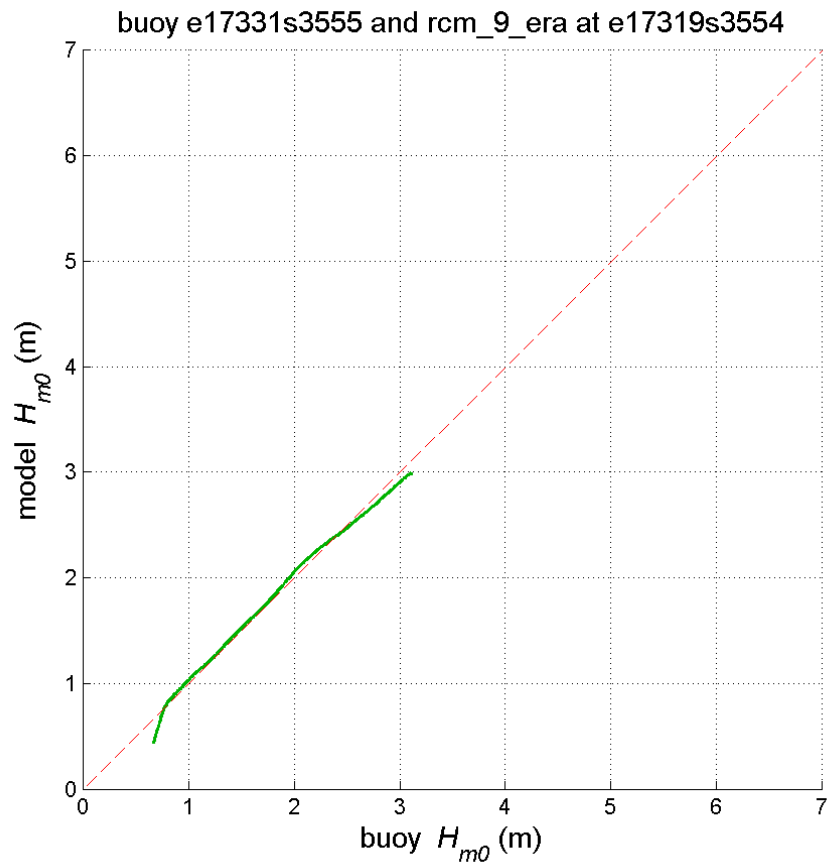
Figure 4-21: Comparison of significant wave height values predicted by the WASP rcm_9_era model with measurements off Mangonui Bluff, near Hokianga Harbour. The green line is a quantile-quantile plot of seasonally-adjusted statistics derived from all records.
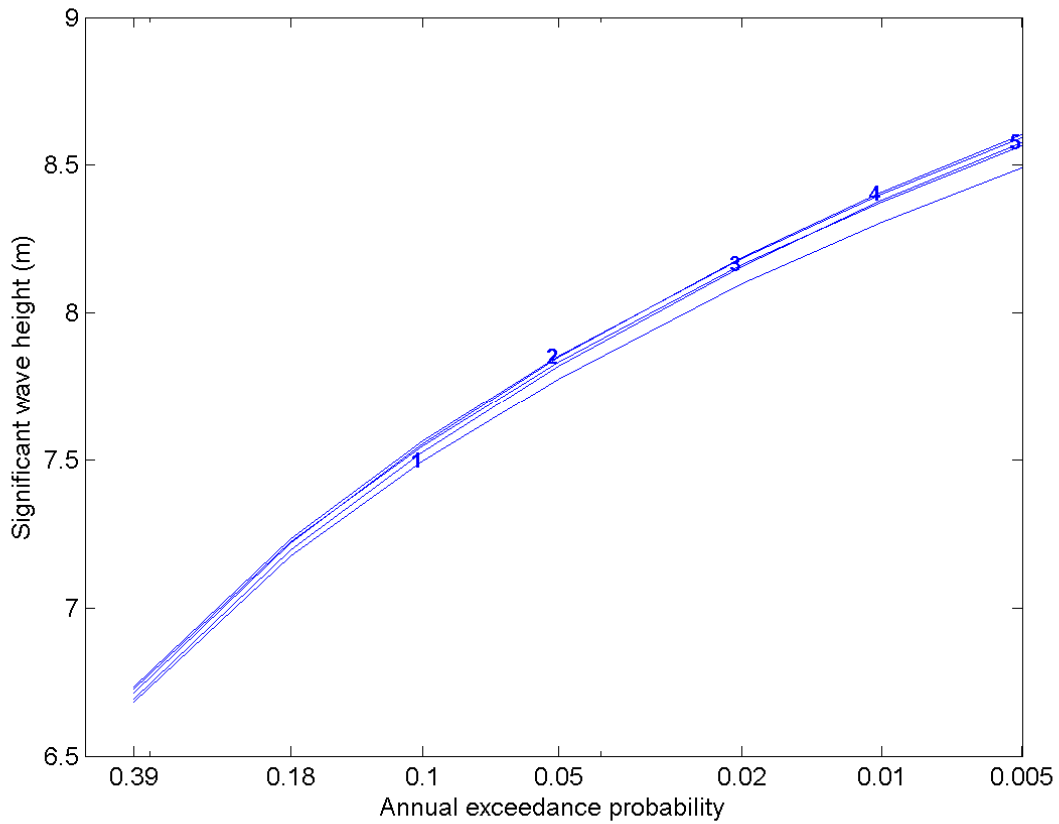
Figure 4-22: Extreme significant wave height (m) along the western open-coast at the 5 sites.

Table 4-6: Extreme significant wave height (m) along the western open-coast.

Site	Easting (NZTM)	Northing (NZTM)	AEP: 0.39 ARI: 2 yr	0.18 5 yr	0.10 10 yr	0.05 20 yr	0.02 50 yr	0.01 100 yr	0.005 200 yr
1	1742786	5876179	6.68	7.18	7.50	7.78	8.10	8.31	8.49
2	1736812	5890706	6.71	7.22	7.55	7.85	8.19	8.41	8.60
3	1729036	5905254	6.73	7.22	7.55	7.83	8.16	8.38	8.56
4	1719636	5933133	6.73	7.24	7.56	7.85	8.18	8.40	8.59
5	1702991	5959977	6.69	7.20	7.53	7.82	8.16	8.38	8.58

4.3.3 Combined storm-tide plus wave setup on the eastern open coast

Joint-probability analyses of extreme storm-tides and waves were undertaken using coinciding significant wave height, wave period, and storm-tide sampled at each high tide. A joint-probability analysis of storm-tides and waves describes the combined likelihood of a high storm-tide and large wave event occurring at the same time (Figure 7-1).

At each location, the highest combined storm-tide plus wave setup elevation was determined for each annual exceedance probability, as described in Section 7.4. These values are presented in Table 4-7. Wave setup contributes approximately 1 m of the total inundation level over and above storm-tide alone, for a joint 1% AEP inundation event (Table 4-8).

Table 4-7:   Maximum storm-tide plus wave setup elevations along the western open-coast. Elevations are relative to AVD-46 and include a +0.15 m mean-sea-level offset.

Site	Easting (NZTM)	Northing (NZTM)	Joint AEP: 0.18 / Joint ARI: 5 yr	0.05 / 20 yr	0.02 / 50 yr	0.01 / 100 yr
1	1742786	5876179	2.90	3.11	3.23	3.30
2	1736812	5890706	2.90	3.13	3.26	3.36
3	1729036	5905254	2.89	3.08	3.20	3.31
4	1719636	5933133	2.87	3.08	3.19	3.26
5	1702991	5959977	2.87	3.09	3.19	3.29

Table 4-8:   Elevation difference (m) between storm-tide + wave setup and storm-tide-only along the western open-coast.

Site	Easting (NZTM)	Northing (NZTM)	AEP: 0.18 / ARI: 5 yr	0.05 / 20 yr	0.02 / 50 yr	0.01 / 100 yr
1	1742786	5876179	0.84	0.92	1.00	1.01
2	1736812	5890706	0.84	0.95	1.03	1.08
3	1729036	5905254	0.85	0.92	0.99	1.05
4	1719636	5933133	0.84	0.93	1.00	1.01
5	1702991	5959977	0.86	0.96	1.01	1.06

5 Glossary of abbreviations and terms

Annual exceedance probability (AEP)
The probability of a given (usually high) sea level or wave height being equalled or exceeded in elevation, in any given calendar year. AEP can be specified as a fraction (e.g., 0.01) or a percentage (e.g., 1%).

AVD-46
Auckland Vertical Datum – 1946 was established as the mean sea level at Port of Auckland from 7 years of sea level measurements collected in 1909, 1917–1919 and 1921–1923.

Average recurrence interval (ARI)
The average time interval (averaged over a very long time period and many "events") that is expected to elapse between recurrences of an infrequent event of a given large magnitude (or larger). A large infrequent event would be expected to be equalled or exceeded in elevation, once, on average, every "ARI" years, but with considerable variability.

Bathymetry
A term for the topography that lies submerged under a water body.

CMA
The **coastal marine area** is defined in s2 of the RMA as meaning:
"The foreshore, seabed, and coastal water, and the air space above the water -
(a) Of which the seaward boundary is the outer limits of the territorial sea.
(b) Of which the landward boundary is the line of mean high water springs, except that where that line crosses a river, the landward boundary at that point shall be whichever is the lesser of -
(i) One kilometre upstream from the mouth of the river; or
(ii) The point upstream that is calculated by multiplying the width of the river mouth by five".

ENSO
El Niño Southern Oscillation. A natural global climate phenomenon involving the interaction between the tropical Pacific and the atmosphere, but has far-reaching effects on the global climate, especially for countries in the Pacific rim. ENSO is the strongest climate signal on time scales of one to several years. The quasi-periodic cycle oscillates between El Niño (unusually warm ocean waters along the tropical South American coast) and La Niña (colder-than-normal ocean waters off South America).

Epoch
A particular period of history that is arbitrarily selected as a point of reference – used in connection with developing a baseline sea level.

GIS
A geographic information system (GIS) is a system designed to capture, store, manipulate, analyse, manage, and present all types of geographical information for informing decision making.

Hindcast
A numerical simulation (representation) of past conditions. As opposed to a forecast or future cast that simulates the future.

IPO
Interdecadal Pacific Oscillation – a long timescale oscillation in the ocean–atmosphere system that shifts climate in the Pacific region every one to three decades.

Joint-probability	The probability of two separate processes occurring together (e.g., large waves and high storm-tide).
LiDAR	Light Detection And Ranging – an airborne laser scanning system that determines ground levels at a very high density (often as little as 1 m spacing between measurements) along a swathe of land underneath the track of the airplane. Most systems used in New Zealand collect data only on land above water levels, but systems are available that can also determine shallow water bathymetry levels in clear water. Vertical accuracy is typically better than ±0.15 m.
Marginal variable	Refers to a single variable (e.g., wave height, or storm-tide) representing one axis, or "margin", of a joint-probability plot.
MCJP	Monte Carlo joint-probability technique. A technique to model extreme sea-level. Suitable for short data records, and provides the flexibility to mix measured and modelled sea-level components (see Table 7-4).
Mean Monthly Sea Level Anomaly (MMSLA)	The sea level anomaly with periods (variations) of one month or greater due to climate variability such as seasonal effects, ENSO and IPO; obtained by detrending MMSL time-series and removing the time-series mean (to a mean of zero).
Mean Sea Level (MSL)	The mean non-tidal component of sea level, averaged over a defined time period, usually several years. New Zealand's local vertical datums were obtained in this way, with AVD-46 being the MSL from sea-level measurements made between 1909 and 1923. Mean sea level changes with the averaging period used, due to climate variability and long-term sea-level rise.
MHWS	Mean high water springs – The high tide height associated with higher than normal high tides that result from the beat of various tidal harmonic constituents. Mean high water springs occur every 2 weeks approximately. MHWS can be defined in various ways, and the MHWS elevation varies according to definition. This has led to subjectivity when defining the CMA for RMA purposes but this report provides a pragmatic solution that builds in variability in tide range and the effect of wave setup on open coasts.
Monthly Mean Sea Level (MMSL)	The variation of the non-tidal sea level on time scales ranging from a monthly basis to decades, due to climate variability, relative to a specified datum. This includes ENSO and IPO patterns on sea level, winds and sea temperatures, and seasonal effects. In some older NIWA reports this might have been referred to as "mean level of the sea" or MLOS.
Open coast	Coastline located outside of sheltered harbours and estuaries, in locations subject to ocean waves and swell.

Perigean spring tide	A perigean spring tide occurs when the moon is either new or full (spring tide) and closest to Earth in its monthly orbit (i.e., the perigee). The coincidence of spring tide and perigee peaks about every 7 months.
Projection	A numerical simulation (representation) of future conditions. Differs from a forecast; whereas a forecast aims to predict the exact time-dependent conditions in the immediate future, such as a weather forecast a future cast aims to simulate a time-series of conditions that would be typical of the future (from which statistical properties can be calculated) but does not predict future individual events.
Quantile-quantile	Quantile-quantile, or Q-Q plots are a graphical method of showing how the frequencies or probabilities of two distributions compare (e.g., model versus measured). If the distributions are similar, then the points will tend to lie on a straight 1:1 line.
Significant wave height H_{m0} (m)	The average height of the highest one-third of waves in the wave record; experiments have shown that the value of this wave height is close to the value of visually estimated wave height.
Storm surge	The rise in sea level due to storm meteorological effects. Low-atmospheric pressure relaxes the pressure on the ocean surface causing the sea-level to rise, and wind stress on the ocean surface pushes water down-wind (onshore winds) and to the left up against any adjacent coast (alongshore winds). Storm surge has timescales of sea-level response that coincide with typical synoptic weather motions; typically 1–3 days.
Storm-tide	Storm-tide is defined as the sea-level peak around high tide reached during a storm event, resulting from a combination of MMSLA + tide + storm surge.
Tidal hysteresis	An additional rise in mean sea level in harbours relative to the open coast, caused by the differential wave speed of the tidal wave between low and high tides in shallow harbours, resulting in a setup of the half-tide level to redress the imbalance in flow capacity between the wave crest and trough.
WASP	The Waves And Storm surge Predictions WASP modelling project recently completed by NIWA produced 45-year (1958–2002) and 30-year (1970–2000) hindcast records of storm surge and waves around the entire New Zealand coast. An aim of the WASP project was to produce a nationally-consistent web-based hindcast of waves and storm surges, from which regional information could be extracted. Data is available on the web via NIWA's Coastal Explorer (http://wrenz.niwa.co.nz/webmodel/coastal).

Wave runup   The maximum vertical extent of wave "up-rush" on a beach or structure above the still water level, and thus constitutes only a short-term upper-bound fluctuation in water level relative to wave setup.

Wave setup   The average temporary increase in mean still-water sea level at the coast, resulting from the release of wave energy in the surf zone as waves break.

6   References

Amos, M.J. (2007) Quasigeoid modelling in New Zealand to unify multiple Local Vertical Datums. *PhD thesis.* Curtin University of Technology, Western Australia.

Andrews, C. (2004) North Shore City sea inundation study. *Tonkin and Taylor Ltd Client Report to North Shore City Council,* No. 21595.

Auckland Harbour Board (1974) Tidal data. Drawing number S90/25 by Tubbs, C.

Auckland Regional Council (2010) Sea level change in the Auckland Region. Report prepared for the Auckland Regional Council by the University of Otago and the National Institute of Water and Atmospheric Research. *ARC Technical Report,* TR065 No. 36 p.

Bell, R.G. (2010) Tidal exceedances, storm tides and the effect of sea-level rise. *Proceedings of the 17th Congress of the Asia and Pacific division of the IAHR,* Auckland, New Zealand, 21-24 February 2010.

Bell, R.G., Dumnov, S.V., Williams, B.L., Greig, M.J.N. (1998) Hydrodynamics of Manukau Harbour, New Zealand. *New Zealand Journal of Marine and Freshwater Research,* 32(1): 81–100.

Bell, R.G., Swales, A., Hill, A.F. (1996) Field studies in Upper Tamaki Estuary for the environmental assessment of the Otahuhu power station heated cooling-water discharge. *Client Report to Kingett Mitchell and Associates, Takapuna,* No. KIM60203/1: 15.

Booij, N., Ris, R.C., Holthuijsen, L.H. (1999) A third-generation wave model for coastal regions 1. Model description and validation. *Journal of Geophysical Research,* 104(C4): 7649–7666.

Britton, R., Dahm, J., Rouse, H., Hume, T., Bell, R., Blackett, P. (2011) Coastal adaptation to climate change: pathways to change. *Report prepared as part of the Coastal Adaptation to Climate Change Project,* No. 106 p.

Coles, S. (2001) *An introduction to statistical modeling of extreme values.* Springer, London, New York: 208.

EurOtop (2007) Wave overtopping of sea defence and related structures: Assessment manual. *Die Küste version, Archive for Research and Technology of the North Sea and Baltic Coast,* No. p.

Fairchild, J.C. (1958) *Model study of wave set-up induced by hurricane waves at Narragansett Pier*, Rhode Island. No. p.

Foreman, M.G.G., Cherniawsky, J.Y., Ballantyne, V.A. (2009) Versatile Harmonic Tidal Analysis: Improvements and Applications. *Journal of Atmospheric and Oceanic Technology,* 26(4): 806–817.

Goring, D.G. (1995) Short level variations in sea level (2-15 days) in the New Zealand region. *New Zealand Journal of Marine and Freshwater Research,* 29: 69–82.

Goring, D.G., Stephens, S.A., Bell, R.G., Pearson, C.P. (2010) Estimation of Extreme Sea Levels in a Tide-Dominated Environment using Short Data Records. *Journal of Waterway, Port, Coastal and Ocean Engineering,* 137(3): 150–159.

Gringorten, I.I. (1963) A plotting rule for extreme probability paper. *Journal of Geophysical Research,* 68(3): 813–814.

Haigh, I.D., Nicholls, R., Wells, N. (2010) A comparison of the main methods for estimating probabilities of extreme still water levels. *Coastal Engineering,* 57(9): 838–849.

Hannah, J. (1990) Analysis of Mean Sea Level Data From New Zealand for the Period 1899-1988. *Journal of Geophysical Research,* 95(B8): 12399–12405.

Hannah, J. (2004) An updated analysis of long-term sea level change in New Zealand. *Geophysical Research Letters,* 31(3): L03307.

Hannah, J., Bell, R.G. (2012) Regional sea level trends in New Zealand. *Journal of Geophysical Research-Oceans,* 117: 1004–1004.

Hawkes, P.J., Gouldby, B.R., Tawn, J.A., Owen, M.W. (2002) The joint probability of waves and water levels in coastal engineering design. *Journal of Hydraulic Research,* 40(3): 241–251.

HR Wallingford (web) *HR Wallingford wave overtopping calculator.* http://www.overtopping-manual.com/calculation_tool.html.

HR Wallingford (2000) The joint probability of waves and water levels: JOIN-SEA - Version 1.0. *User Manual,* No. TR 71: 12.

HR Wallingford and Lancaster University (2000) The joint probability of waves and water levels: JOIN-SEA, a rigorous but practical new approach. No. SR 537: 47.

Ministry for the Environment (2008) *Coastal Hazards and Climate Change: A Guidance Manual for Local Government in New Zealand.* 2nd edtition revised by Ramsay D. and Bell R. (NIWA). Prepared for the Ministry for Environment, Wellington: 127.

Mullan, B., Carey-Smith, T., Griffiths, G., Sood, A. (2011) Scenarios of storminess and regional wind extremes under climate change. *NIWA Client Report to Ministry of Agriculture and Forestry,* WLG2010-031: 80.

Oldman, J.W., Black, K.P. (1997) Mahurangi Estuary numerical modelling. *Client Report to Auckland regional Council,* No. ARC60208/1; TR 2009/041. p.

Oldman, J.W., Gorman, R.M., Lewis, M. (2007) Central Waitemata Harbour Contaminant Study. Harbour hydrodynamics and sediment-model calibration and implementation. . *Client Report for Auckland Regional Council,* No. HAM2007-102.

Pritchard, M., Stephens, S., Measures, R., Goodhue, N., Wadhwa, S. (2012) Kaipara Harbour 2-dimensional hydrodynamic modelling. *Client Report to Auckland Council,* No. HAM2012-128: 36.

Pugh, D.T., Vassie, J.M. (1978) "Extreme sea-levels from tide and surge probability.*" Presented at the Proceedings of the 16th Coastal Engineering Conference,* Hamburg, 911–930.

Pugh, D.T., Vassie, J.M. (1980) Applications of the joint probability method for extreme sea-level computations. *Proceedings of the Institution of Civil Engineers Part 2*: 959–979.

Ramsay, D., Altenberger, A., Bell, R., Oldman, J., Stephens, S. (2008a) Review of rainfall intensity curves and sea levels in Manukau City. Part 2: Sea levels. *Consulting Report to Manukau City Council, No. HAM2007-168*: 74.

Ramsay, D., Stephens, S., Altenberger, A., Oldman, J. (2008b) The influence of climate change on extreme sea levels around Auckland City. *Consulting Report to Auckland City Council,* No. HAM2008-093: 74.

Reeve, G., Pritchard, M. (2010) Manukau Harbour enhancement project: hydrodynamic modelling calibration report. *NIWA Client Report to Watercare Services Limited,* No. HAM2010-019: 49.

Reinen-Hamill, R., Shand, T. (2005) Assessment of potential sea levels due to storms and climate change along Rodney's East Coast. *Tonkin and Taylor Ltd Client Report to Rodney District Council,* No. 22239.

Ris, R.C., Holthuijsen, L.H., Booij, N. (1999) A third-generation wave model for coastal regions 2. Verification. *Journal of Geophysical Research,* 104(C4): 7667–7681.

Stanton, B.R., Goring, D.G., Bell, R.G. (2001) Observed and modelled tidal currents in the New Zealand Region. *New Zealand Journal of Marine and Freshwater Research,* 35: 397–415.

Stephens, S.A., Bremner, D., Budd, R., Edhouse, S., Goodhue, N., Hart, C., Reeve, G., Wadhwa, S. (2011a) Kaipara Harbour hydrodynamic data collection. *Client Report to Auckland Council,* No. HAM2011-131: 20.

Stephens, S.A., Coco, G., Bryan, K.R. (2011b) Numerical simulations of wave setup over barred beach profiles: implications for predictability. *Journal of Waterway Port Coastal and Ocean Engineering-ASCE,* 137(4): 175–181.

Stephens, S.A., Reeve, G., Goodhue, N. (2011c) Coastal storm-tide levels in the Auckland Region. Phase 1: Rationalising and updating previous studies. *Client Report to Auckland Council,* No. HAM2011-102: 63.

Stephens, S.A., Wadhwa, S. (2012) Development of an updated Coastal Marine Area boundary for the Auckland Region. *Client Report to Auckland Council,* No. HAM2012-111: 63.

Stephenson, A., Gilleland, E. (2005) Software for the analysis of extreme events: The current state and future directions. *Extremes,* 8(3): 87–109.

Stockdon, H.F., Holman, R.A., Howd, P.A., Sallenger, A.H. (2006) Empirical parameterization of setup, swash, and runup. *Coastal Engineering,* 53(7): 573–588.

SWAN (2011) *SWAN User Manual - SWAN Cycle III Version 40*: 85.

Tawn, J.A., Vassie, J.M. (1989) "Extreme sea-levels: the joint probabilities method revisited and revised". *Presented at the Proceedings of the Institute of Civil Engineering Part 2,* 429–442: 87.

Tawn, J.A., Vassie, J.M. (1991) Recent improvements in the joint probability method for estimating extreme sea levels. *In*: Parker, B.B. (ed) *Tidal Hydrodynamics*: 813–828, Wiley, New York.

Tolman, H.L. (1991) A third-generation model for wind waves on slowly varying, unsteady, and inhomogeneous depths and currents. *Journal of Physical Oceanography,* 21: 782–797.

Tolman, H.L. (2007) "The 2007 release of WAVEWATCH." *Presented at the 10th International Workshop on Wave Hindcasting and Forecasting and Coastal Hazard Symposium,* North Shore, Oahu, Hawaii, November 11-16, 2007.

Tonkin & Taylor Ltd (1986) Manukau Harbour resources study. *Consulting report on behalf of Maunkau Harbour Maritime Planning Authority*.

Uppala, S.M., KÅllberg, P.W., Simmons, A.J., Andrae, U., Bechtold, V.D.C., Fiorino, M., Gibson, J.K., Haseler, J., Hernandez, A., Kelly, G.A., Li, X., Onogi, K., Saarinen, S., Sokka, N., Allan, R.P., Andersson, E., Arpe, K., Balmaseda, M.A., Beljaars, A.C.M., Berg, L.V.D., Bidlot, J., Bormann, N., Caires, S., Chevallier, F., Dethof, A., Dragosavac, M., Fisher, M., Fuentes, M., Hagemann, S., Hólm, E., Hoskins, B.J., Isaksen, L., Janssen, P.A.E.M., Jenne, R., McNally, A.P., Mahfouf, J.F., Morcrette, J.J., Rayner, N.A., Saunders, R.W., Simon, P., Sterl, A., Trenberth, K.E., Untch, A., Vasiljevic, D., Viterbo, P., Woollen, J. (2005) The ERA-40 re-analysis. *Quarterly Journal of the Royal Meteorological Society,* 131(612): 2961–3012.

Van Rijn, L.C. (2010) Modelling erosion of gravel/shingle beaches and barriers: Concepts and Science for Coastal Erosion Management. *Report No. D13b.*

Walters, R.A., Goring, D.G., Bell, R.G. (2001) Ocean tides around New Zealand. *New Zealand Journal of Marine and Freshwater Research,* 35: 567–579.

7 Appendix A – How extreme sea-levels were calculated – details

The aim of an extreme sea-level analysis is to determine the height and likelihood of occurrence of unusually high (or low) sea levels. In particular, extreme sea-level analyses usually require estimation of the probability of sea levels that are more extreme than any that have already been observed (Coles 2001).

7.1 Ways to describe extreme sea level likelihood

The likelihoods associated with extreme storm-tides and/or waves, are reported in terms of their probability of occurrence. The **annual exceedance probability** (AEP) describes the chance of an event reaching or exceeding a certain water level in any given year. For example, if a storm-tide of 2.2 m has a 5% AEP, then there is a 5% chance of a storm-tide this high, or higher, occurring in any 1-year period. So it is unlikely in any single year, but could still happen and should be planned for. Furthermore, although the occurrence probability is only 5%, more than one storm-tide this high or higher could occur in any given year.

Alongside AEP, the likelihood of extreme events can also be described in terms of their **average recurrence interval** (ARI), which is the average time interval between events of a specified magnitude (or larger), when averaged over many occurrences. Table 7-1 shows the relationship between AEP and ARI; small relatively common events have a high annual exceedance probability and a low average recurrence interval, and *vice versa* for large, rare events.

Table 7-1: Relationship between annual exceedance probability (AEP) and average recurrence interval (ARI). $AEP = 1 - e^{(-1/ARI)}$.

AEP (%)	99%	86%	63%	39%	18%	10%	5%	2%	1%	0.5%
ARI (years)	0.2	0.5	1	2	5	10	20	50	100	200

ARI (or its often used surrogate "return period") is an easily misinterpreted term, with the public often assuming that because one large event has just occurred, then the average recurrence interval will pass before another such event. The term AEP better conveys the message of continuous probability that large events could occur at any time.

This report provides occurrence likelihoods for extreme storm-tide and wave height magnitudes and their joint occurrences. This knowledge is only one aspect of the planning process. Another essential planning component is to consider the planning timeframe, or lifetime, of interest. For example, a typical planning lifetime for residential housing is about 100 years. Table 7-2 presents the likelihood that events with various occurrence probabilities will occur, *at least once*, within a specified planning lifetime. The likelihoods are shaded according to their chance of occurring in the specified timeframe:

- **> 85%**   Almost certain
- **60%–84%**   Likely
- **36%–59%**   Possible
- **16%–35%**   **Unlikely**
- **< 15%**   Rare

For example, a relatively common (smaller) event with a 39% AEP is *almost certain* to occur over a 20-year lifetime. However, a rare (larger) 2% AEP event is *unlikely* to occur over the same 20-year lifetime. 1% AEP's are a commonly used planning event magnitude, and 100-year planning lifetimes are common for affected infrastructure; Table 7-2 shows that a 1% AEP event is *likely* to occur over a 100-year planning lifetime.

In Table 7-3, the event average recurrence intervals have been converted into the expected *average number of exceedances* for various asset planning lifetimes. The *average number of exceedances* is a useful measure for estimating *risk*, because it tells us how often, *on average*, we can "expect our feet to get wet" over a given planning lifetime, for a specified event magnitude. To use the above examples, in 20 years there are likely to be 10 exceedances of a relatively common (smaller) event with a 39% AEP, but < 1 exceedances of a rare (larger) 2% AEP event over the same period. The *average number of exceedances* is a useful way to illustrate the effect of sea-level rise on the likely number of coastal inundation events.

Table 7-2:   Likelihood of at least one exceedance event occurring within planning lifetimes
The likelihood of occurrence is described by AEP and/or ARI. $P = 1 - e^{-L/ARI}$, where L = planning lifetime and P = probability of occurrence within planning lifetime.

AEP (%)	ARI (years)	Planning lifetime (years)						
		2	5	10	20	50	100	200
39%	2	63%	92%	99%	100%	100%	100%	100%
18%	5	33%	63%	86%	98%	100%	100%	100%
10%	10	18%	39%	63%	86%	99%	100%	100%
5%	20	10%	22%	39%	63%	92%	99%	100%
2%	50	4%	10%	18%	33%	63%	86%	98%
1%	100	2%	5%	10%	18%	39%	63%	86%
0.5%	200	1%	2%	5%	10%	22%	39%	63%

Table 7-3: *Average number of exceedances* occurring within planning lifetimes, for event magnitudes with a specified probability of occurrence (AEP / ARI). $N = L / ARI$, where L = planning lifetime and *ARI* = average recurrence interval.

AEP (%)	ARI (years)	Planning lifetime (years)						
		2	5	10	20	50	100	200
39%	2	1	2.5	5	10	25	50	100
18%	5	< 1	1	2	4	10	20	40
10%	10	< 1	< 1	1	2	5	10	20
5%	20	< 1	< 1	< 1	1	2.5	5	10
2%	50	< 1	< 1	< 1	< 1	1	2	4
1%	100	< 1	< 1	< 1	< 1	< 1	1	2
0.5%	200	< 1	< 1	< 1	< 1	< 1	< 1	1

7.2   Introduction to extreme sea-level analysis

Extreme sea-level analyses are based on extrapolation from past sea-level measurements. The quality, frequency and length of the sea-level record control the accuracy and uncertainty of the extreme sea-level analysis and can govern the choice of extreme sea-level method. Each extreme sea-level method has unique data requirements; for example, the GEV fitted to annual maxima requires observed annual maximum sea levels, whereas the Monte Carlo joint probability technique (MCJP) requires a high-quality digital dataset sampled at least hourly. Extreme sea-level analyses are sensitive to outliers (erroneous large measurements). Data preparation is extremely important, and the most time-consuming component of an extreme sea-level analysis. Raw sea-level records are seldom perfect and can be affected by siltation of the recorder, timing errors (e.g., daylight saving), datum shifts and gaps in the record, for example. Sea-level measurements must be quality assured before use in an extreme sea-level analysis. No analysis technique can make up for poor data.

The results of an extreme value analysis depend on the sampling frequency and duration of the underlying data, because these factors influence the sea-level processes that are included. For example, high-frequency data (e.g., 1, 5 or 10 minute sampling) may include short-term fluctuations due to waves or seiche, whose inclusion can raise extreme sea-level estimates. Modern sea-level gauges commonly measure as frequently as every minute, which is useful for identifying short period processes such as seiche or tsunami in ports and harbours. For extreme sea-level analysis it is common to subsample the data to ½-hour or 1-hour intervals, which is sufficient to resolve the processes contributing to the storm-tide while avoiding the contribution of waves and seiche.

7.2.1   Direct extreme sea-level techniques

Direct methods are so called because they "directly" analyse the observed/measured sea level maxima that occur during storm-tides. The measured storm-tide maxima "directly" include all the components of higher than normal sea-level that can occasionally combine to produce unusually high sea levels, such as monthly mean sea level, spring tide, and storm surge. Direct methods use techniques based on extreme value theory, which in simple terms

involves fitting an "extreme-value model" to the most extreme sea-level maxima in the record (subject to appropriate data sampling). There are certain limitations that come with the adoption of extreme value theory:

1.   The results can be inaccurate when applied to short sea-level records.

2.   The models themselves are developed under idealised circumstances, which may not be exact (or even reasonable) for a process under study. For example, direct methods analyse the observed extremes of sea level, which in New Zealand are usually a coincidence of a moderate to high storm surge and a high spring tide. Extreme value theory is a valid approach for modelling the storm surge component of sea level because it is an approximately stochastic process. However, the tide, which makes up most of the sea-level variance, is deterministic, and so the direct application of extreme value theory is compromised.

3.   The models may lead to wastage of information when implemented in practice.

The above limitations imply that extreme value theory is best applied directly to sea levels when long records (sea level measured over many decades) are available, and when the stochastic storm surge component is relatively large in comparison to the tidal component. These limitations do not mean that direct methods cannot and should not be used for modelling extreme sea levels, they are widely applied, but the practitioner should be aware of the limitations and associated uncertainty when interpreting the results. (Haigh et al. 2010) showed that direct methods using extreme value theory underestimate the long (> 20 years) period return levels when the astronomical tidal variations of sea level (relative to a mean of zero) are about twice that of the non-tidal variations. In New Zealand, tidal variability is more than twice storm surge.

Direct extreme value techniques invoke the *extreme value paradigm*, which for sea level is: "under suitable assumptions, for a large number of sea-level observations, the approximate behaviour of the maximum sea-levels (after dividing the sea-level observations into blocks (e.g., annual maxima)), can be described by a certain family of extreme value models that can be calibrated to the observed sea-level maxima" (Coles 2001).

Examples of these classical extreme-value models are the generalised extreme value (GEV) and the generalised Pareto distribution (GPD). The GEV model is fitted to block maxima such as annual or monthly maxima, or several maxima per year (*r*-largest). The GPD model is fitted to maxima that exceed some high threshold. A basic assumption is that the sea-level maxima used to calibrate the extreme-value models are independent from one another. In practice, for New Zealand storm surge and wave data, this means separation using at least a 3-day time threshold, which separates the meteorological conditions that create them.

Another assumption is that the sea-level observations must exhibit stationary behaviour[12], i.e., there are no long-term trends such as sea-level rise or ENSO and IPO climate variability. From sea level data it may be necessary to obtain an estimate of the maximum sea level likely to occur in the next 100 or 1000 years. How can we estimate what levels may occur in the next 1000 years without knowing what climate change might occur? Although the pattern of sea-level variation may not appear to have changed in the last 50 years of measurement

---

[12] A data time-series is stationary if it has random variability, but the mean and variance of that random variability remains unchanged with time. Thus a sea-level record is not stationary if it includes long-term sea-level rise.

record, such stability may not persist in the future. The "1000-year average recurrence level" is only meaningful under the assumption of stability (or stationarity) in the prevailing process. We have predicted extreme sea levels for a maximum 200-year average recurrence level, but caution that climate change could have a pronounced influence on extreme sea-levels over a 100-year timeframe as required by the New Zealand Coastal Policy Statement.

7.2.2 Indirect extreme sea-level techniques

Indirect methods involve splitting the sea level into its deterministic (predictable) tidal and stochastic (e.g., unpredictable, storm-driven) non-tidal components, and analysing the two components separately before recombining. Indirect methods are more complicated and require stringent data quality control, but make more efficient use of the available data and so give better results for short data records. The indirect methods also overcome the main theoretical limitations of extreme value theory application to sea levels, and average return sea levels can be estimated from relatively short records (<5 years) because all measured storm surge events are utilised, not just those that lead to extreme levels. The revised joint probability method (RJPM) (Pugh & Vassie 1978; Pugh & Vassie 1980; Tawn & Vassie 1989; Tawn & Vassie 1991) is a widely-applied indirect method, and the newly-developed Monte Carlo joint probability technique (MCJP) is being applied in New Zealand (Goring et al. 2010). An advantage of the MCJP relative to the RJPM is that it gives robust confidence intervals, and incorporates additional sea-level components such as MMSL. NIWA has working versions of both the RJPM and MCJP.

Generally, the methods that make use of more of the available sea-level measurements are more accurate and have the least uncertainty – they make more "efficient" use of the data and are preferred where accuracy is important. Techniques that use less data are easier to apply and are preferred where a low-effort or approximate analysis is required, and/or where long records are available.

Table 7-4:   Summary of extreme value techniques used here for estimating the probabilities of extreme still water levels. GEV = generalised extreme value model; GPD = generalised Pareto distribution.

	Advantages	Disadvantages
Direct methods	**GEV fitted to annual maxima**	
	▪ Simple to apply (no thresholds) with easily-obtained software.	▪ Inefficient use of data (wastage). About 40-years of Annual Maxima required for 100-year ARI estimate.
	▪ Simple data treatment and post-processing (Annual Maxima easily obtained and quality checked).	▪ Long sea-level record required (large uncertainty for short records). In some locations this is partially compensated by Annual Maxima records that extend beyond modern digital records.
	▪ Annual Maxima records sometimes extend beyond the modern continuous digital records.	▪ Sensitive to large outliers in the data.
	GPD fitted to peaks-over-threshold	
	▪ Most efficient data use of the direct methods (highest confidence, lowest uncertainty).	▪ Requires subjective choice of threshold – user experience, or trial and error.
	▪ Commonly applied with easily-obtained software.	▪ At least 10-years of data required for a 50 to 100-year ARI estimate.
		▪ Use of more data requires more stringent data quality check.
Indirect methods	**Monte Carlo Joint Probability (MCJP)**	
	▪ Most efficient use of data.	▪ Sensitive to data errors, requires stringent data quality assurance.
	▪ Suitable for short records (< 5-years).	
	▪ Higher confidence (lower uncertainty).	▪ Complex and time-consuming to apply – requires high level of user experience relative to direct methods.
	▪ Stable in the presence of large outlying events.	▪ Less commonly applied and available software.
		▪ Assumes tide and storm surge are independent, which may not be true in estuaries

7.2.3 Extreme storm-tide methods used in this project

For this project we used the indirect Monte Carlo joint probability technique (Goring et al. 2010) to calculate extreme storm-tide elevations, and cross-checked these analyses using direct techniques fitted to sea-level maxima. The MCJP technique is more accurate for the relatively short observational datasets we have available in the Manukau and Kaipara Harbours. Above all, it is more flexible in allowing us to include historical events and combine measured and modelled datasets to predict extreme storm-tide elevations. Previous studies in the Waitemata Harbour (Ramsay et al. 2008b; Stephens et al. 2011c) used a GEV model fitted to annual maxima, but this has larger uncertainty than the MCJP technique, and are

also less stable when fitted to simulated sea levels, due to the strong influence that data outliers can have. Thus the extreme storm-tide elevations produced here are considered to supersede those produced in previous studies. Likewise, a hydrodynamic model with better spatial resolution has been used to re-model tidal amplification in the Manukau Harbour, leading to improved upper-harbour extreme sea-level estimates compared with Stephens et al. (2011b).

The Monte-Carlo joint-probability method (Goring et al. 2010) was used to predict the storm-tide height for a range of AEP's. The technique works by splitting the sea-level record into contributions by:

- Astronomical tide – tidal harmonic analysis is used to calculate the tidal component of the measured sea-level. The astronomical tide is subtracted from the raw sea level to obtain a non-tidal residual sea level.

- Storm surge – a wavelet filter is applied to the non-tidal residual sea level to separate periods of sea-level variability that are expected to be associated with synoptic weather systems, or "storms". Sea-level oscillations with periods of motion from 1–16-days are separated and assigned to "storm surge".

- Monthly mean sea level anomaly – a wavelet filter is used to separate periods of sea-level variability of 1-month or greater from the non-tidal residual, and assigned to "MMSLA".

The components: tide, storm surge, and MMSLA are then independently recombined using a random (Monte Carlo) sampling technique that preserves the likelihood of occurrence (and coincidence) of each component. In this way, thousands of years' worth of sea-level component combinations are simulated (assuming stationarity), which leads to tighter confidence intervals on the estimates.

Extreme sea-level frequencies and magnitudes are then calculated using the thousands of years of simulated sea levels. A count-back technique is used to calculate frequency–magnitude relationships, for example, if 1000 annual maxima are simulated, then the 10th-highest value represents the 100-year average recurrence interval.

In New Zealand and in the Auckland region, the most important sea-level component is the tide. An analysis of historical storm-tide events in New Zealand showed that extreme storm-tide levels around the open coast of New Zealand are dominated by very high tides coinciding with small to moderate storm surges (Bell 2010). Thus the tidal regime is the most important quantity to model; fortunately it is also the easiest component to model and predict.

7.2.4 Extreme wave heights

Wave heights cannot easily be separated into various components like storm-tides can. Therefore the *direct* extreme-value techniques listed above (Table 7-4) are suitable for extreme wave analysis. We used the generalised Pareto distribution (GPD) fitted to peaks-over-threshold (POT) wave data to predict the likelihood of extreme wave heights, because the POT approach makes use of more data and so has higher efficiency than the annual maxima technique. GPD was fitted to the largest 5% of significant wave heights, using code from Coles (Coles 2001), converted for use in R software (Stephenson & Gilleland 2005). The GPD was fitted to wave height peaks from independent storms separated by at least

three days (POT). Given the 30-year record of modelled wave data from WASP we can reliably estimate up to a 1% AEP event (Coles 2001).
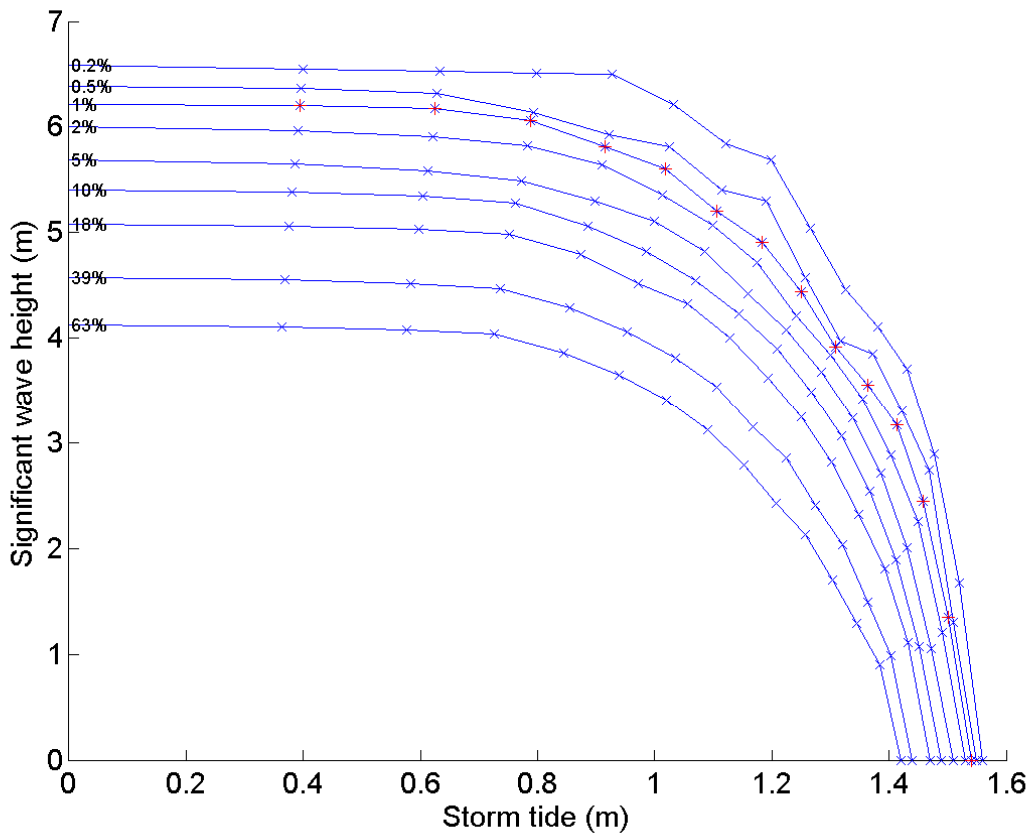
7.2.5 Joint probability of storm-tides and waves

A joint-probability analysis of storm-tides and waves describes the combined likelihood of a high storm-tide and large wave event occurring at the same time. In the absence of a joint-probability analysis design conditions are sometimes derived by superimposing an extreme storm-tide and an extreme wave together. However this results in over design, because the chances of this joint occurrence are very small. For example, assuming storm-tide and wave heights are independent, the coincidence of a 1% annual exceedance probability (AEP) storm-tide (100-year average recurrence interval (ARI)) with a 1% AEP wave height has a 0.01% AEP (10,000-year ARI). In New Zealand the astronomical tide is the largest source of sea-level variability and its amplitude forms the largest component of storm-tide. Therefore, most large storm-tides in New Zealand result from high perigean spring tides combining with a small to moderate storm surge. Because the astronomical tide is independent of storms, dependence between storm-tides and waves is relatively weak compared with some overseas locations. However, there is often a dependence between waves and the storm surge component of the storm-tide, because both storm surges and waves are meteorologically forced and may be heightened by the same storm, and this needs to be accounted for. The joint-probability software models the dependence between storm-tide and wave height and steepness.

Joint-probability analyses of extreme storm-tides and waves were undertaken using the JOIN-SEA software developed by HR Wallingford (Hawkes et al. 2002; HR Wallingford 2000; HR Wallingford and Lancaster University 2000). The software requires coinciding significant wave height, wave period, and storm-tide sampled at each high tide, giving 706 pairs of values per year.

The software fits a generalised Pareto distribution (GPD) to the largest 5% of waves and storm-tides to model extreme values, and samples from the empirical distribution to model more frequent event magnitudes. The software fits a bivariate normal distribution to account for any dependence between the storm-tides and waves.

The results assign AEP for each combination of storm-tide and significant wave height. Figure 7-1 illustrates these joint probability curves for Mangawhai Beach.

Figure 7-1: Joint-probability of storm-tide and significant wave height at Mangawhai Beach. Red crosses mark storm-tide and wave combinations that have an annual exceedance probability of 0.01 (100-year ARI).

Each joint AEP corresponds with a curve of wave height and storm-tide pairings. Given a beach profile for that location the total inundation level at the shoreline can be estimated for each point on the curve. By selecting the highest combined storm-tide and wave setup level from a chosen joint AEP contour the maximum joint wave and storm-tide inundation level is calculated.

7.3   Methods for calculating extreme sea levels in harbours

Extreme sea-levels in the Waitemata, Kaipara and Manukau Harbours were calculated as follows:

- Extreme sea-level analyses were undertaken using the Harbour tide gauge records. These analyses return the frequency–magnitude relationship for extreme storm-tides at the gauge locations.

- Hydrodynamic models were used to simulate ~30-year sea-level time-series at multiple locations throughout the Harbours, including the tide-gauge locations.

- Extreme sea-level analyses were undertaken based on the simulated sea-level records.

- At the tide-gauge locations the extreme sea-level analyses from simulated and measured data were compared as a validation check.

Extreme sea levels are, by definition, rare events. Only by observing a system for a long period of time can an understanding of the frequency and magnitude of extreme sea levels be attained. For the calculation of extreme sea levels, a sea-level record would ideally meet the following criteria:

- Sea-level gauge surveyed to datum.

- Accurate: no long-term drift or sensor subsidence, no siltation or blockage of the gauge. Known tectonic movement or local subsidence at gauge site.

- ≥ 50-years length to incorporate up to two IPO and multiple ENSO climate variability cycles.

- Sample at least hourly to capture storm-tide peak.

- Includes all extreme sea-levels that occurred (no data gaps at crucial times).

The Port of Auckland tide gauge is a rarity where we have high-quality sea-level measurements over 107 years since 1904, and we can model the frequency and magnitude of extreme sea levels there with confidence. Shorter sea-level gauge records were available from the Kaipara Harbour at Pouto Point (2001–present) and the Manukau Harbour at Onehunga (2001–2011). Although less than ideal, these records are sufficiently long to be modelled using the Monte-Carlo joint-probability technique (Goring et al. 2010) that was specifically designed for short records, and provide a comparison for extreme-value analyses using simulated datasets.

As explained in Sections 2.1 and 7.2, extreme sea levels result from combinations of high tide, storm surge, monthly mean sea level, and wave setup that combine in different ways. All of these processes interact in different ways with the local environment such as the underwater bathymetry, topographic constriction, and wind and wave exposure. Thus the extreme sea-level frequency–magnitude relationship changes with location. For example, the tide amplifies as it shoals into the Waitemata Harbour, so the tide range is larger in the upper harbour than at Port of Auckland where the long-term sea-level record was located. It is not possible to obtain a long series of sea-level measurements everywhere. The solution is to use numerical hydrodynamic models that simulate tidal and storm long-wave propagation, calibrate them against sea-level measurements, and use them to predict extreme sea levels at many locations within the harbours.

Numerical hydrodynamic models solve the set of mathematical equations that describe the forced motion of fluids by tide, wind, storm-surge, etc. The equations are solved at a grid of discrete points within the area of interest (called the domain). The bathymetry at each point on the grid is assigned as well as a starting water level and velocity. The numerical model then calculates new water levels and velocities for each grid point as it steps forward through time. Forces such as tide level changes on the open boundary of the domain, or wind blowing across the water surface affect the fluid in the domain (numerically within a computer simulation). The accuracy of hydrodynamic models depends on several factors that include:

- Accurate bathymetry to describe the model domain.

- Accurate description of the forcing at the model boundaries, such as tidal water level elevation changes, for example.

- Accurate solutions to the numerical equations.

- Accurate representation of sub-grid scale processes (such as bottom friction).

- Sufficiently fine grid resolution to resolve the important bathymetric features that control water flow, such as sub-tidal channels and inter-tidal flats.

- Sufficiently fine computational time-step.

- The finer the grid resolution and time step, the more accurate the model (assuming accurate bathymetry and boundary forcing), but the greater the computational requirements. There is always a compromise between model accuracy and computational efficiency to be made. The model is a schematisation of the real-world environment that should be sufficiently accurate to examine the main processes of interest with confidence.

Hydrodynamic models were used in two ways to represent extreme sea levels:

1. The models were used to simulate an approximately 30-year time-series of sea levels at numerous locations throughout the Waitemata, Kaipara and Manukau Harbours. An extreme sea-level analysis was then able to be undertaken using these simulated sea-level time-series at each location.

2. The 23 January 2011 storm-tide event was simulated in the Waitemata Harbour. This is the highest storm-tide event on record at the Port of Auckland, and has an estimated average recurrence interval of approximately 100 years. The simulated extreme sea-levels on 23 January 2011 were compared to 100-year ARI sea-level estimates made using method 1 above.

To dynamically simulate the hydrodynamics in the three harbours for 30 years would take time and computational resources beyond the scope of this project. Hence, a workaround was used that employed hydrodynamic models to simulate various sea-level *components*, which were then recombined, along with the sea-level gauge data, to estimate sea-level time-series throughout the Harbours. The approach used was to separately model the three major components of storm-tide: tide, storm surge and monthly mean sea-level anomaly, and recombine them to produce simulated storm-tide sequences. This approach treats the three sea-level components as independent from one another; it assumes for example that the size of the storm surge is not influenced by the state of the tide. Our tide-gauge analyses show that there is a significant dependence between storm surge and tide elevation inside the constricted Harbours, and the assumption of independence is not adhered to. However, analyses of historical storm-tides in New Zealand has shown that the highest storm-tides have resulted from very high tides combining with a low to moderate storm surge (Bell 2010), because the tide is the largest source of sea-level variability. Therefore, we simulated the storm surge component at high spring-tide levels, based on the reasonable assumption that the highest storm-tides will mostly coincide with the highest spring tides, thus modelling the tide–surge dependence at these highest of tides.

A crucial part of the sea-level reconstruction was the analysis of the tide-gauge records. The tide-gauge records were used as a "base", while the hydrodynamic models were used to spatially extrapolate from the tide-gauge locations.

The sea-level time-series were reconstructed as follows:

- Tides were simulated for a full lunar month, including two spring-neap cycles, which covered all combinations of the three main semi-diurnal tides M_2, S_2 and N_2 that dominate tidal variability in the Auckland region. The tide models were forced at the open boundary using NIWA's New Zealand tide model (Stanton et al. 2001; Walters et al. 2001)[13]. Simulated tides were output at many locations throughout each harbour, including the tide-gauge locations.

- For each simulated location, the simulated tide time-series were used to derive a quantile-quantile scaling factor relative to the tide-gauge location.

- Tidal harmonic analysis (Foreman et al. 2009) was used to analyse the sea-level gauge records and predict the tides at the gauge locations. The tides were predicted at the gauge site to match the duration of the available meteorological records that were used to reconstruct the storm surge.

- The quantile-quantile scaling relationships were used to reconstruct tide records at other locations throughout the Harbours, by applying them to the tides predicted from the tide-gauge. This approach ignores that fact that tidal shoaling will change the shape of the tide full wave as it propagates up and back out of the estuary. This is OK, because the subsequent extreme-value analyses sub-sample the simulated sea-level time-series only at times of peak high tide and discard the rest of the sea-level time-series. This approach of scaling the tide (peaks) was preferred to undertaking tidal harmonic analyses from simulated time-series at all locations in the harbour, because wetting and drying and the distortion of the tidal wave makes harmonic analysis problematic in some shallow upper-harbour locations.

- Storm surge consists of two components: 1) an inverse-barometer sea-level rise caused by a drop in atmospheric pressure and 2) wind stress pushing water up against the land boundary. The local wind-driven component was simulated by applying a wind of constant speed and direction for the duration of a semi-diurnal tide cycle. At each output location the peak wind-driven storm surge amplitude was obtained by subtracting the maximum elevation from a simulation using only the tide (high-tide peak), from the maximum elevation from the tide + wind simulation. The base tide for the simulations was a sinusoidal tide of 12.42-hour period with perigean spring tide amplitude = M_2 + S_2 + N_2. Winds were simulated from the northeast, southeast, southwest and northwest quadrants, at wind speeds of 0–25 m s^{-1} (0–90 km/hr) in increments of 5 m s^{-1}. For each output location, a wind-driven storm surge response matrix was created. The matrix relates wind vector to wind-driven storm surge response at spring tide peak. The matrix was matched with the local

---

[13] http://www.niwa.co.nz/services/online-services/tide-forecaster

meteorological wind record to interpolate a wind-driven storm surge component time-series for the duration of the meteorological record.

- The inverse-barometer component of storm surge was assumed to apply ubiquitously throughout the Harbours as low-pressure storm systems are mostly much larger spatially than a harbour. It was calculated from the local meteorological record using Equation 7-1. The inverse-barometer factor (IB_{factor}) was used as a calibration parameter to match the extreme sea-level frequency–magnitude relationships from measured and modelled data at the tide-gauge locations (more details below). The simulated inverse-barometer storm surge component was added to the simulated wind-driven component to obtain total storm surge.

- The monthly mean sea-level anomaly was obtained from the tide-gauge record by low-pass filtering the non-tidal residual component of sea-level. MMSLA is a slowly-varying sea-level component and was assumed to apply ubiquitously throughout the Harbours.

- At each output location within the Harbours, extreme sea-level analyses were undertaken using the simulated tide, storm surge and MMSLA time-series, applying the Monte-Carlo joint-probability technique described in Section 7.2.3.

7.3.1 Inverse barometer

Inverse-barometer sea level was calculated from the local meteorological record using Equation 7-1. The IB_{factor} varies between locations and also in time for a given location, depending on the local topography and the travel speed and direction of the passing pressure system. Goring (1995) found a long-term average IB_{factor} of 0.67 for the Waitemata Harbour. However, we are most interested in correctly predicting the IB_{factor} for storm events, when it is often larger.

Equation 7-1:   **Inverse-barometer sea-level equation.**   Calculates the sea-level response to barometric pressure change. MSLP = mean sea level pressure in hecto-Pascals, and IB_{factor} is the inverse barometer factor that gives the local sea level response to changes in atmospheric pressure.

IB (m) = [MSLP – mean(MLSP)] $\times$ (-10 $\times$ IB_{factor} ÷ 1000)

Storm-surge in harbours consists of a component that is generated locally inside the harbour (usually wind setup), but also has a component generated in the open sea outside the harbour, which propagates as a storm-surge wave through the harbour entrance. The modelling used in this project only simulated storm-surge generation inside the harbour, by local wind setup and inverse-barometer. Thus the total simulated storm-surge would be under-predicted because the simulations are missing the external storm-surge wave. This was overcome by using a larger IB_{factor} to compensate.

The IB_{factor} was used as a calibration tool to match extreme storm-tide elevations derived from modelled data with those from measured data. It was adjusted, using trial and error, to best match the extreme storm-tide distributions predicted from modelled and measured data at the tide-gauge locations (e.g., Figure 3-7, Figure 3-14 and Figure 3-24). The treatment was slightly different for each of the three major harbours, reflecting differences in harbour response to storm-surge. In the Waitemata Harbour the IB_{factor} was set to 1.0, and a linear

ramp was applied to increase IB_{factor} from 1.0 to 1.4 for atmospheric pressures between the 95th and 100th percentile. In the Manukau Harbour the IB_{factor} was set to 0.7, and a linear ramp was applied to increase IB_{factor} from 0.7 to 2.3 for atmospheric pressures between the 99th and 100th percentile. In the Kaipara Harbour the IB_{factor} was set to 1.2, and a linear ramp was applied to increase IB_{factor} from 1.2 to 1.4 between the 95th and 100th percentile.

The inverse-barometer sea-level was applied uniformly to the entire harbour, because the size of the meteorological pressure systems is larger than the harbour.

7.4   Methods for calculating extreme sea levels on the open coast

For the purposes of this study the "open coast" is defined as coastline located outside of sheltered harbours and estuaries, in locations subject to ocean swell. It is important to consider the contribution of waves to the total sea level on the open coast, because wave setup can be large, up to 1 m for example (e.g., Fairchild 1958). Whereas storm-tides are the main inundation hazard inside the harbours of the Auckland region, the highest sea-levels on the open coast are likely to result from a combination of storm-tide plus wave setup. This means that measurements or models of both storm-tides and waves are required. Furthermore, the likelihood of various combinations of storm-tide and wave magnitudes must be modelled.

Combined storm-tide and wave setup elevations on the open coastlines of the Auckland region were calculated as follows:

- Model wave and storm-tide conditions for a 30-year (1970–2000) period at locations offshore from the surf zone along the open coast. The WASP project models were used.

- Undertake a joint-probability analysis between storm tides and waves at each output location. The joint-probability analysis calculates the likelihood of various storm-tide and wave combinations.

- Use beach profile data and an empirical wave setup formula to calculate wave setup at the shoreline for all wave conditions in the joint-probability analyses.

- Add storm-tide and wave setup to calculate the total combined storm-tide plus wave setup elevation.

The Waves And Storm surge Predictions WASP modelling project recently completed by NIWA produced 45-year (1958–2002) and 30-year (1970–2000) hindcast records of storm surge and waves around the entire New Zealand coast. An aim of the WASP project was to produce a nationally-consistent web-based hindcast from which regional information could be extracted. This will help create a more standardised approach by local government, infrastructure operators and coastal communities in their efforts to adapt to climate-change impacts. The information provides a wider basis for sustainable resource-management planning decisions for the coastal margin that adequately accounts for not only sea-level rise impact (which currently tends to be the main focus), but also potential changes to waves and storm-surge and their impact on coastal hazards. Data is available on the web via NIWA's Coastal Explorer,[14] at the 50 m depth contour at regular intervals around the New Zealand

---

[14] http://wrenz.niwa.co.nz/webmodel/coastal

coastline. This provides "offshore" conditions that can be used in situ, or as boundary conditions to drive more detailed coastal models. The first hindcast simulation used wind and atmospheric pressure forcing data from the global ERA40 reanalysis (Uppala et al. 2005) which covers the 45-year period 1958-2002 with a resolution of 1.225 degrees (~140 km). An additional hindcast for the thirty-year period 1970-2000 was computed used dynamically down-scaled forcing data. This "regional climate model" (RCM) which has a finer resolution of 0.27 degrees (~30 km) and the ERA40 data for boundary conditions was used for this project.

Time-series of storm-tide sea-level for 1970–2000 were estimated by adding the following three sea-level components:

- Astronomical tide – predicted using NIWA's New Zealand tide model (Stanton et al. 2001; Walters et al. 2001)[15].

- Storm surge – hindcast by the WASP models.

- Monthly mean sea-level anomaly – derived from the nearest long-term tide gauge record as described in Section 2.1 (Port of Auckland for east coast and Anawhata for west coast).

Time-series of wave statistics (e.g., height, period and direction) were derived from WASP hindcasts. These were used directly on the west coast. There are many islands offshore from Auckland's east coast that affect the wave climate through wave refraction and sheltering, and the spatial resolution of the New Zealand-regional-scale WASP models was too coarse to resolve these features in the Hauraki Gulf. Therefore, the WASP hindcast was used to drive a nested wave model with sufficient spatial resolution to translate the WASP wave predictions from offshore in deep water to the Auckland coastline of the inner Hauraki Gulf.

Further coast-specific detail on the prediction of open-coast combined storm-tide plus wave setup elevations is given later in Sections 4.1 and 4.2.

7.4.1 Beach profiles

Beach profile data were obtained from Auckland Council, for Browns Bay, Campbells Bay, Cheltenham, Kawakawa, Long Bay, Mangawhai/Pakiri, Maraetai, Milford, Muriwai, Omaha, Piha, and Takapuna Beaches (see Figure 7-2 for an example for Pakiri Beach).

Many beaches have a composite slope with flatter slopes at lower tide mark and steeper slopes at high-tide mark. At most profile locations, numerous beach profiles were available over many years, showing considerable profile variability over time (as in Figure 7-2). A representative beach slope for use in Equation 2-1 was selected as follows:

- Profiles from each location were split into a number of profile sets depending on length of record, with an approximately equal number of profiles in each set. Splitting the records was necessary to enable a clear visual examinations of the profiles; plots containing all profiles were too cluttered to analyse.

- The MHWS elevation was marked relative to the profile datum, based on known MHWS elevations in the region (Stephens & Wadhwa 2012).

---

[15] http://www.niwa.co.nz/services/online-services/tide-forecaster

- For each of the profile sets, a line was fitted by eye to the steepest slope that crossed the MHWS line, as in Figure 7-3.

- The representative beach slopes obtained from the profile sets were averaged at each location.

- Beach slopes for all locations were compared (as in **Table 7-5**). They were remarkably consistent around the coastline, probably as a result of tending to fit to the steepest profiles over the steepest part of the beach.

- A representative beach profile slope of 1 in 9 was adopted for Mangawhai/Pakiri, and a slope of 1 in 7 was adopted for all other beaches in the Auckland region.

- These beach slopes are considered conservative in that they are relatively steep representations of the measurements over the profile near the MHWS elevation (the steepest part of the beach). Thus they will tend to return higher wave setup calculations than the use of shallower slopes in equations such as Equation 2-1.

Table 7-5: Representative beach profile slopes at MHWS elevation for Auckland east-coast beaches.

Location	Beach slope (β_s) 1:X
Browns Bay	1:10
Campbells Bay	1:6
Cheltenham	1:6
Long Bay	1:9
Mangawhai	1:9
Maraetai	1:6
Milford	1:8
Omaha	1:9
Pakiri	1:8
Takapuna	1:8
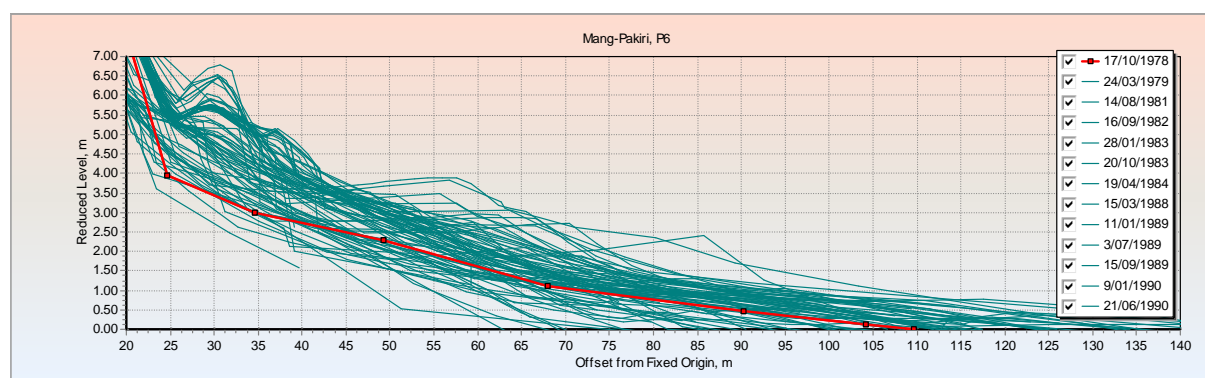
Figure 7-2: Pakiri Beach profiles, at site P6.
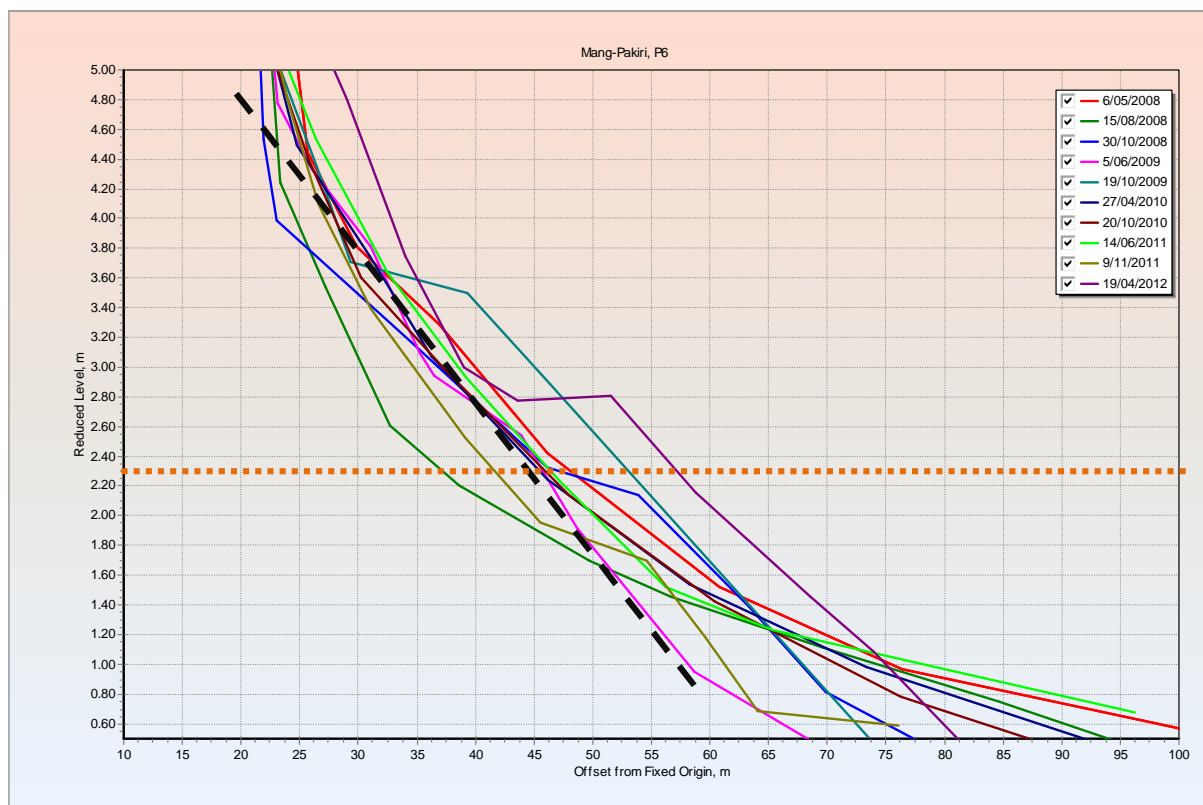
Figure 7-3: Pakiri Beach profiles near the high-tide line; profile P6. A selection (1 of 3 for this profile location) of beach profiles (2008–2012). The orange dashed line marks the MHWS line relative to profile datum. The black dashed line marks a best fit by eye to the steepest slope of these beach profiles at the MHWS elevation.

7.5 Methods for calculating extreme sea levels in small east-coast estuaries

There are a number of estuaries on the east coast of the Auckland region for which there are no measured or modelled sea-level data. These estuaries include Tamaki Inlet, Whangateau, Matakana, Orewa and Weiti, for example. For these locations, we used a simplified approach.

The joint-probability of storm-tides and waves was calculated offshore from the estuary entrance, as described in Section 7.4 above. The storm-tide component was assumed to amplify within these small estuaries, and an amplification factor was applied that increased with distance from the entrance of each estuary. The applied amplification rate was equivalent to the tidal amplification between the Port of Auckland and Salthouse Jetty gauges in the Waitemata Harbour, being 4.2 mm of elevation per km of horizontal distance. We also calculated tidal harmonic constituents (and tidal amplification rates) using existing sea-level records at Pakuranga Bridge in Tamaki Estuary, (Bell et al. 1996) and Dawsons Landing in Mahurangi Estuary, (Oldman & Black 1997). The Tamaki estuary had a similar tidal amplification rate to the Waitemata Harbour, whereas the Mahurangi Harbour rate was approximately double. Thus there is uncertainty in the amplification rates used for the smaller

estuaries that have no sea-level records. This causes an uncertainty of about 3 cm elevation, which is of minor significance to the calculation of the extreme sea-level inundation lines. The wave setup component at the entrance was assumed to translate inside the estuary, so was added to the amplified storm-tide elevations inside the estuary.

8 Appendix B – Mapping inundation areas

Auckland Council has LiDAR data available for the entire region. This provides the council with detailed topographic information and digital elevation models which includes the coastal margins across the region. LiDAR data utilises the AVD-46 for its elevation baseline, bearing in mind that present-day MSL is now about 0.15 m above this datum. The zero LiDAR contour therefore provides a historic MSL that is slightly lower than present-day MSL for the entire region, but is nevertheless tied into the widely-used AVD-46 vertical datum. Contouring above this line typically has a resolution of 0.125 m ground sampling distance (GSD) for urban areas and 0.5 m GSD for rural areas.

By intersecting extreme sea-level estimates with a digital elevation model constructed from LiDAR, a set of flooded coastlines can be generated that represent the inland extent of flooding from the sea. Land lying seaward of the flooded coastlines and below the extreme sea-level elevations can be mapped as flooded.

This section outlines the methods used to produce inundation area maps within GIS. To demonstrate the method, results are shown for the 0.01 annual exceedance probability (100-year ARI) event along the east coast of the Auckland region and then focussing on the Whangateau Estuary to illustrate the final mapping. The methods are the same for all regions and all annual exceedance probability scenarios. The mapped scenarios are listed in Table 1-1.

The process used to develop the inundation polygon in GIS is now described, for a single AEP scenario:

Open coast

- Extreme sea-levels at model-output locations around the Auckland coastline were loaded into GIS (Figure 8-1).

- Extreme sea-levels were interpolated between along connecting lines (Figure 8-2).

- The sea-level elevations were transferred to the coastline using nearest-neighbour interpolation.
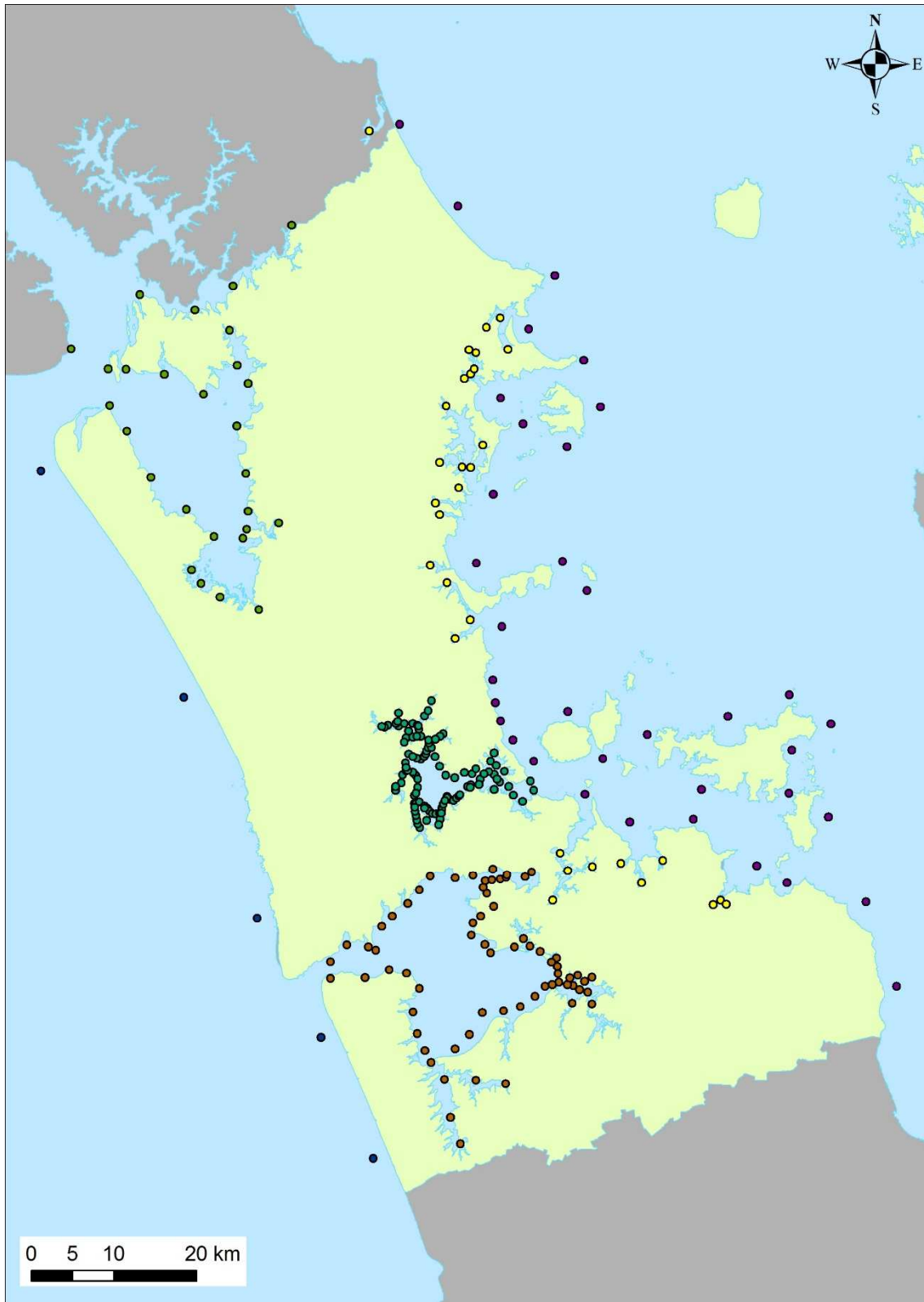
Figure 8-1: Map of the Auckland Region with 0.01 AEP storm-tide elevations marked at model-output locations.

Figure 8-2: Map of the Auckland Region with interpolated elevations on the lines connecting model output locations, and elevations transferred from offshore lines to points along the coastline.

Waitemata, Kaipara and Manukau Harbours, and small east-coast estuaries

- For each extreme sea-level model-output location, the nearest point on the coast was identified and designated as a "hot point", and the extreme sea-level elevations were transferred to it. All other coast vertices in between the hot points remain empty.

- Linear interpolation was used to interpolate extreme sea-level elevations along the guiding coastline, from the hot points to all vertices between (Figure 8-3).

Figure 8-3: Map of Waitemata Harbour with interpolated elevation values on the simplified coastline. "Hot points" along the coastline are marked in red, modelled sea-level output locations in purple.

Creating a regional extreme sea-level surface and generation of inundation polygons

- The interpolated 0.01 AEP extreme sea-level elevations for the Auckland region are shown in Figure 8-4.

- A study area polygon was created from approximately the + 20 m contour inland and to ~ 1 km offshore, to be used as the analysis area (Figure 8-5). This study area polygon can be described as a "window" within which the GIS looks for the intersection of the extreme sea-level elevation with the LiDAR DEM.

- 600,000 random points were picked within the study area and assigned the extreme sea level of the near coastal vertex. We used this dataset to create a 1 m raster of the spatially varying extreme sea level. This is shown in Figure 8-6 for the present-day 0.01 AEP extreme sea-level elevation line, up to 1 km from the coastline.

- Sea-level rise scenarios of +1 m and +2 m were added to some of the present-day extreme sea-level scenarios (Table 1-1).

- Figure 8-7 and Figure 8-8 give examples of the inundation polygons in Whangateau Harbour for 0.01 AEP extreme sea-level scenarios for present-day mean-sea-level and present-day plus 2 m sea-level rise.
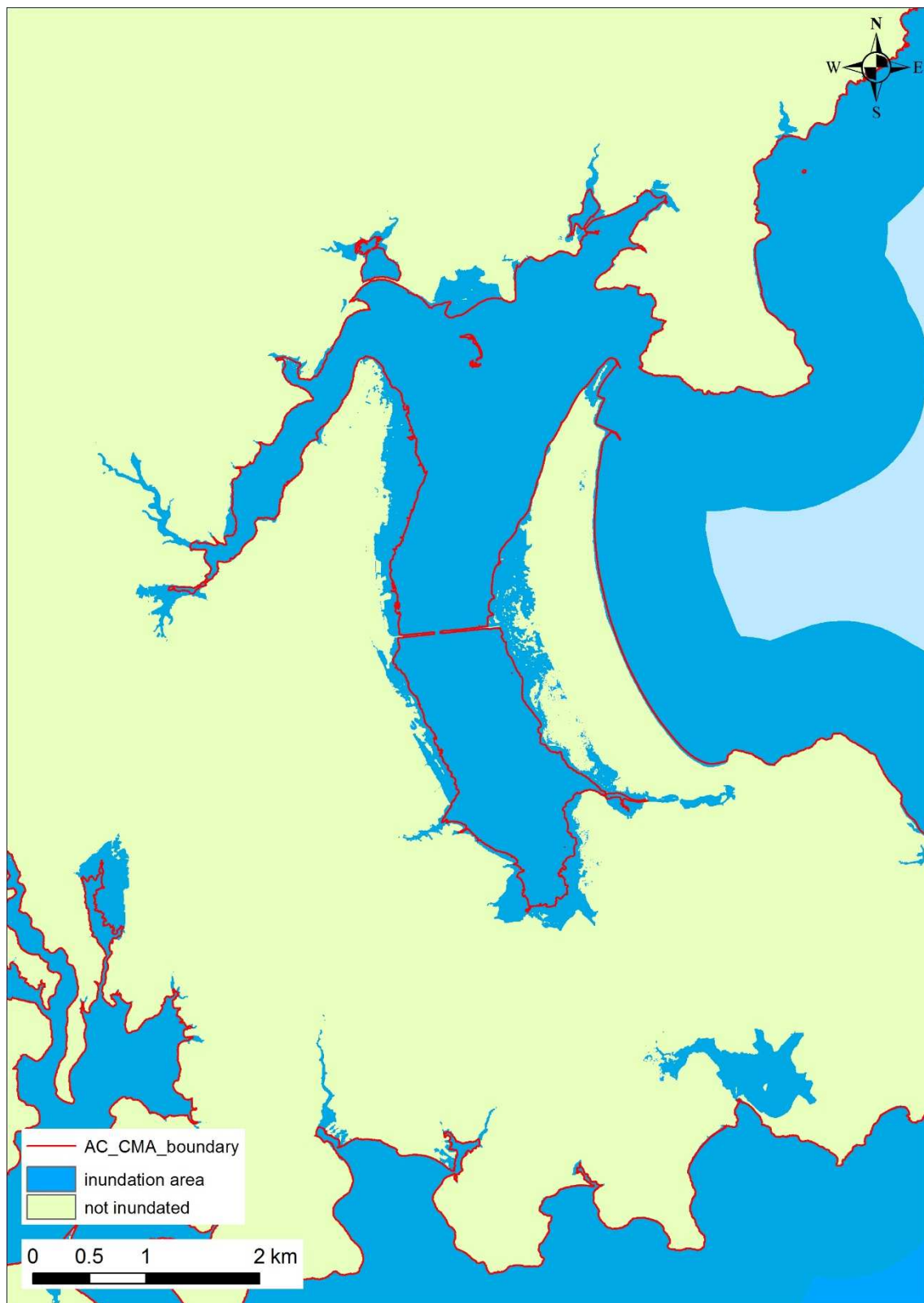
Figure 8-4: Map of Auckland region with interpolated elevation values on simplified coastline.

Figure 8-5: 600,000 random points in the analysis area.

Coastal inundation by storm-tides and waves in the Auckland region
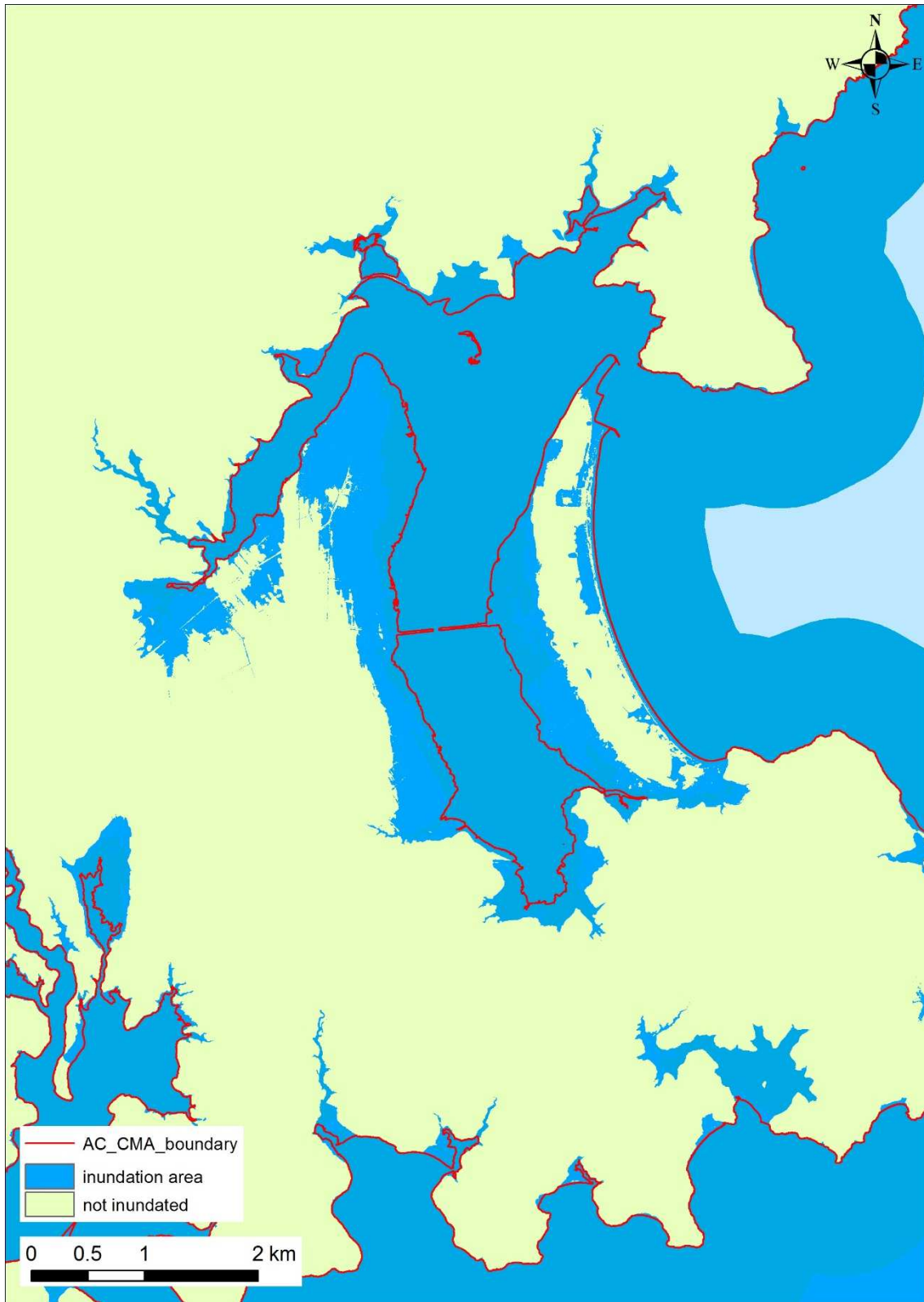
Figure 8-6:   Map of Auckland region with water surface for 0.01 AEP (100-year ARI) elevations.

Figure 8-7:   Inundation area from 0.01 AEP (100-year ARI) extreme sea-level scenario, including present-day +0.15 m mean-sea-level offset to AVD-46, in Whangateau Harbour. AC_CMA_boundary is the CMA boundary for the Auckland region (Stephens et al. 2012).

Figure 8-8: Inundation area from 0.01 AEP (100-year ARI) extreme sea-level scenario, including present-day +0.15 m mean-sea-level offset to AVD-46 + 2.0 m sea-level rise, in Whangateau Harbour.

Connection by rivers and drains

The raw polygons contained numerous ponded areas that were unconnected to the sea. This occurred because they were lower than the extreme sea-level being modelled, but separated from the sea by a strip of higher land. Therefore, the final process was to overlay a GIS layer containing the drainage network. If a ponded area was connected by a river or drain, then it was included in the flood map, and if not it was deleted. In the data layers supplied to Auckland Council, these areas are flagged 'connected by drain or river'. The connections are based on the storm water and river network locations supplied by Auckland Council. Our 'bathtub' approach assumes that if an inland area is connected to the open coast via a drain/river then this area will be inundated to the equivalent level as the adjacent open coast (i.e., no lags or diminished volumes assumed in flooding through these connections.

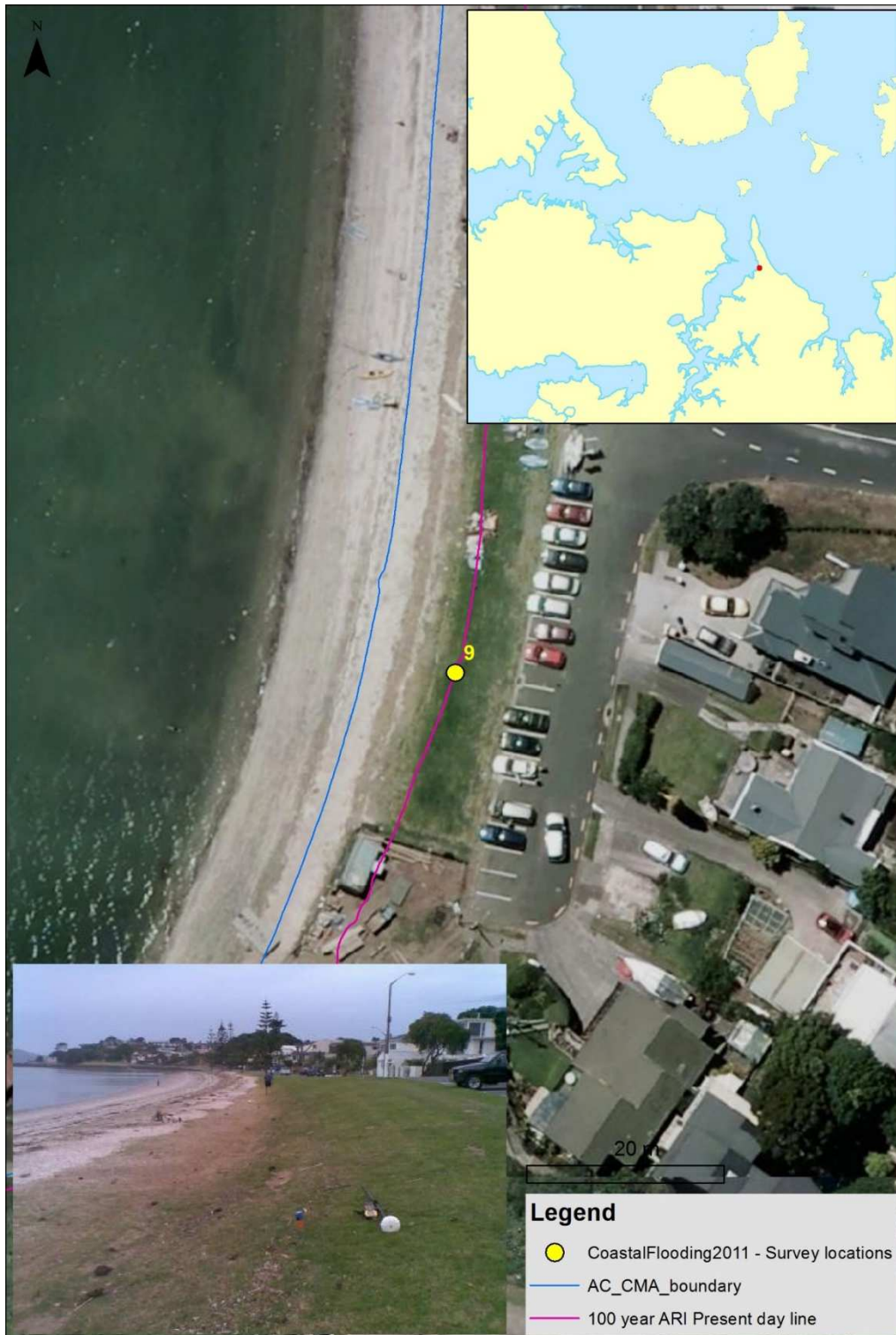## Verification of present-day 0.01 AEP inundation polygons

The 23 January 2011 storm-tide was the highest on record at the Port of Auckland (Waitemata). The average recurrence interval for this storm-tide has been estimated at 88 years (Stephens et al. 2011c), and 126 and 205 years, depending on the method used, but the difference between a 100-year and a 200-year ARI event is only ~6 cm (Section 3.1.1). Therefore, the 100-year ARI inundation area polygon at present-day mean sea level should compare closely to the coastal flooding that occurred on 23 January 2011. The 0.01 AEP (100-year ARI) inundation polygons were validated by visually comparing it with ground photographs from the 2011 storm-tide event, for the east coast of the Auckland region. Surveys of the areal extent of inundation (from Auckland Council) were also used, and photographs during the storm-tide were also used for validation at few locations.

Verification against surveys of the 2011 storm-tide

Auckland Council surveyed locations that marked the inland edge of coastal flooding during the 23 January 2011 storm-tide. These locations are plotted alongside the landward boundary of the 0.01 AEP polygon, overlaid on aerial photographs, in Figure 8-9–Figure 8-13. The comparisons appear to verify the modelling for the 0.01 AEP scenario for present-day MSL.

Figure 8-9: Verification of present-day 0.01 AEP (100-year ARI) storm-tide line against surveyed location of maximum flood incursion during 23 Jan 2011 storm-tide, at Kohimarama. Pink line marks modelled 0.01 AEP storm-tide line. Blue line marks coastal marine area (CMA) boundary.

Figure 8-10: Verification of present-day 0.01 AEP (100-year ARI) storm-tide line against surveyed location of maximum flood incursion during 23 Jan 2011 storm-tide, at Half-Moon Bay. Pink line marks modelled 0.01 AEP storm-tide line. Blue line marks coastal marine area (CMA) boundary.

Figure 8-11: Verification of present-day 0.01 AEP (100-year ARI) storm-tide line against surveyed location of maximum flood incursion during 23 Jan 2011 storm-tide, at Saint Heliers Bay. Pink line marks modelled 0.01 AEP storm-tide line. Blue line marks coastal marine area (CMA) boundary.

Figure 8-12: Verification of present-day 0.01 AEP (100-year ARI) storm-tide line against surveyed location of maximum flood incursion during 23 Jan 2011 storm-tide, at Saint Heliers Bay (east). Pink line marks modelled 0.01 AEP storm-tide line. Blue line marks coastal marine area (CMA) boundary.
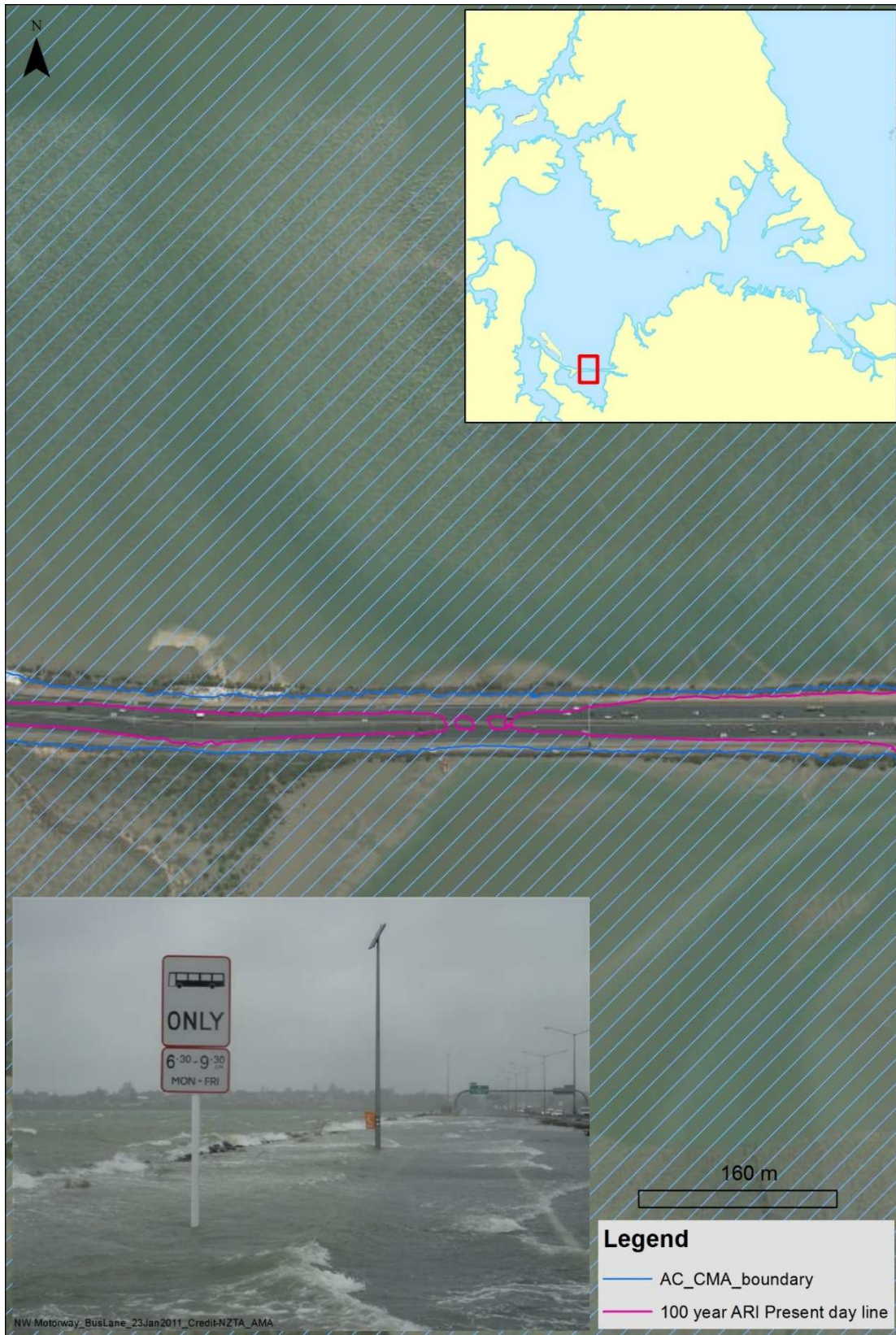
Figure 8-13: Verification of present-day 0.01 AEP (100-year ARI) storm-tide line against surveyed location of maximum flood incursion during 23 Jan 2011 storm-tide, at Saint Marys Bay. Pink line marks modelled 0.01 AEP storm-tide line. Blue line marks coastal marine area (CMA) boundary.

Verification against photographs of the 2011 storm-tide

The present-day 0.01 AEP GIS polygons were compared with photographs of flooding over the North-western (SH16) and Northern (SH1) motorways, with the model showing a close match (Figure 8-13, Figure 8-14). On the northern motorway the GIS polygons show inundation on the north bound lane, which did not occur because the water was stopped by a low median barrier between the north-bound and south-bound lanes, not captured in the LiDAR data (Figure 8-14).

Figure 8-14: Verification of present-day 0.01 AEP (100-year ARI) storm-tide line against photograph of observed flooding on the north-western motorway during the 23 Jan 2011 storm-tide.

Figure 8-15: Verification of present-day 0.01 AEP (100-year ARI) storm-tide line against photograph of observed flooding on the Northern motorway during the 23 Jan 2011 storm-tide.

Coastal inundation by storm-tides and waves in the Auckland region